

Master Thesis

# **On the Optimum use of Mg II Index as a Proxy for UV SSI Variation Models**

Neda Darvishsefat

Matriculation number: 2959969

February 29<sup>th</sup>, 2016

Supervisor and Referees:

Dr. Mark Weber  
Prof. John P. Burrows



Postgraduate Program in Environmental Physics (PEP)  
Institute of Environmental Physics (IUP)  
University of Bremen

## **Acknowledgement**

This thesis would have not been possible without the support of many people. First of all the staff and coordinators of PEP international graduate program, for providing the opportunity to study in a comfortable environment, surrounded by great classmates from all over the world. Special thanks to Lars Jeschke and Anja Gatzka for their assistance throughout the entire master's program.

I would like to thank my supervisor Dr. Mark Weber, for his continuous understanding and support throughout this thesis. As well as my head supervisor Prof. Dr. John Burrows, for his guidance. Also special thanks to Martin Budde and Stefan Boetel for their ongoing assistance and teachings.

Most of all I thank my family for their never ending support and believe in me.

# Table of Contents

Abstract.....	3
1 - Introduction and Motivation.....	4
2 - Scientific Background	
2-1 Structure of the Sun & Irradiance Variability.....	7
2-1-1 Sunspots.....	9
2-1-2 Faculae.....	10
2-2 Solar Spectrum Irradiance (SSI) .....	11
2-3 Mg II Index.....	14
2-4 Solar Models.....	17
3- Instruments of SSI Datasets	
3-1 SORCE SOLSTICE.....	18
3-2 UARS SOLSTICE & SUSIM.....	19
3-3 Instrument Degradation in the UV.....	20
3-4 Mg II Index Composite.....	22
3-5 NRLSSI2 .....	23
4 – Method	
4-1 Approach.....	24
4-2 Correlation of Mg II index with SORCE SOLSTICE.....	25
4-3 Sensitivity Analysis at 205 nm.....	26
4-4 Detrending Data.....	32
5 – Results	
5-1 SORCE SOLSTICE	
5-1-1 Analysis at 130 nm and 300 nm.....	38
5-1-2 Summary Plots.....	43

5-2 UARS SOLSTICE.....	49
5-3 UARS SUSIM.....	55
5-4 Sensitivity Comparison for all Instruments.....	59
5-5 NRLSSI2.....	61
5-6 Comparisons of all Instruments with NRLSSI2.....	63
6 – Summary .....	67
Appendix .....	69
Bibliography .....	73

## Abstract

Time series of Solar Spectral Irradiance (SSI) are an important input parameter for climate models. But its measurements are not consistent either throughout the spectrum or in time. Therefore, proxy based solar models are used to represent the SSI in climate models. The Mg II index is a useful proxy to model SSI in the UV spectral region. In order to confirm how suitable the use of this proxy is, the correlation of the Mg II index composite with the available SSI satellite data from SORCE SOLSTICE (2003-present), UARS SOLSTICE (1991-2001) and UARS SUSIM (1991-2005) has been analyzed. The observation periods of each of these instruments cover solar minima and maxima of the 11-year cycle. The spectral range investigated is from 115 to 300 nm in the UV. The SSI sensitivity with respect to changes in the Mg II index has been obtained and its stability over the 11-year solar cycle is discussed. The results show for all three instruments in most parts, stability of the sensitivity within its uncertainty range through the observation time, particularly for the lower wavelengths in the UV region. For higher wavelengths above about 250 nm additional parameters like sunspots have to be considered in the linear regression in order to achieve better results.

SORCE SOLSTICE covering the solar minimum years, does not always show firm stability specially in the peak of solar minimum years, but has overall low absolute values and low uncertainties. UARS SUSIM covering solar maximum and minimum years, shows better stability of the sensitivity, but with higher uncertainties at the same time and lower absolute values. It also covers the maximum years very well with lower uncertainties. The UV proxy sensitivity from UARS SOLSTICE covering the same solar minimum years as UARS SUSIM, has lower uncertainties, with relatively stable sensitivity with time, along with higher absolute values. In addition the obtained sensitivities from the three instruments have been compared to the SSI output from the NRLSSI2 model which uses SORCE SOLSTICE for its linear regression, and is widely used in climate models. The comparisons show a high difference between modeled data and UARS SOLSTICE instrument with more irregularities and higher values, indicating more SSI variations if it had been used for the model, but also more instrument irregularities. UARS SUSIM in contrast shows lower values indicating lower SSI variability than NRLSSI2.

# Chapter 1

## Introduction and Motivation

As we know the sun is the main source of energy on earth. Important features of the Earth's atmosphere, for example its thermal structure, composition and dynamics, are dependent on the Solar Spectral Irradiance (SSI). This dependency appears through processes like photodissociation, photoionisation, thermal absorption and photoabsorption (Thuillier et al., 2012).

But the total solar irradiance (the SSI integrated over all wavelengths, also called the solar constant) is not a constant and has variations of 0.1% over the 11-year solar cycle. Solar variations are the result of the magnetic activities on the sun's surface, leading to temperature variations, and so affecting its outgoing radiation. Even though this variation percentage is generally small, there is higher a impact in the UV region of the solar spectrum where the irradiance values are lower, but the variability can reach up to 100% (Ermolli et al., 2013). There have been SSI time series measurements, mainly through satellite observations, as well as attempts to reconstruct the SSI for longer times, and more extended wavelength coverage, using solar models (Ermolli et al., 2013).

In order to better understand the role of these variability on earth's climate, climate models require for their input reliable solar spectral irradiance (SSI) time series. Even though there have been various SSI measurements through satellite instruments over the past decades for establishing its time series, the data have gaps either in time or in wavelength coverage or both. On top of that the achieved data from space suffer from instrument degradation specially in the UV region. Therefore there has been attempts of constructing solar models to represent SSI data for further use climate models. Currently used solar models for SSI are the semi-empirical models, like NRLSSI2 and SATIRE- S (Ermolli et al., 2013). In these models proxies for different regions of the spectrum are being used as input parameters in order to construct the final SSI data. These proxies are measured quantities representing the solar spectral irradiance.

Several proxies are being used for this purpose, such as the Mg II and Ca II core-to-wing ratio, the solar radio flux F10.7, the He II (1083 nm) line intensity, the sunspot number (measured since 1609)

and the cosmogenic isotopes Be10 and C14 available back to 7000 BC (Thuillier et al., 2012). The decimetric flux F10.7 and the Mg II index are suitable proxies for the EUV and UV, while sunspots number for visible wavelengths (Pagaran et al., 2009) (Thuillier et al., 2012). The most suitable proxy in the UV region is the Mg II index (Deland et al., 1993) (Dudokde Wit et al., 2009). The Mg II index which is a core-to-wing ratio of the Mg II doublet near 280 nm, measures the solar chromospheric activity and faculae brightening and is frequently used as a proxy for UV irradiance solar models (Riaz, 2012). Therefore, the Mg II composite is a widely used component in stratospheric research, thermospheric and ionospheric research areas along side with Total Solar Irradiance (TSI) and SSI models which are important in the climate change studies (Viereck et al., 2004).

The importance of reconstruction of reliable solar models, amplifies the need for accurate proxies that are able to fully represent the solar variability. For this reason the relationship between each of the proxies and SSI has been analyzed for different regions of the UV spectrum. Focusing on the UV region and the Mg II index, this thesis zooms in the relationship of the Mg II index and SSI. How well the Mg II index correlates with the SSI data in the UV range, shows how suitable this proxy is for use in SSI models.

Analysis of this relationship includes sensitivity analysis of SSI datasets with respect to the Mg II index, along with determining uncertainty. Converting the proxy sensitivity (SSI change per Mg II index unit) to a solar cycle percentage, will provide a value, that can be related directly to existing SSI variability estimations (Domingo et al., 2009). The slope of the linear regression of SSI against the Mg II index for different years of SSI measurements, will determine how well this relationship functions and how stable the proxy sensitivity is with time. In order to do so, the SSI change per change of Mg II index, for continuous wavelengths from 115 to 300 nm will be examined over the observed period of time of SSI satellite timeseries. The focus of discussions will be mostly during solar minimum and maximum years, since most of the changes happen in these years. If the stability of the derived proxy sensitivity is stable from solar minimum to maximum, considering also the uncertainties, then it would demonstrate the suitability of Mg II index as a proxy for UV SSI variations.

The uncertainty derived from this linear regression for each year, as well as the standard deviation from the mean of the annual sensitivity values for each wavelength, provide a measure of the uncertainty. On

top of that there are additional uncertainties due to instrument measurements. Specially in the UV region the instruments suffer from optical material degradation, which further increases the uncertainties. In order to reduce the degradation uncertainties, all data sets have been detrended. This means that the proxy sensitivity is mainly derived from the 27 day solar rotation, which are in fact superimposed on the long term 11- year solar cycle. Thus the solar cycle percentage is also determined from this rotational time scales of solar variability. This will reduce the degradation effect of long term observational periods from the space instruments, which are a great issue in the UV region.

Furthermore, 3 different datasets of SSI measurements through different satellite instruments (two SOLSTICES and SUSIM) have been used as a final comparison of the absolute values and uncertainties of the obtained sensitivity. These three instruments have the longest observational time spans. They cover up different time spans of the solar cycles, mostly during solar maximum and minimum years in order to have a thorough outlook over the entire 11 year solar cycle. In addition, a final comparison of the obtained results from these datasets have been made with the SSI output of the NRLSSI2 reconstruction, that is also partly based on solar proxies. This model already uses SORCE SOLSTICE measurement data for its linear regression (Lean, 2012). The difference between the results from the model and the three satellite data will provide an outlook on the uncertainty of the NRLSSI2.

This thesis starts by giving an introduction to the scientific background of solar variability (Chapter 2). The three satellite instruments used here, along with the model have been described afterwards (Chapter3). Continued by a brief description of the method to derive the proxy sensitivity (Chapter 4) Then the results have been shown and discussed in details, for 3 chosen wavelengths from different parts of the UV region for each of the studied instruments (Chapter 5). In this chapter the compatibility of the obtained results from the different instruments has been discussed, along with a final comparison of the results from the measured data with the output of the solar model NRLSSI2. A summary and conclusion is provided in the final chapter 6.

# Chapter 2

## Scientific Background

### 2-1 - Structure of the Sun

The main source of energy received by the Earth is from solar radiation. Part of it is absorbed and scattered by the atmosphere and part of it is received at the earth's surface. This incoming radiation is the main driver for weather changes, oceanic circulations and climate variations.

Generally the incoming solar radiation is considered a constant of  $1367 \text{ W/m}^2$  in simplistic studies. But there are cyclic variations of 0.1% in time due to the variations in the magnetic field of the sun, which reach up to 100% in the UV region (Domingo et al., 2009). The solar radiation is known to vary from its maximum (active sun) to its minimum (quiet sun) in a 11-year cycle. In addition there is also the 27 day cycle due to the rotational period of the sun (Rühedi et al., 2004).

These cycles depend on the sun's structure and its magnetic activity. The sun is a gaseous sphere mainly composed of hydrogen and helium, along with several heavier constituents like oxygen, carbon, calcium, magnesium, iron. The solar energy is a result of the fusion of four hydrogen atoms into one helium atom at very high temperatures. Therefore it emits a large amount of electromagnetic radiations in all wavelengths. A total output of  $3.99 \cdot 10^{26} \text{ W}$  is generated, from which the earth receives  $1367 \text{ W/m}^2$  (solar constant, TSI) at the top of Earth's atmosphere (TOA).

The sun and its atmosphere can be divided into several subcomponents as described below (Hanselmeier, 2004):

Sun's interior:

- The core which is the center of the sun where the energy is generated
- The radiation zone where the energy flows into the outer layers through emission and absorption processes.
- the convection zone that is just below the surface

The sun's atmosphere is divided into several layers

- The photosphere is the region where most of the light is emitted and is considered to be the first 500 km from surface of the sun. The photospheric temperature is stable and about 5775 K.
- The chromosphere follows the photosphere by expanding to 2 Mm
- The transition region with a strong increase in temperature
- The corona is the outermost part of the sun with very high temperatures reaching millions of K

Figure (1) depicts this structure in details.

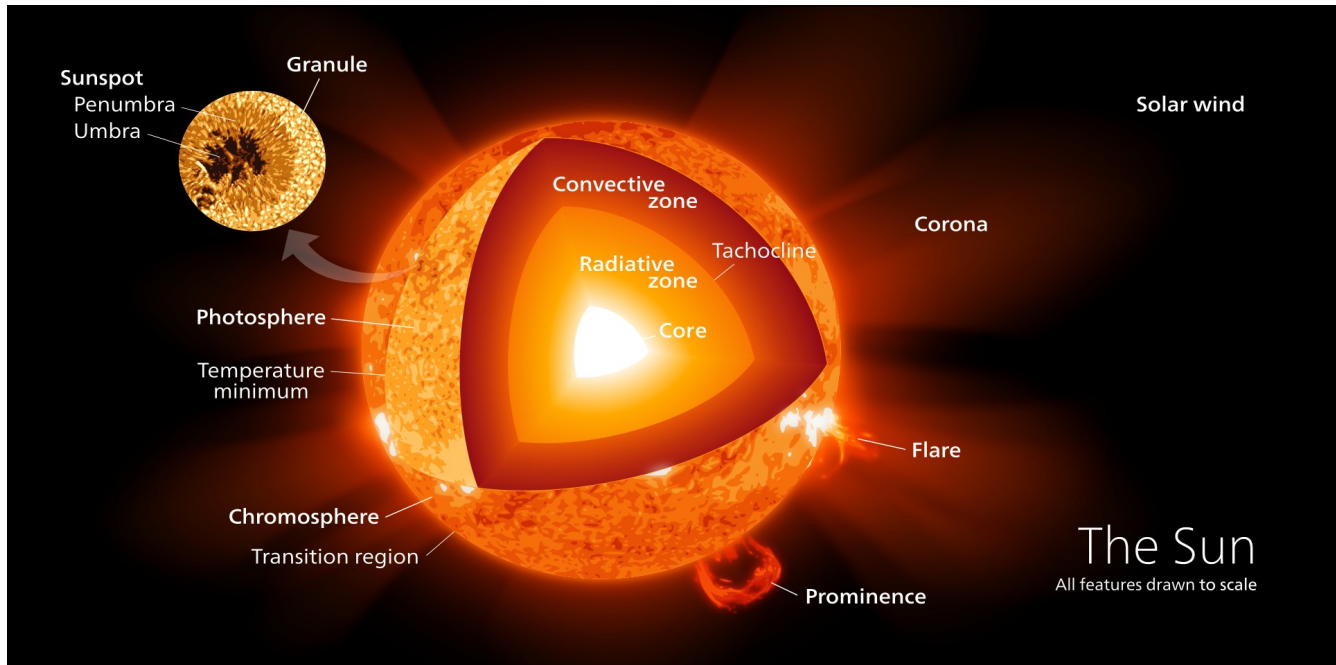


Figure (1): The sun's structure and components [<https://en.wikipedia.org/wiki/Sun>]

The sun's interior is the source of high energy production through nuclear fusion. The energy is transferred towards its outer layers, and from the photosphere the energy is radiated out to the sun's atmosphere and out into the space. The magnetic activities in the photosphere and the sun's atmosphere are the main cause for the variation in its radiation. Sunspots and faculae are two main magnetic activities responsible for solar variations.

Since the sun is gaseous and not solid, it has different rotation periods at different solar latitudes. On the surface around its poles it rotates with a 35 day period and at the equator in 25.7 days, and as a mean the sun spins with a 27 days rotation period as it would be seen from an observation point on earth (Shakeri, 2010). This causes a differential rotation on the solar surface and is known as the 27-days Carrington cycles.

## 2-1-1- Sunspots

Due to high magnetic fields, visible dark spots appear in the photosphere. They are cooler compared to the temperature of the surrounding photosphere due to the outflow of the magnetic field from the sun's surface (Riaz, 2012). These strong magnetic spots lead to intense heating in the solar atmosphere and cause active regions which are also the cause of mass ejections in the corona (Rühedi et al., 2004). Sunspots are composed of dark central regions that are called umbra surrounded by a less dark area called penumbra (Hanselmeier, 2004). Sunspots appear at low latitudes near equator and never on the poles (Hanselmeier, 2004).

Solar activity is related to sunspots as a result of solar magnetic activity. A key indicator of the solar magnetic activity is counting the number of sunspots observed in time (Hanselmeier, 2004). This method was introduced by Schwabe and led to the discovery of the 11-year solar cycle. The daily observations of sunspots has been organized and carried out from 1849 known as the international sunspot number. (Hathaway, 2010)

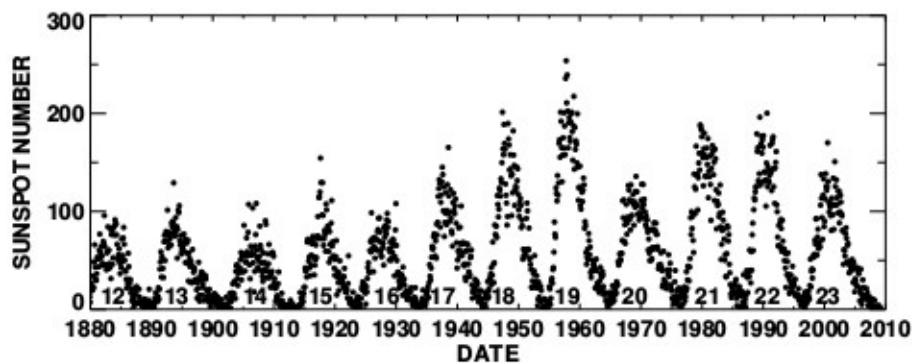


Figure (2): Monthly averages of the daily International Sunspot Number (Hathaway, 2010)

When the sunspot numbers are at a minimum, the sun is quiet, which is termed the solar minimum. When the sunspot numbers are at their peak, the solar maximum is reached and the sun is active (Shakeri, 2010). Figure (3) shows how the number of sunspots varied over the last centuries, where for later than 1750 year, various and unsystematic observations have been used. It suggests stable cycles of solar activity over the last 200 years but a significant drop in the Maunder Minimum years (1645 – 1715) (Hathaway, 2010).

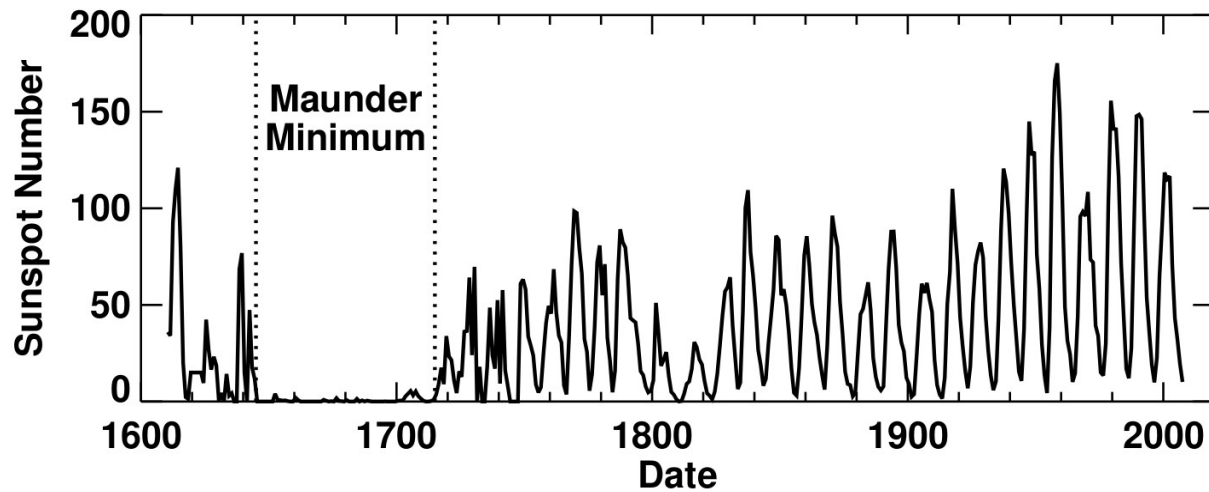


Figure (3): The yearly averages of the daily Group Sunspot Numbers are plotted as a function of time. The Maunder Minimum (1645 – 1715) is well observed in this dataset (Hathaway, 2010).

## 2-1-2 - Faculae

There are brighter areas in the photosphere called faculae, which are concentrated hot material formed through small scaled magnetic flux tubes.

They are important for the energy balance between sunspots which are cooler in temperature and the rest of the photosphere in order to maintain a stable temperature. The faculae are generally surrounding the sunspots and appear more when the sun is more active. Their number is higher and they also persist longer on the photosphere compared to the sunspots, and since these bright spots have higher emittance, solar radiation is increased, particularly in the UV during active sun periods (Hanselmeier, 2004) (Shakeri, 2010).

Sunspots and faculae cause temperature variations on the higher layer of the sun, the chromosphere. Therefore chromospheric activities are a result of the magnetic activities on the photosphere.

Establishing a faculae index is also possible but more difficult and they lack long term observations, and so the observation of faculae has not been as well established as it is for sunspots. Therefore chromospheric flux ratios like the Mg II index, are used as alternatives, which offer much better advantages over faculae indices (Froehlich and Lean, 2004).

## 2-2 - Solar Spectral Irradiance (SSI)

The solar radiation received at the top of the atmosphere is the most important source of energy for this planet. Due to its major influence on the components of the earth system, it has been measured and observed for a long time. Generally for simple calculations in the earth system, and considering the sun as a black body with a temperature of 5800 K, the radiation (integrated over the entire spectral range) at the Earth's TOA is about  $1367 \text{ W/m}^2$ . The solar irradiance as a function of wavelength defines the solar spectral irradiance (SSI) or the solar spectrum (Figure (4)).

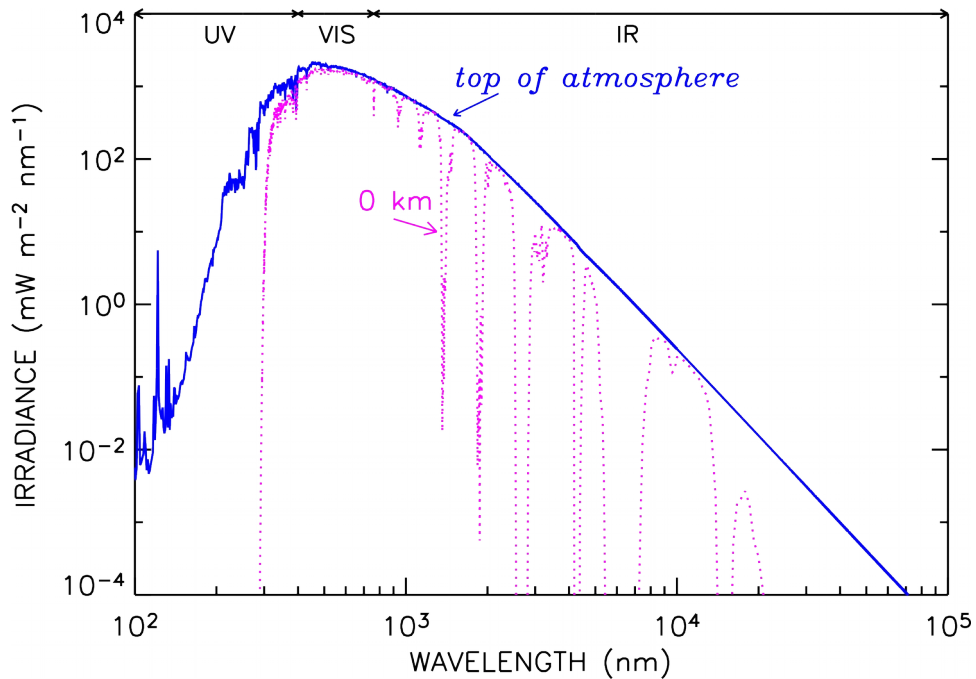


Figure (4): Solar irradiance spectrum (Froehlich and Lean, 2004)

The integration over all the wavelengths and the area under the spectral irradiance curve then is defined as the total solar irradiance (TSI) or solar constant (Fox, 2004). Over a 11-year solar cycle the TSI varies by about 0.1% around the mean value of  $1367 \text{ W/m}^2$ . The variability reaches up to 100% in the UV region as depicted in figure (5). The red curve shows the SSI over the wavelength spectrum, and the blue curve shows its corresponding variability at the same wavelength. The variability has a high value until around 100 nm, and then it decreases greatly on to very low values for higher wavelengths. Therefore solar activity studies are of more importance in the UV region, and less significant in the higher wavelengths.

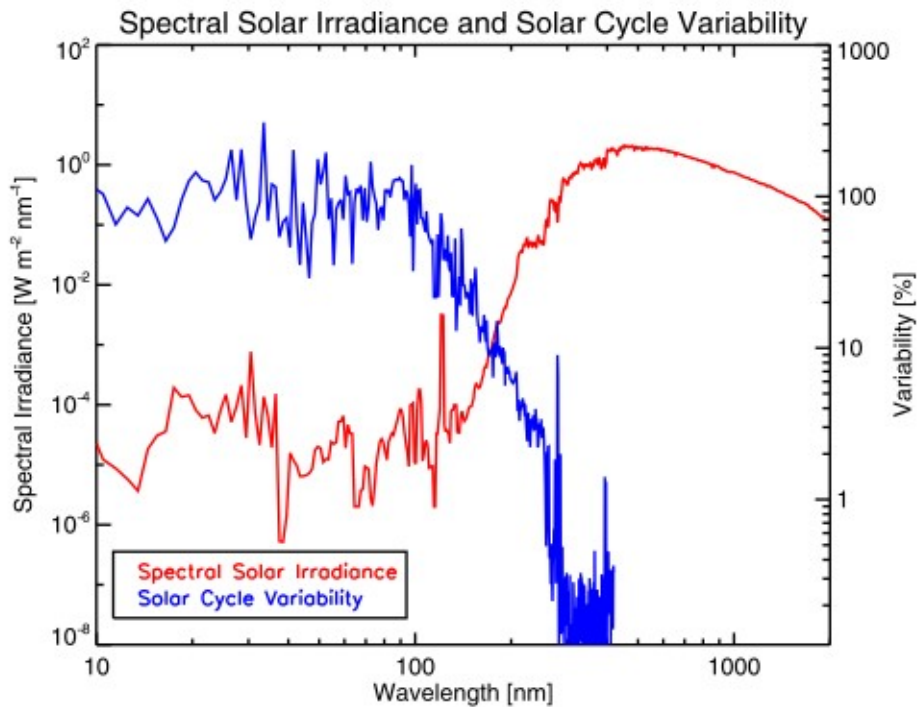


Figure (5): SSI and its variability (Domingo et al., 2009)

These variations over time have been measured through several instruments, as well as various proxies in order to establish a time series of the solar irradiance as depicted in figure (6). Obtaining long term time series of SSI is necessary for further use in climate research.

### Solar Cycle Variations

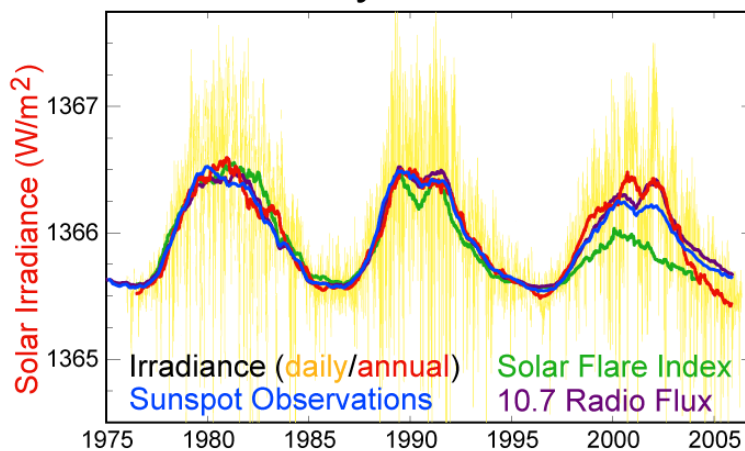


Figure (6): Solar variation over time, the curves show measurements with various solar variation indicators

[\[https://en.wikipedia.org/wiki/Solar\\_cycle\]](https://en.wikipedia.org/wiki/Solar_cycle)

There exist species in the solar atmosphere absorbing its outgoing radiation. Therefore the received

spectrum on earth has absorption and emission lines, known as the Fraunhofer lines. These species from O, H, HE to metals like Mg and Ca exist at different altitudes. As it is seen in figure (7), the temperature decreases with height at first to a minimum of around 4500 K and then increases with altitude until million degrees in the corona. At different temperatures there is the probability of different electronic transitions of species, which leads to the formation of absorption lines in different altitudes (Shakeri, 2010).

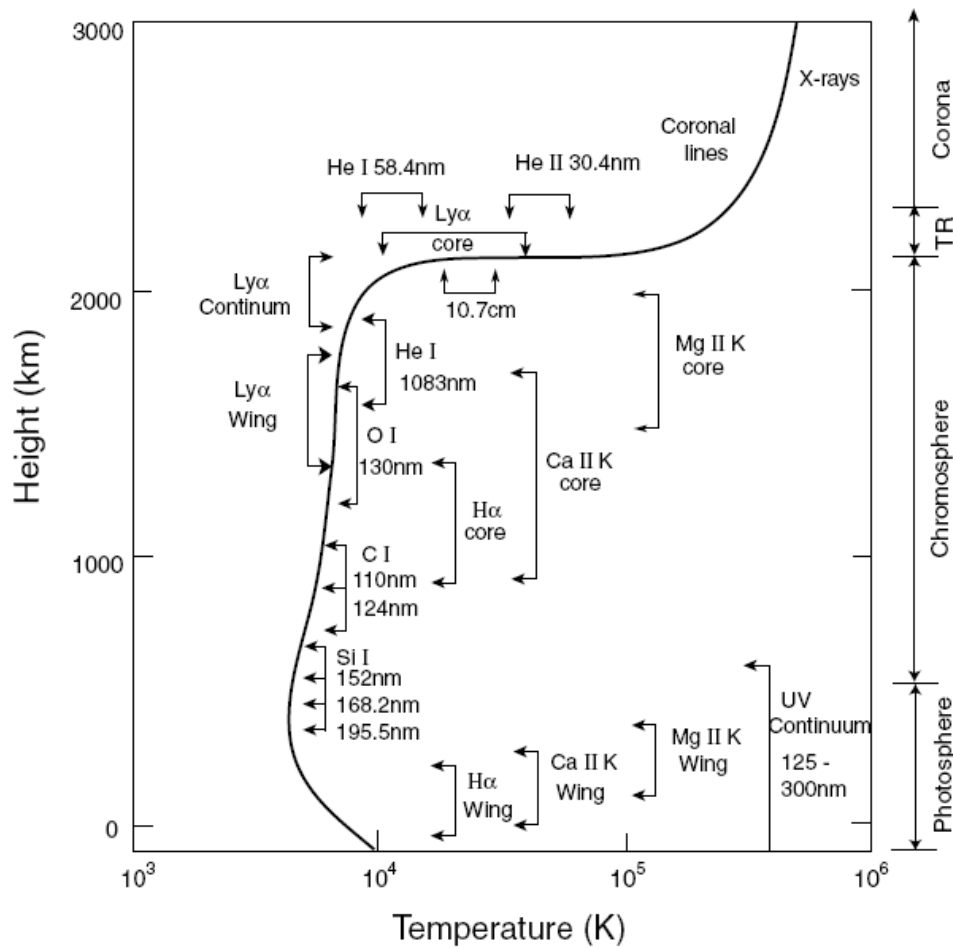


Figure (7): The temperature structure of the solar atmosphere and the regions above it where absorption lines are formed. (Lean et al., 1987)

Through measuring the absorption lines of these species it is possible to detect solar variability. This case is true specially when the core of the absorption line exist in the chromosphere, compared to its wings in the photosphere with a more stable temperature. The core absorption line will vary according to the variation of the chromospheric temperature variation, and therefore can detect chromospheric activities. Particularly of interest are Mg II, Ca II and He I (Froehlich and Lean, 2004). In this thesis the focus will be on Mg II as a chromospheric proxy.

## 2-3 - Mg II index

Magnesium absorption lines are observed in the solar spectral range. These lines have been discovered in 1962 by Kachalov Yakovleva (Lemaire & Skumanich, 1973). Many of the lines are electronic transitions of ionized magnesium. This ion is in fact a good means of studying the physical nature of stars, nebulae, stellar atmospheres, and the interstellar medium. The presence of magnesium in stellar atmospheres is mainly due to the fact that it can be easily built up in higher energy conditions of supernova stars from three helium nuclei (Cholakyan, 1986).

The absorption of magnesium at 280 nm are seen as pairs of lines, called doublets. The two lines which are very close to each other in wavelength, are indicated as h and k lines in order to avoid confusion. The h line peaks at 280.27 nm wavelength and k at 279.55 nm (Shakeri, 2010). This is due to the magnesium atomic structure, where the last two electrons jump from 3s to 3p when excited. Then because of spin-orbit interaction the energy level from 3p is split into two adjacent energy levels (Rühedi et al., 2004). This difference in the energy levels splits the final spectral line into two separate lines. This effect is known as the splitting of spectral lines and is observed in many emission lines of the spectrum. The energy levels are depicted in figure (8).

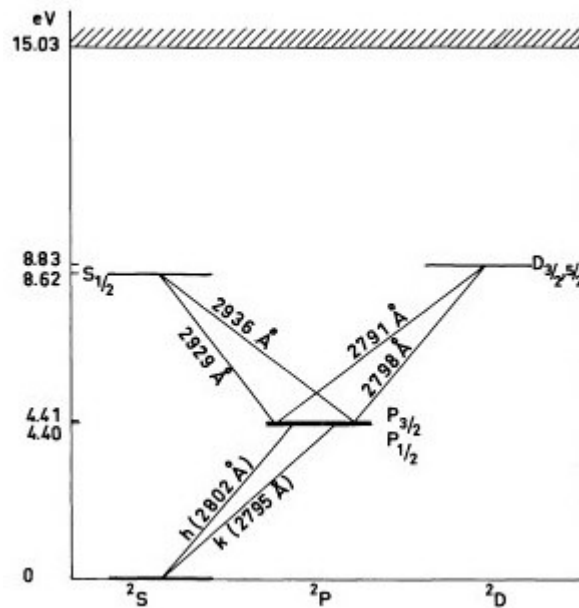


Figure (8): Mg II energy diagram (Lemaire & Skumanich, 1973)

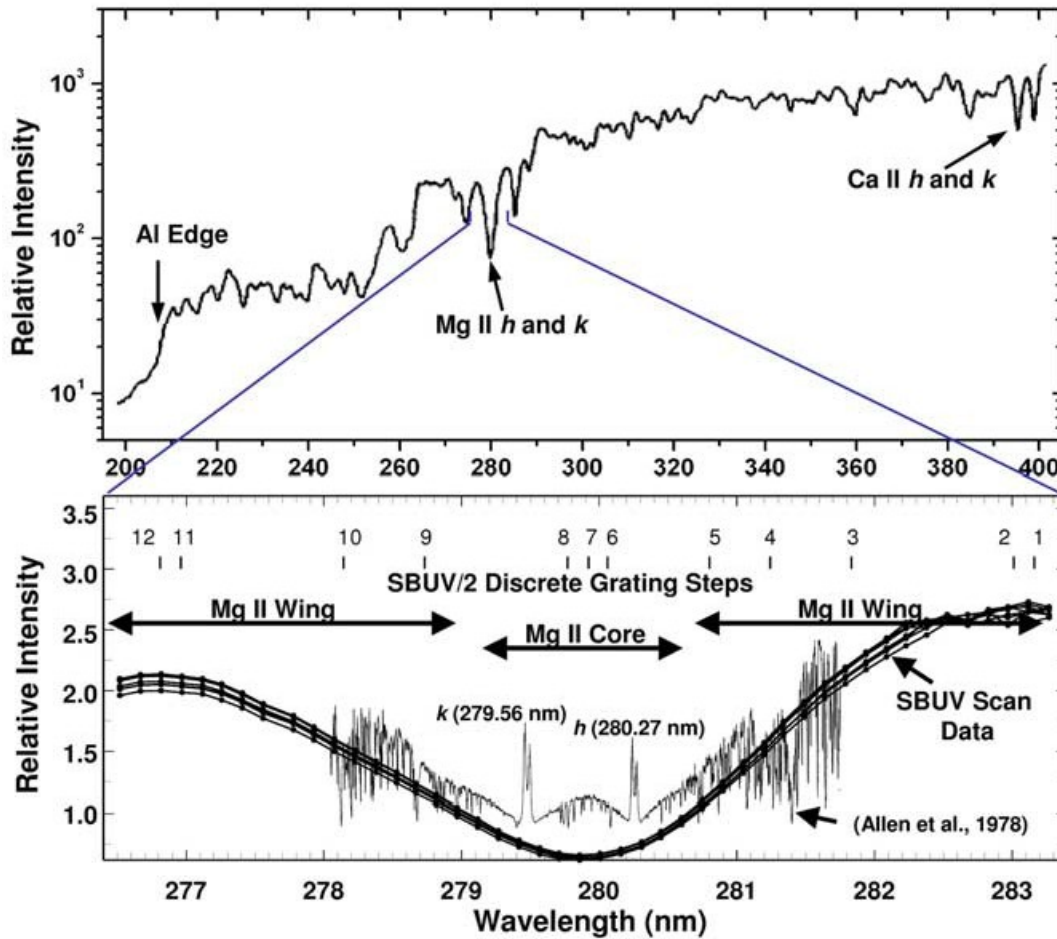


Figure (9): Mg II core and wing region (Vierrick et al., 2004)

The Mg II index is specified as the core-to-wing ratio, which is the ratio of the narrow core of the emission line to that of the wing of the broader absorption lines. The intensity of the core emission indicates the intensity of the temperature in the chromosphere and, therefore, varies during the solar maximum and minimum. The intensity of the absorption wing originating in the photosphere remains relatively stable from solar minimum to maximum, as the temperature of the photosphere is stable. Therefore, the Mg II index is an indicator of the UV solar or chromospheric activity (Vierrick et al. & Rühedi et al., 2004)(Shakeri, 2010). Figure (9) shows the solar UV spectrum near the Mg II absorption lines, from 250-400 nm measured by NOAA9 solar backscatter ultraviolet (SBUV)/2 instrument. In the bottom plot it is focused around Mg II, with several curves from low resolution SBUV scan that do not show the two h & k lines, and a high resolution curve that shows all the detailed absorption lines. The wing and core region which includes the two h & k lines are shown here (Vierrick et al. 2004).

A Mg II index composite time series is derived by putting together several data sets of SSI from various satellite instruments in different periods. The timeseries started in 1978 and continues until today as seen in figure (10). The solar cycles 21, 22, and 23 are shown clearly in this time series which only extends until 2004. The cycle 23 appears a bit smaller than the other two cycles, indicating less activity of the sun during that time. On top of the 11-year solar cycle signal, the apparent noise indicates the 27-day solar rotation signal. The solar rotation signals also have amplitudes near solar maximum, and show almost as large as the 11-year solar cycle amplitudes (Viereck et al., 2004).

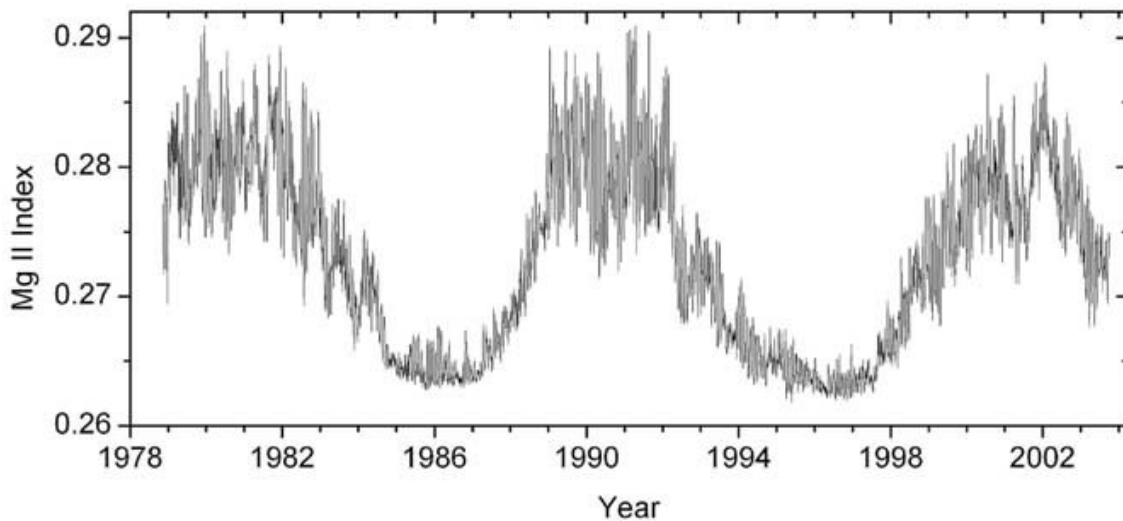


Figure (10): Timeseries of Mg II Index (Viereck et al., 2004)

Since this index is a core-to-wing ratio, and therefore does not change due to the optical instruments' degradations due to harmful UV radiations, it can be used as a proxy in the UV region.

Solar proxies are good indicators of solar activities and can serve as input parameters for solar models. As it was mentioned before, there exist no reliable longterm time series of SSI. Therefore it is attempted to construct SSI through solar models, where it is important to have reliable solar proxies for each region of the spectrum. There are several proxies available to represent solar activity. Some of the proxies used so far are the F10.7cm solar radio flux, Mg II 280 nm, Ca II 394 nm, He I 1083 nm, Lyman alpha, and sunspot numbers (Viereck et al., 2004) (Pagaran et al., 2009). It is also shown in figure (6) how they indicate the solar variation. Since the Mg II index has been shown to have the best correlation with SSI datasets in the UV spectrum, it is preferred over other proxies like F10.7 in this region (Viereck et al., 2001).

## 2-4 - Solar Models

Generally a model is a description of a system in terms of its dependable variables and components. In physics, models are represented through the mathematical language. Equations built up from several variables which describe the specific system of study. The variables can contain real life data sets obtained from measurements, which then the model would be named as empirical models. They can also consist out of abstract concepts (Snow et al., 2005).

There are generally two types of solar models, proxy models and physical models. Proxy models have single or multiple parameters and use proxies as their parameters. Physical models use physical components for the calculation of the solar spectrum and are often semi-empirical models (Fox, 2004). In this study only the single parameter proxy model of irradiance measurements is discussed which is presented as (Fox, 2004):

$$I(\lambda, t) = b \times X(\lambda_0, t) + I_0 \quad (1)$$

Here  $I(\lambda, t)$  is the irradiance as a function of a particular wavelength  $\lambda$  and time  $t$ ,  $I_0$  is a constant at a certain time,  $X(\lambda_0, t)$  is the proxy at a certain  $\lambda_0$ , and  $b$  is a scaling factor obtained from the regression to determine the proxy sensitivity (Fox, 2004).

In this study the correlations of the Mg II index and the SSI at various wavelengths are investigated. In the above equations  $X$  represents the Mg II index and the sensitivity is the ratio of variation of SSI over the variations of the Mg II index:

$$SSI_{\lambda}(t) = \frac{\Delta SSI_{\lambda}(t)}{\Delta Mg II(t)} \times Mg II(t) + c_{\lambda} \quad (2)$$

This equation holds true for each wavelength in the spectrum. Here  $c_{\lambda}$  is just a beginning point at a specific reference time. The desired parameter to be analyzed is the sensitivity parameter

$\frac{\Delta SSI_{\lambda}(t)}{\Delta Mg II(t)}$ . If this parameter is stable over time with little change, then it suggests the suitability of the proxy Mg II index as a UV SSI proxy.

# Chapter 3

## Instruments of SSI datasets

The SSI was measured by several instruments and by different techniques from the ground or from space. Reliable timeseries measurements are obtained from satellites on top of the atmosphere.

The SSI measurement data used here is obtained from SORCE SOLSTICE (2003-present), UARS SOLSTICE (1991-2001) and UARS SUSIM (1991-2005). These three instruments have the longest observational time spans compared to other solar measurements from space, along with the most consistent datasets. The two SOLSTICES cover mainly two of the recent solar minimums, and SUSIM covers in addition to the UARS SOLSTICE, a solar maximum time period. They cover up different time spans of maxima and minima years in order to have a thorough outlook over the entire 11 year solar cycle, as well as a good comparison between the obtained results from the instruments when the observational time overlaps. However all these satellite data have a measurement uncertainty of roughly 2%. In addition to that, the uncertainty rises up due to degradation in their operating optical systems specially in the UV region (Hill et al. & Tarrío et al., 2011). This uncertainty is considered throughout the analysis process in this thesis.

In the end, the data output of the model NRLSSI2 has been used as a final comparison. This comparison will provide information about the difference between the obtained results from the three instruments and the modeled data which has used the Mg II index as a proxy for its construction.

### 3-1- SORCE SOLSTICE

SORCE is a NASA- satellite launched in 2003 with the mission of measuring incoming x-ray, ultraviolet, visible, near-infrared, and total solar radiation. It measures the sun's output, mainly used for climate change studies, through several detectors, spectrometers, radiometers,... which are engineered inside instruments mounted aboard this satellite. SORCE carries four instruments TIM, SIM, XPS and SOLSTICE (NASA, 2016).

The SOLar STellar Irradiance Comparison Experiment (SOLSTICE) is an instrument aboard SORCE

satellite and operated from 25<sup>th</sup> of January 2003 until present, mainly in the UV region (115-320 nm) with a spectral resolution of 1 nm and an absolute accuracy of better than 5%. It is the second improved version of the same instrument, previously used on board UARS satellite. Its specifics are listed in Table (1) (McIntock et al. & Snow et al., 2005).

This instrument has two spectrometers covering different parts of the spectrum. In the end its dataset is split into two parts as well. Part A covers from 115 nm to 180 nm, and Part B covers from 180 nm to 310 nm (McIntock et al. & Snow et al., 2005).

Table (1) : SOLSTICE properties [<http://lasp.colorado.edu/home/sorce/instruments/>]

Instrument Type	Modified Monk-Gilleison spectrometers
Detector Type	photomultiplier tubes
Wavelength Range	115 – 310 nm
Resolution	1 nm
Absolute Accuracy	1.2-6%
Relative Accuracy	0.2-2.6%/year
Dimensions (H×W×D)	18.3 × 38.7 × 84.6 (×2) cm
Mass	36.0 kg (total)
Power	33.2 watts (total)
Nominal Data Rate	738 bps (total)
Field-of-View	1.5° × 1.5° (uncalculated) and 0.75° × 0.75° (calculated)

### 3-2- UARS SOLSTICE and SUSIM

UARS (Upper Atmosphere Research Satellite) is a satellite launched by NASA from 1991 to 2005 at 600 km altitude, in order to study earth's atmosphere. There are 10 instruments on board this satellite to observe and measure various components and variables regarding the atmosphere. This satellite measures ozone and related chemical species to the ozone layer, as well as winds and temperature in the stratosphere, along with the solar irradiance (UARS, 2016). The two instruments of interest here are SOLSTICE and SUSIM.

The first version of SOLSTICE on board UARS was operated from 1991 to 2001 by LASP laboratories. It has daily measurements of 1 nm resolution for the 120 to 410 nm wavelength region. It has an absolute accuracy of 5% and relative accuracy of 1%. It is a three channel spectrometer for both solar and stellar observations. The three overlapping channels are the G channel from 119 nm to 190 nm, the F channel from 170 to 320 nm, and the N channel from 280 nm to 420 nm. The channels are identical but with different mirror coating for better instrument sensitivity(SOLSTICE, 2016).

SUSIM (Solar Ultraviolet Spectral Irradiance Monitor) is a dual dispersion spectrometer instrument for measuring the UV wavelengths of 115-410 nm. It operated from 1991 to 2005. It has a daily resolution of 1 nm to 5 nm, and also a weekly resolution of 0.15 nm. The data used here has a resolution of 1 nm. It has an absolute accuracy of 6% and a relative accuracy of 2% (SUSIM, 2016).

### **3-3- Instrument degradation in the UV region**

Optical instruments operating in space suffer greatly from degradation in the UV region. At this wavelength region the high energy of the photons affect greatly the optical materials and environment. The adsorption of water and carbonaceous molecules in the vacuum environment on the optical surfaces and mirrors. This will damage the surface when the molecules undergo photon stimulated decompositions. Dissociation of water molecules causes oxidation of the surface, and decomposition of carbon molecules leads to carbon deposit on the surface of the optical materials, and results to blackening of the mirrors. This will cause for uncertainty in the final obtained data (Hill et al. & Tarrío et al., 2011).

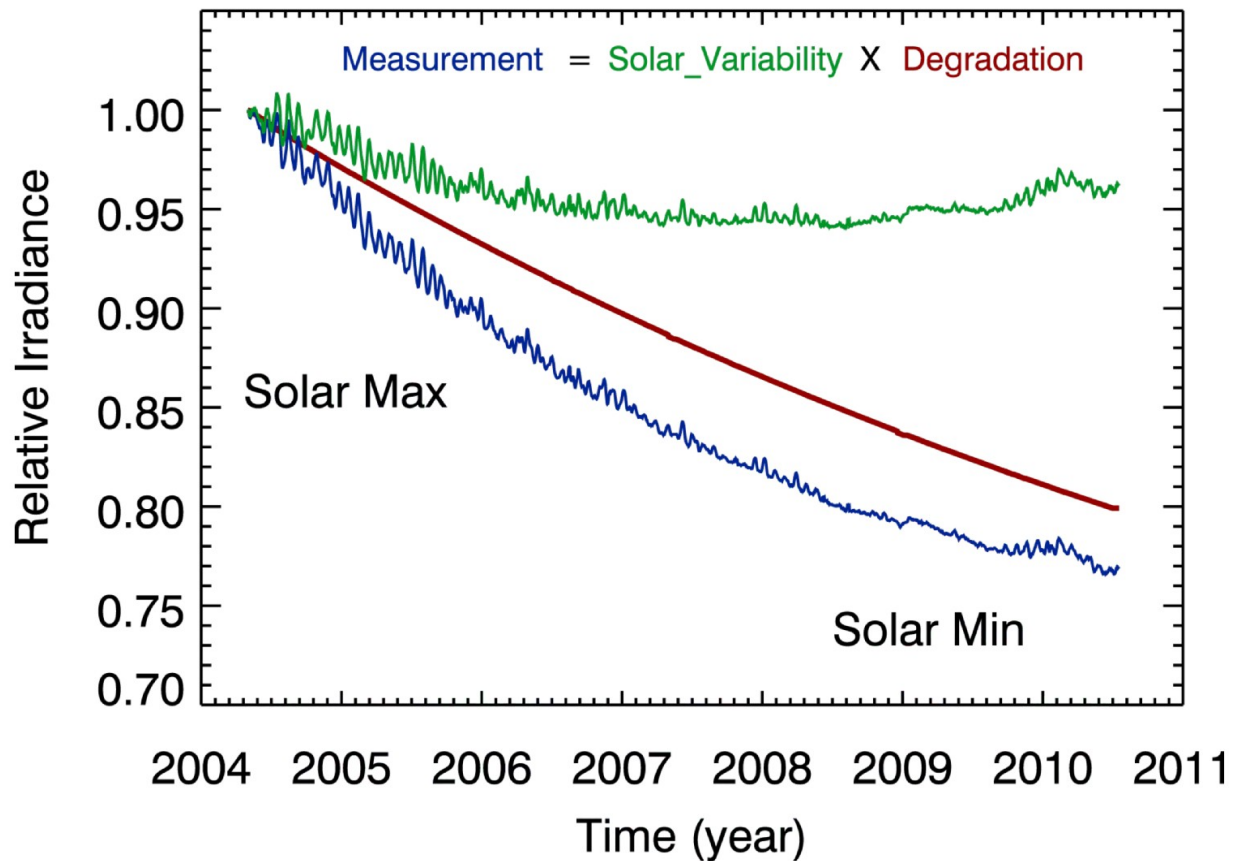


Figure (11): Effect of optical degradation [Woods, 2012] [<http://www.pages-igbp.org/download/docs/meeting-products/presentations/2012-1st-solar-forcing-wshop/woods.pdf>]

Since solar variation measurements are more important in the UV region, the uncertainty caused by degradation of the instruments has to be considered throughout the analysis. As it is seen in figure (11) obtained from the measurements of a similar instrument SIM, this degradation causes for more drift between measured data and the expected values, and so an increase of uncertainty which is more evident during the solar minimum years of the 11-year cycle.

There are several ways to reduce instruments degradation. One way is to control the exposure time on the optical materials. The UV radiation are measured for 1 minute and then exposure time is closed, in order to reduce stray light. One instrument measures daily, the other only once per month, and so it is possible to calibrate. Another way is to have a double spectrometer, but there is uncertainty in getting perfect alignment. Also a way is to calibrate with the UV stars which radiate constant UV radiation, compared to the sun which has high variability in the UV. But even with all these attempts to reducing

degradation, the problem is still not removed and there are uncertainties (Hill et al. & Tarrío et al., 2011).

As a way to reduce this uncertainty from the data is to detrend the data from the long term solar variations for the final analysis, and so reduce the long term effect of degradation.

### 3-4- Mg II index composite

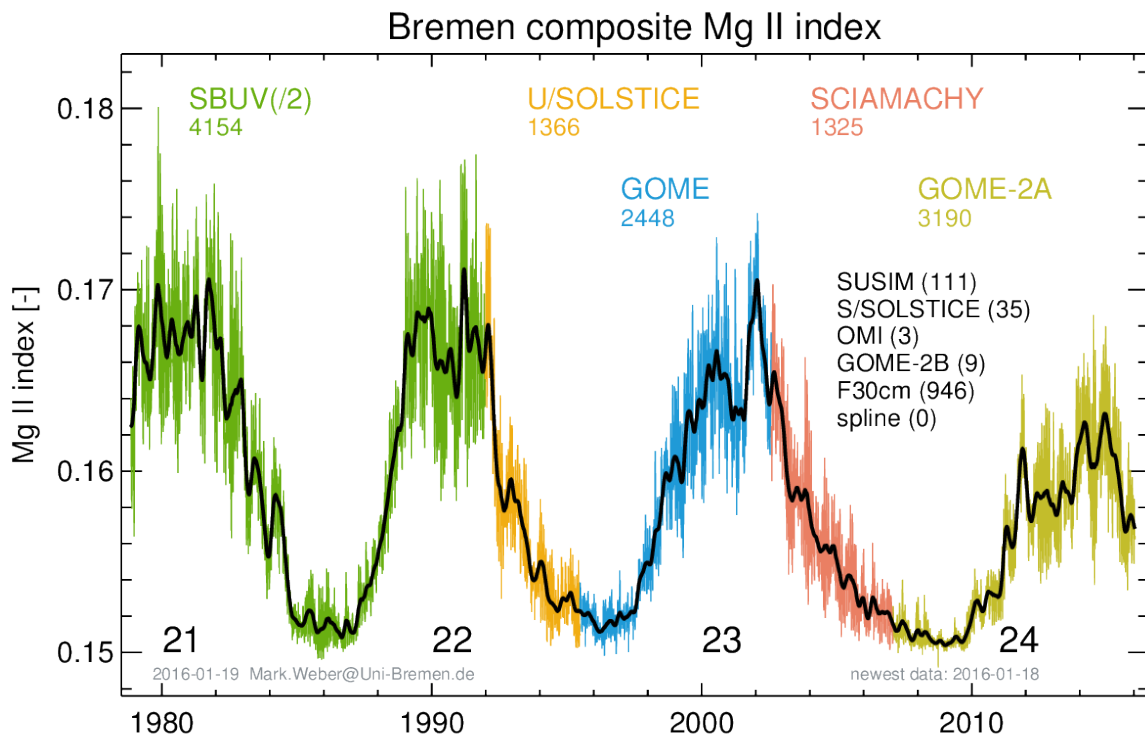


Figure (12): Mg II Index composite [<http://www.iup.uni-bremen.de/UVSAT/research/solarradiation>]

Figure (12) shows the composite of the Mg II index created at the University of Bremen. It is a construction of Mg II datasets obtained from different satellite data. The major contributions from the specific satellite are shown with the different colors. This time series covers the solar cycles 21 from 1978, until present, the solar cycle 24. The black line is smoothed data for twice the 27-days solar rotation cycle.

### 3-5- NRLSSI2

The NRLSSI2 is the second version of NRLSSI solar model developed by Dr. Judith Lean, and is being used as input to climate models in the current fifth IPCC report. SATIRE-S is another SSI model that provides reliable dataset for climate models (Ermolli et al., 2013). Compared to measured data, these models provide information over long time spans and the entire spectrum. Therefore it is used instead of measured data which cover only decades of observation times, along with a limited spectrum for each observation.

This model uses several proxies of sunspots and faculae brightening, including the Mg II index, in order to construct the entire spectrum of the solar irradiance from EUV to IR. It covers the wavelength range from 120 (nm) in the UV to 100000 (nm) in the infrared region. It has a binning resolution from 1 nm in the lower wavelengths, to 25 nm at higher wavelengths. It covers the time span from 1950 to the present with a daily output. At the same time with a monthly output it covers up to 1882 and annually since 1620 covering the Maunder minimum years (Lisirid, 2016).

The formulation used for this model, mainly in the UV, visible and near IR region, uses similar equation to equation (2) with additional terms for covering the spectrum (Lean et al., 2005).

$$I(\lambda, t) = I_{quiet}(\lambda) + \Delta I_{Faculae}(\lambda, t) + \Delta I_{spots}(\lambda, t) \quad (3)$$

The above equation shows in a simple form how this model is formulated. The solar irradiance is represented with  $I$  as a function of wavelength and time. The term  $I_{Faculae}$  includes faculae brightening and Mg II index time series. The  $I_{spots}$  term includes sunspot darkening for higher wavelengths. The  $I_{quiet}$  term represents quiet sun and serves as  $I_0$ , a reference value (Lean, 2012).

In the UV region NRLSSI, the previous version of the same model used mainly UARS SOLSTICE observation data for its derived SSI through a linear regression (Ermolli et al., 2013). For higher wavelengths above 220 nm, SUSIM SSI data is most compatible with NRLSSI data compared with SORCE SOLSTICE (Ermolli et al., 2013). But the NRLSSI2 uses SORCE SOLSTICE which is the improved second version of the same SOLSTICE instrument, as the main data set for its linear regression (Lean et al., 1997)(Lean, 2012).

# Chapter 4

## Method

### 4-1- Approach

This thesis is about determining how suitable the Mg II index is to be used as the input parameter in the solar model described in equation (2). Here SSI is a measured quantity that is dependent on time and wavelength, and therefore for each wavelength there exists a SSI time series that is related with this equation to the Mg II index time series. According to this equation, there should be a linear relationship between SSI and the Mg II index at each wavelength. Therefore obtaining the distribution of SSI against Mg II index is the first step of analysis.

In order to determine how well the changes in the Mg II index, corresponds to the changes in the SSI, a sensitivity analysis, has been performed in this thesis. For this purpose the correlation of Mg II dataset with a SSI dataset, measured from a specific satellite instrument is examined through a scatterplot. The distribution of the data will show visibly whether there exists good or poor correlation between the two datasets. Since the data sets have some gaps in time, they have been synchronized with the Mg II index at first, and so the missing data parts have not been considered during the analysis. Through a linear regression analysis of this dataset, and by determining the slope of the linear fit known as the sensitivity parameter along with the uncertainty of this linear fit and its Pearson's correlation coefficient, this analysis can be further investigated. In the end the sensitivity values have been converted to a solar cycle percentage value to have a more general and independent value from the type of Mg II composite that has been used. For further details and better analysis, both Mg II index and SSI data have been smoothed and detrended. Both data are smoothed over a 55 days cycle which is twice the 27 day cycles of the solar activities. Then the detrended time series is derived from the original timeseries minus the smoothed time series, where the 11 year solar cycle and long term instrument trends are eliminated. Here the effects of instrument degradation is reduced, which is a cause for inaccuracies in the final correlation.

This approach has been carried out for the UV spectrum of 115-300 nm. Three different datasets from the satellite instruments SORCE SOLSTICE, UARS SOLSTICE and UARS SUSIM have been

analyzed for further comparison, throughout different time decades. In this way the time spans from solar maxima and minima within 11- year cycle were covered by each dataset. In the end the obtained results from all three instruments is compared to the sensitivity of the modeled NRLSSI2 data. In order to show more details, only some of the results are shown for a low, middle and high wavelength in the UV spectrum as examples. 130, 205 and 300 nm, although there will be summary plots in the end for the entire spectrum. In this chapter the analysis is explained in details only for the specific wavelength of 205 nm from SORCE SOLSTICE.

#### 4-2- Correlation of Mg II index with SORCE SOLSTICE

The Mg II index composite created in the University of Bremen expands from year 1978 until present (Snow et al.,2014) is shown in figure (13). This data shows clear variations with the 11-year solar cycle and 27-day rotation. When averaging the daily data into monthly data the 11-year cycle signatures are even more clearly evident. The years 1980, 1991, 2002 are solar maximum years, while 1986, 1997, 2009 are solar minimum years.

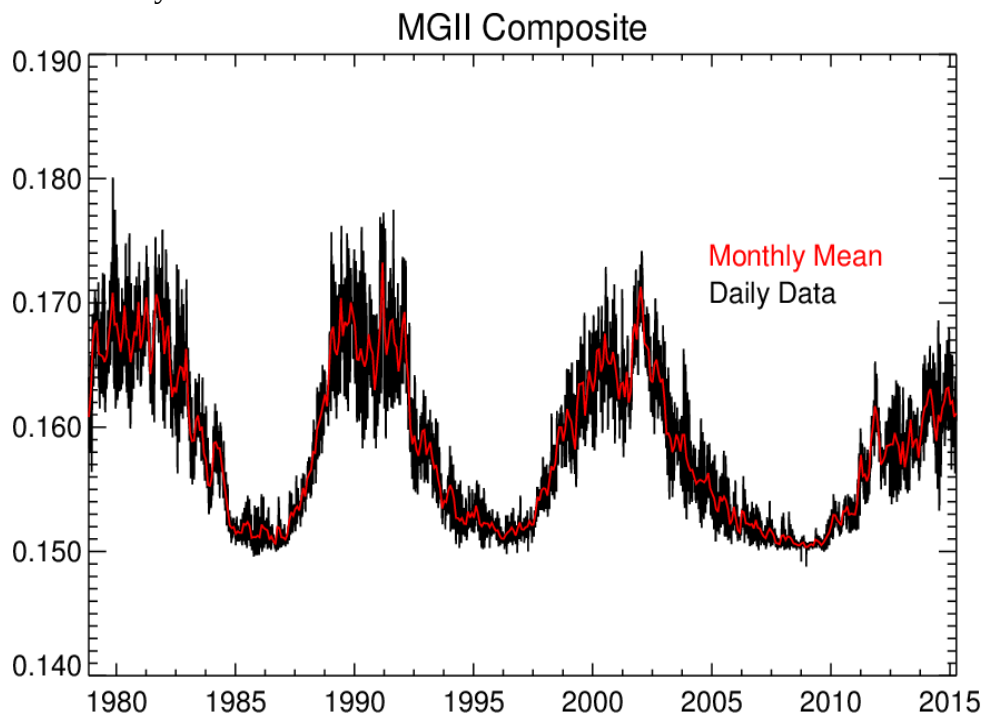


Figure (13): Mg II Composite as daily and monthly data

The SORCE SOLSTICE data set of SSI covers almost 10 years from 2003 until 2013. The time series for 205 nm is shown in figure (14). They cover the end of solar cycle 23 and the rise of solar cycle 24 after minimum in 2009. Also there is a peak in high activity by the end of 2011. The highest activity though, is observed in year 2004. This data set includes measurements for continuous wavelengths in two separate data sets from 115 nm to 179 nm and from 180 nm to 309 nm and is gridded for every 1 nm. The data has some gaps by the end of 2013.

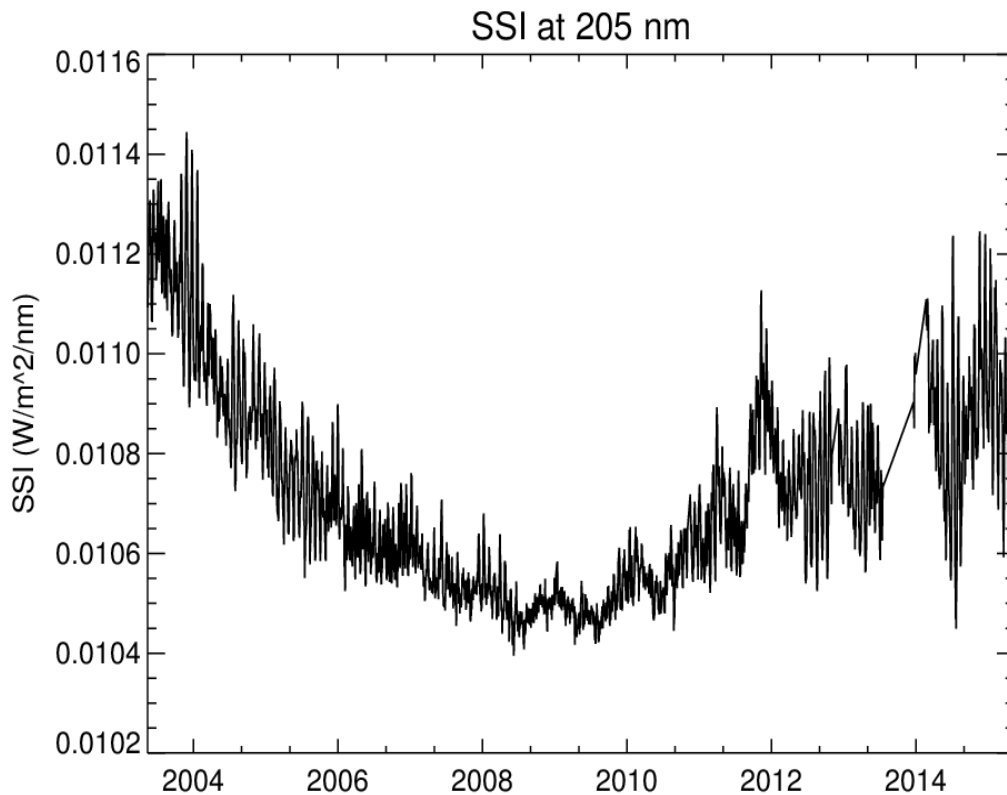


Figure (14): Daily SSI (W/m<sup>2</sup>/nm) from SORCE SOLSTICE at 205 nm

### 4-3- Sensitivity Analysis at 205 nm

The correlation of the SORCE SOLSTICE SSI at 205 nm with the Mg II index over the entire observation period is shown in Figure (15) along with its linear fit which is the red line. Through a scatter plot the correlation and dependency of the Mg II index and the SSI at a specific wavelength, which is now 205 nm, can be seen directly. In scatter plots usually the dependent variable is plotted on the x axis and the codependent variable on the y-axis. Since the Mg II index is considered

the stable variable, it is drawn on the x-axis, and the SSI data on the y-axis. In the scatter plots of this entire analysis, the x- axis will remain the same data set, and the y-axis changes for different wavelengths and instruments.

A positive correlation can be identified easily when the pattern of dots would slope from lower left to upper right. A distribution sloping downwards can be identified as negative correlation (Cleveland et al., 1993).

The scatter plot shows a firm spread cloud from the lower left up to the upper right, with a higher density at the lower left part. It shows a positive correlation with a high correlation coefficient of 0.813. This number would be much higher if the data cloud was not split in two. In this case both SSI and Mg II were not detrended (see discussion in next section).

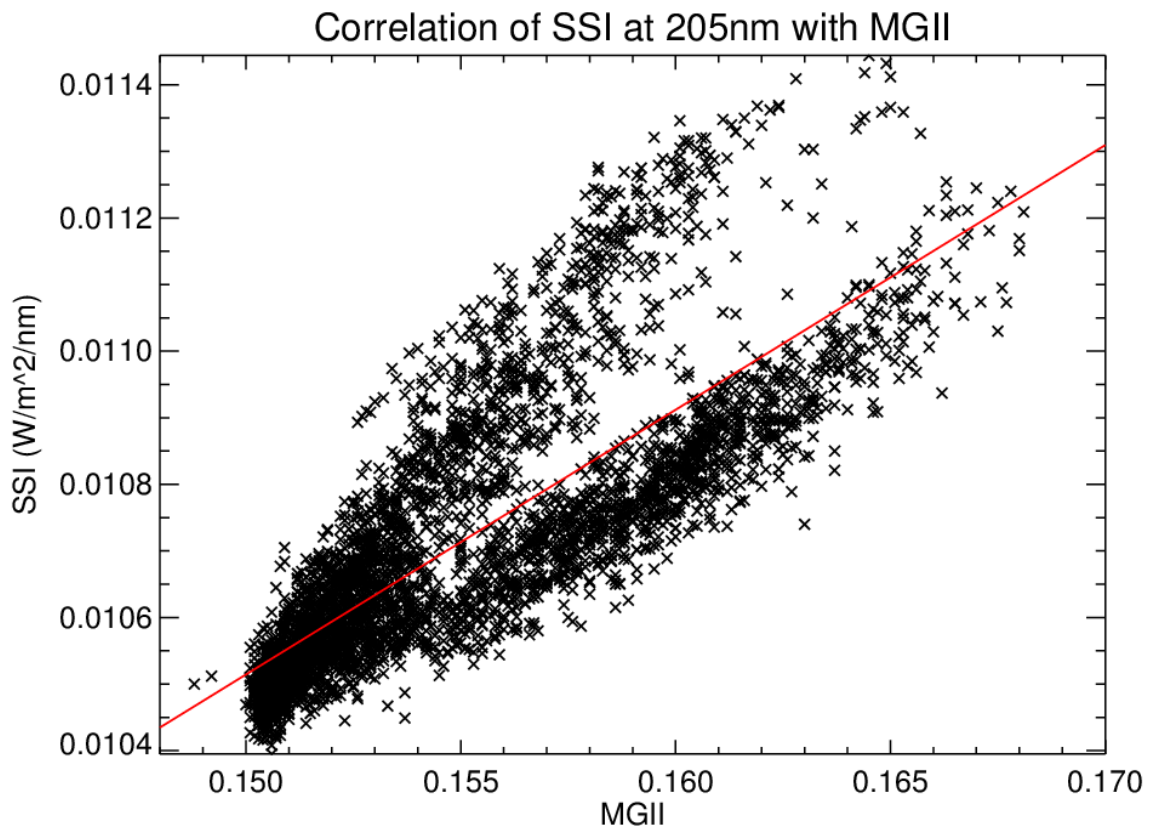


Figure (15): Scatter plot of SORCE SOLSTICE SSI data versus Mg II index at 205 nm

As an example of a very high correlation, the scatter plot for 280 nm is shown in figure (16). This distribution also shows a positive and very high correlation, as there is a very uniform distribution

along the fit line. This high correlation is expected, since this is the location of the Mg II doublet, from which the Mg II index composite has been obtained in the first place.

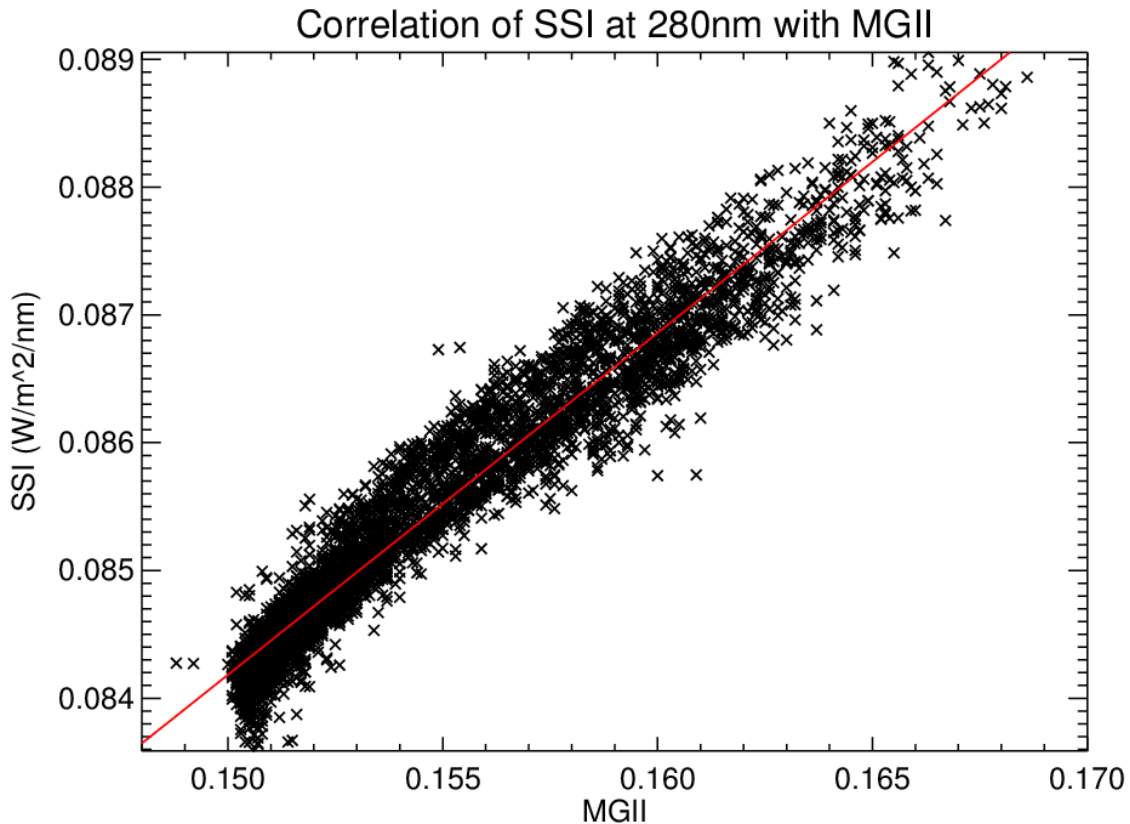


Figure (16): Scatter plot of SORCE SOLSTICE SSI data at 280 nm versus Mg II index

In order to examine this correlation in more details, the two data sets are separated into yearly data. Figure (17) shows the separated data and their corresponding linear fit with each color representing a different year. Now it is seen that the split of data is separated by years. There are higher values at the beginning years of the observation time span. They decrease with the passing years, reach the solar minimum year, and then increase again. This perfectly shows the change in intensity of the measured SSI with the solar 11-year cycle. But the values do not reach the same intensity as the previous years. This difference is due to instrument degradation. Since the instrument has been exposed to UV radiation in the space for a longer time, the measured data decreased, particularly in the early years.

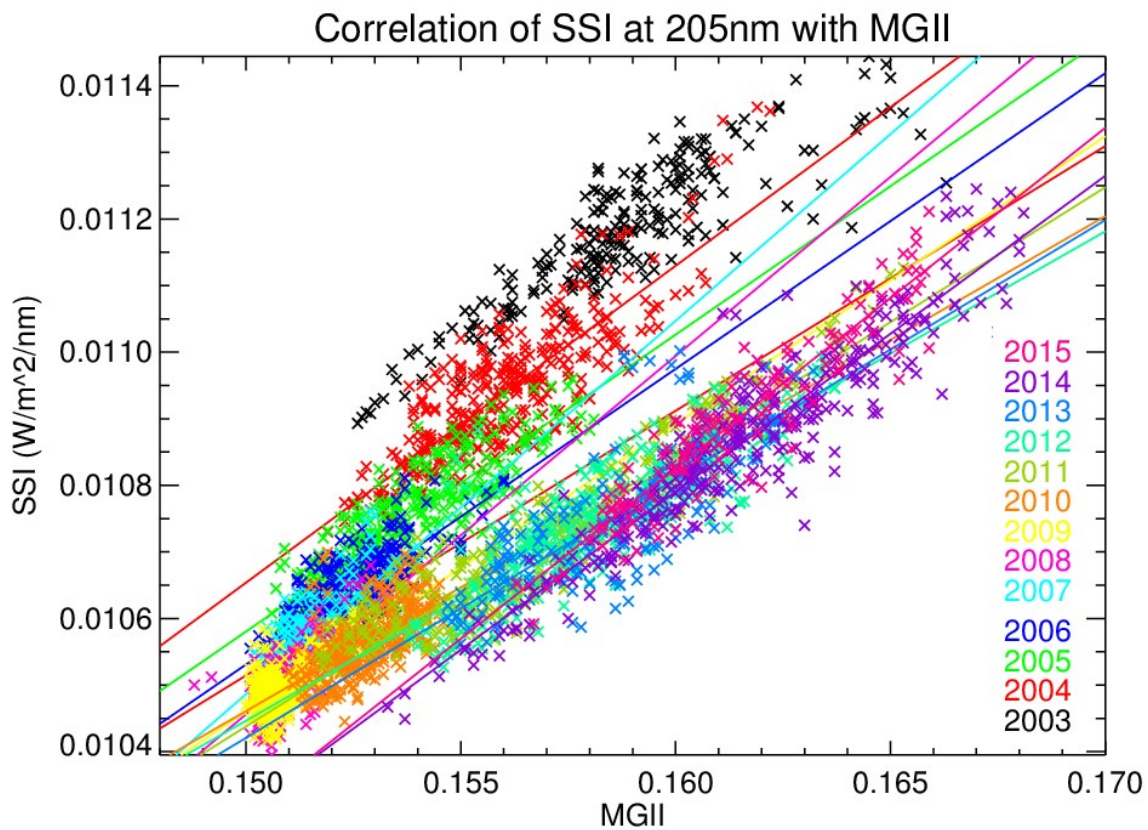


Figure (17): Correlation of SOLARcycle SSI at 205 (nm) with Mg II index separated in yearly data with their correspondent linear fit results.

The yearly correlation coefficients are plotted as a function of time in Figure (18). It is seen that the correlation decreases from 2003 until 2010 and is at its minimum in year 2010. These years are during solar minimum and therefore the correlation is weaker. In 2011 and 2012 there is significant increase in the correlation when the sun activity raises again. But in general most of the years have a high correlation of more than 0.5 which is a positive result.

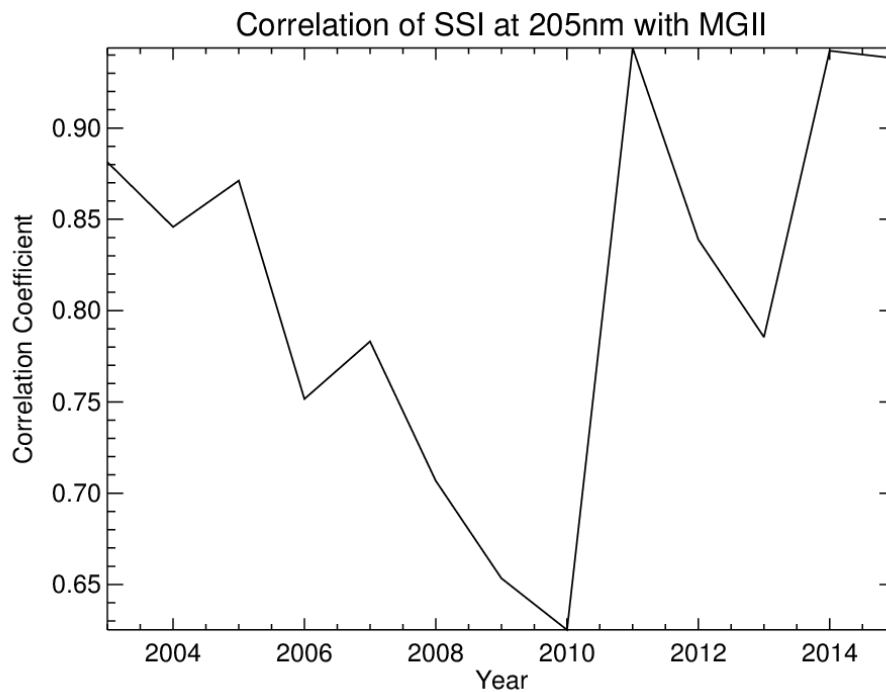


Figure (18): Correlation coefficients for each year of correlation of SORCE SOLSTICE SSI at 205 (nm) with Mg II index

As mentioned in section (2-4) about solar models, the slope of the linear fit represents the sensitivity of the solar proxy model. The slope of the lines along with their uncertainty, is plotted as a time series in figure (19). This has been done with the LINFIT function in IDL, and the error bars are obtained from the SIGMA of the same function of this linear fit as as 1-sigma uncertainty, which then has been plotted as 2 sigma uncertainty.

Here it is seen that the sensitivity values fluctuate around the overall mean value, shown as a blue line, over this time period. The fluctuations are 0.01 ( $W/m^2/nm$ ) from the mean value at most. And mainly within the range of its 2 times standard deviation shown with the dashed light blue line. It is also seen that when the fluctuations increase, the errors that are obtained from the  $2\sigma$  of the linear fits and are shown with the red error bars, also increase.

In fact from 2006 to 2010, which are close to solar minimum years, the sensitivity shows more variability and at the same time the errors are also high. This shows that during solar minimum the errors in the sensitivity are higher compared to solar maximum years, which is expected as the variation with the 27-day solar rotation is much weaker. During years 2004-2006 and 2011-2013, there is little change in the sensitivity, and at the same time smaller error bars are seen. During these times the sun activity is higher and therefore there are less errors. By the end of year 2013 and early 2014,

there is a lack of data, in the dataset. As there has been a battery problem for SORCE SOLSTICE leading to cooling the instrument and the degradation caused data problems. This part has been excluded for the analysis and has been synchronized with the Mg II index. Therefore the obtained sensitivity in this part does not include as many data points as the other years, and the increased value might not be quiet reliable.

As long as the error bars overlap with each other, it can be concluded that the changes are stable within their uncertainty. This does not seem to be the case at some points in this plot, where the changes are greater than the error's limits, and there seems to be greater fluctuations compared to their corresponding errors.

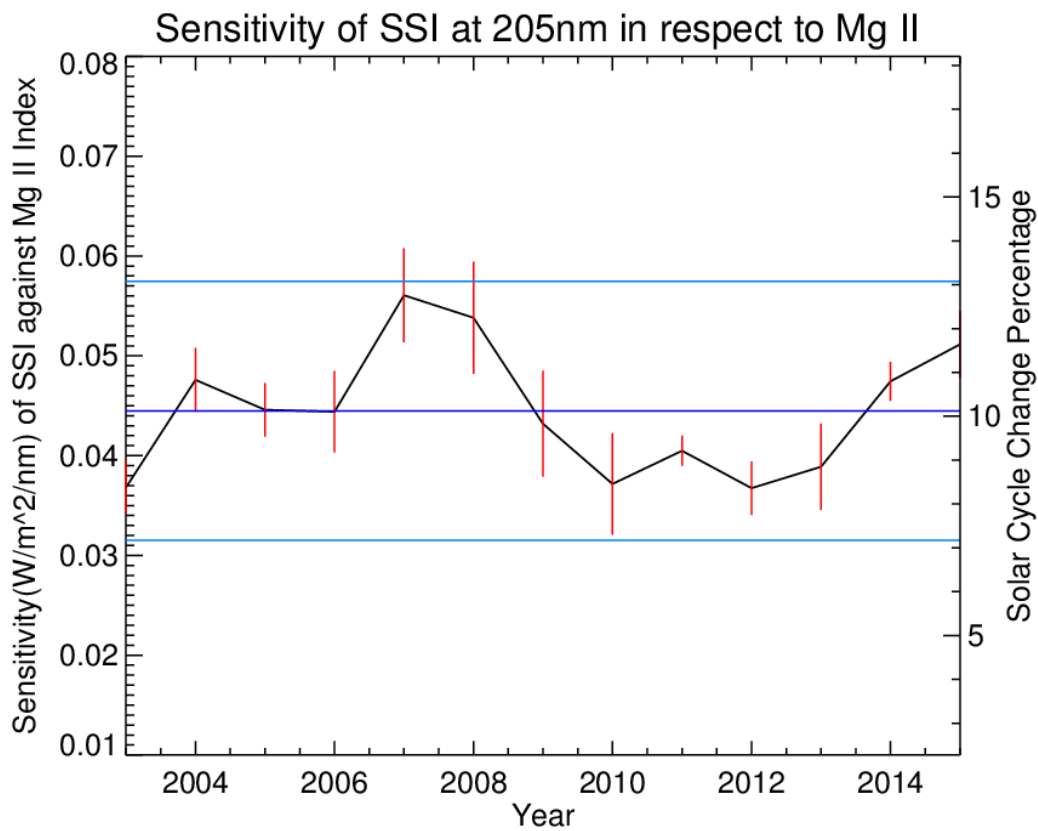


Figure (19): Sensitivity analysis of SORCE SOLSTICE SSI at 205 nm with respect to the Mg II index with their corresponding 2 sigma uncertainty of the linear fit. Blue line is the mean value over the years along with its 2 times standard deviation.

The values of proxy sensitivity are not very intuitive, since it is dependent on the Mg II index values. Since there are different Mg II index composites with different values, so the proxy sensitivity can

change according to which composite is being used. That's why a percentage number is more useful for comparisons. This solar cycle percentage is obtained by scaling the proxy sensitivity over the Mg II index values and therefore is not dependent on its value any longer. And so will provide a reliable quantity that is better to be used to compare for all the different data sets.

The percentage of change (of sensitivity) per solar cycle is calculated as follows:

$$\delta(\lambda, t) = \frac{\frac{\Delta SSI(\lambda, t)}{\overline{SSI_\lambda}}}{\frac{\Delta Mg II(t)}{[max(Mg II(t)) - min(Mg II(t))]}]} \times 100 \quad (4)$$

Here the sensitivity value is divided over the mean absolute value of SSI at each wavelength, and multiplied by the difference of the maximum and the minimum value of the Mg II index during a specific solar cycle. The extreme values for the Mg II index are scaled from the solar cycle 22-23 from 1993.12 to 2002.12.

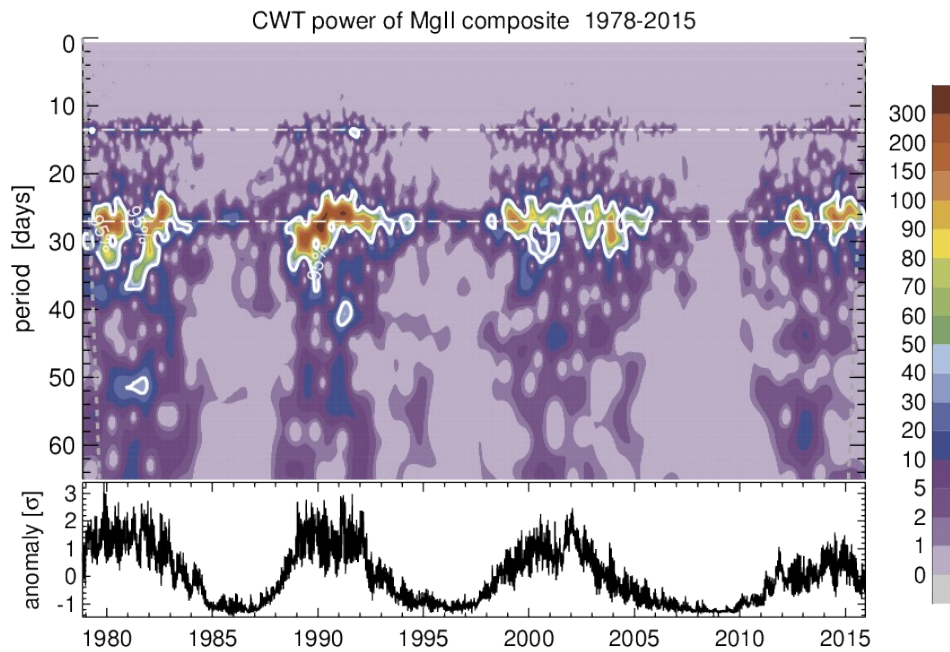
The right side of y-axis in figure (19) shows the same diagram as the sensitivity plot with the values of the solar cycle variability in percent. There is a minimum expected solar cycle change of almost 8% in years 2003 and 2012, and a maximum of almost 13% in 2007. Showing 5% variation over the entire observation period.

#### 4-4 - Detrending data

Usually in a time series there is some gradual change in some of its properties, which can be stated as a trend. Trends can be considered as long term changes and fluctuations over the mean in the time series. Detrending is the mathematical process to remove the trend in the time series. It is usually used to remove the distortion from the desired parameter of study. It is also used as a preprocessing step to prepare the time series for analysis in methods that assume stationarity and stability (Mecko, 2015). The detrending process can be done in several ways. One common way is to use a smoothing function. By smoothing with a desired parameter of variability and then subtracting it from the original data, a detrended data set for the parameter of interest will remain without all the unnecessary distortions.

The SSI time series proxy model is a linear equation, therefore taking away the trend from its variable results in dealing with a stationary process with less inaccuracies. In the UV region, optical instruments in space suffer from degradation due to high level of energy of the photons, which results to higher uncertainty in the final achieved data. Therefore removing longterm trends of the data, also results to reducing the effect of instrumental degradation, and so reducing the uncertainty levels.

Detrending the SSI data over the 27 days cycle, removes the longterm trends in the dataset. The corrected signal will indicate the short term solar variability visibly. Although now the data shows the short term 27 day cycles, they are superimposed on the long term 11 year cycles (Lean et al., 1997). The 11 year solar cycles leave their impact on the rotational cycles, and therefore during the solar minimum years, the rotational cycles are also weaker in signal. Studies suggest a linear correlation between the 11 year cycles and the 27 days cycles. Figure (20) shows the continuous wave transformation power spectrum of the Mg II index focused on the solar rotation cycles. It is visible here that during solar maximum years, the intensity of Mg II index also increases on the 27 days periods. Therefore, even though the long term effect have be reduced, there is still information available about the long term solar cycle, by solely examining the short term cycles.



Figure(20): Continuous wave transformation power spectrum of the Bremen Mg II composite index, [courtesy of M. Weber]

Both Mg II index data and the same SSI dataset have been smoothed over 55 days which covers two times the 27 days cycle. For this purpose the SMOOTH function in IDL has been used with the width parameter of 55 and \EDGE\_TRUNCATE option to apply for all data points. Then subtracting the smoothed time series from the original, will result to a time series showing dominantly the 27-days rotational solar cycles. As seen in figure (21), in the new detrended time series, the 11-year solar cycle signature is removed.

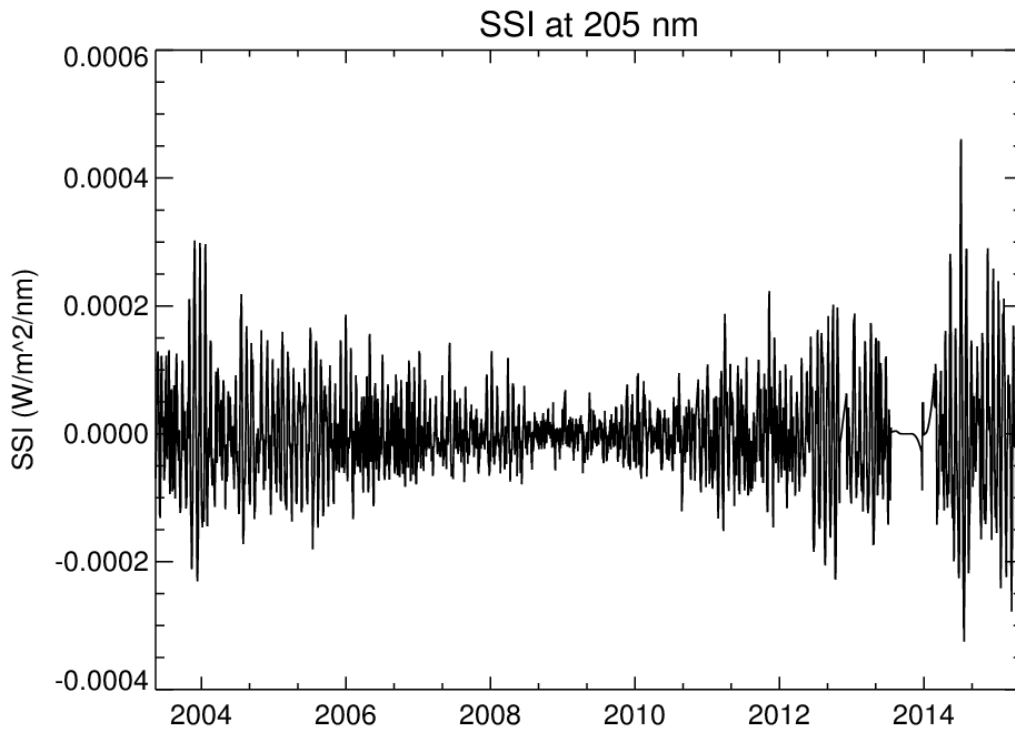


Figure (21): Detrended SSI data from SORCE SOLSTICE over 55 days at 205 (nm)

Now proceeding with the same approach in the analysis, the distribution of SSI against the Mg II index is shown in plot (22) for each year. It is now seen that there is uniform distribution, without the split in the data as was seen before. Now the long term degradation effects of the instrument is no longer visible, which was seen through the split of the data in the previous plot (17). This proves that by removing the long term cycles, also the long term degradation effects of the instrument on the data, has been removed.

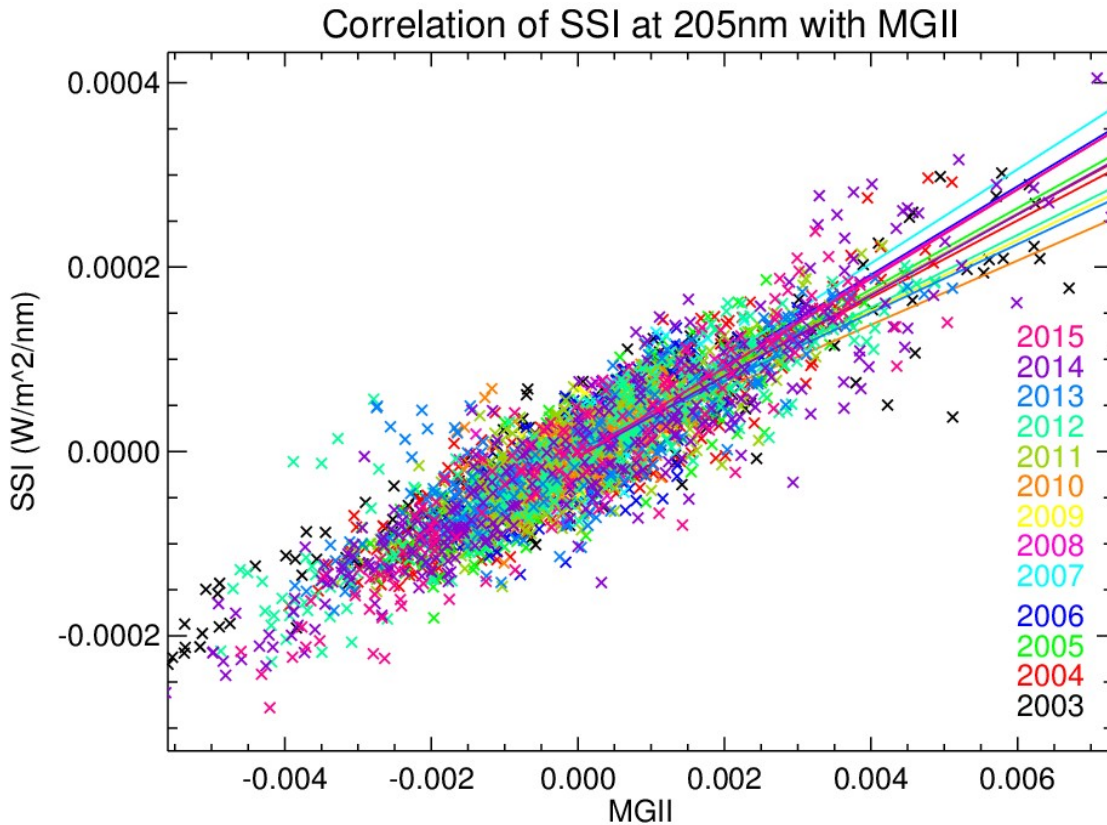


Figure (22): Correlation of SOLAR SOLSTICE SSI at 205 nm with Mg II index separated in yearly data with their correspondent linear fit results.

The obtained sensitivity of each year is shown in figure (23). It is seen that now the sensitivity fluctuates less around its mean value, and the difference of the values from the maximum until the minimum is reduced compared to the data without detrending. Now the errorbars seem to cover up more of the fluctuations over the mean value, and most importantly the 2 sigma errorbars overlap with each other. Still the pattern, more change with higher error bars, is present during the solar minimum years. With this plot it is more evident to see the stability of the sensitivity within its error bars. But as discussed before, during solar minimum years the stability decreases and there are a few years exception like in 2009 and 2011, that can not be considered as stable.

The percentage of the solar cycle change shown on the right side of the y-axis, now has a maximum at around 11% and a minimum at 8 %, which makes a difference of nearly 3.5% instead of the previous 5%.

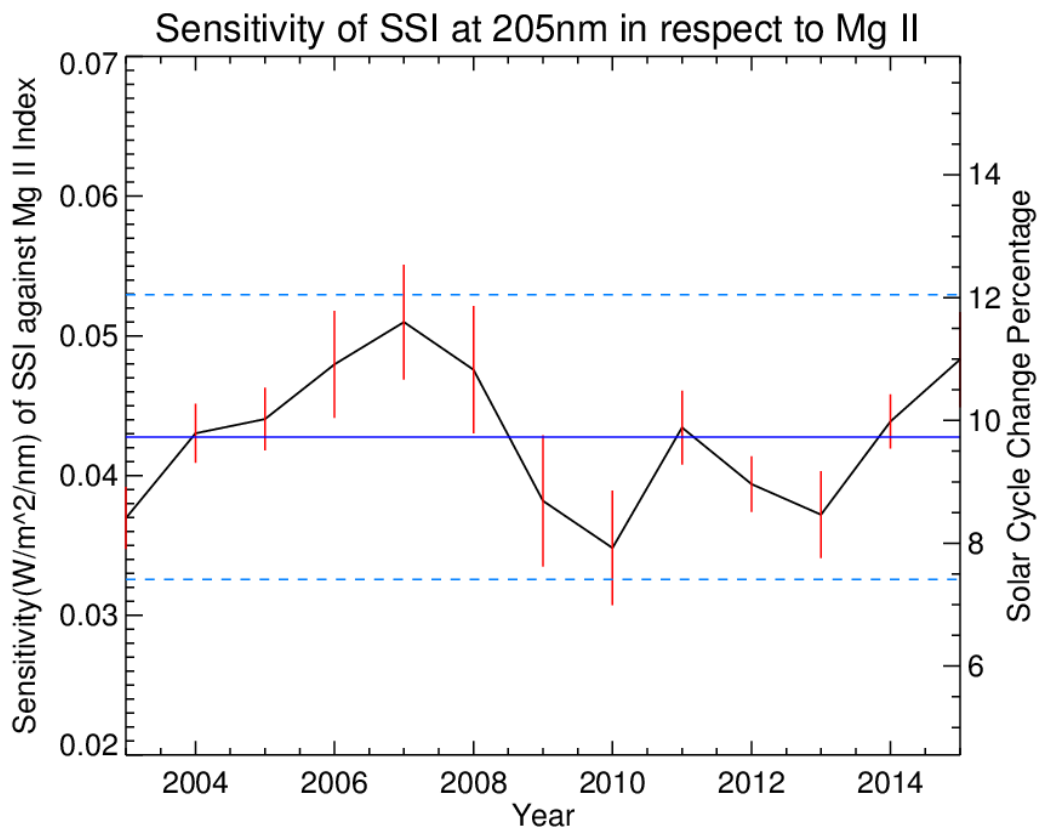


Figure (23): Sensitivity analysis of detrended SORCE SOLSTICE SSI at 205 nm with respect to the Mg II index with their corresponding 2 sigma uncertainty of the linear fit. Blue line is the mean value over the years along with its 2 times standard deviation.

The comparison for the correlation coefficient shown in figure (24) demonstrates that the correlation between SSI and Mg II is generally higher when using detrended data. The minimum correlation has shifted to 2009, which is closer to the peak in solar minimum years following the solar cycle 23.

The results of detrending both data before analysis, indicate less change of values and better stability than what was previously calculated before detrending the data. Therefore, in the continuing analysis for other wavelengths and instruments only detrended data will be used hence forward.

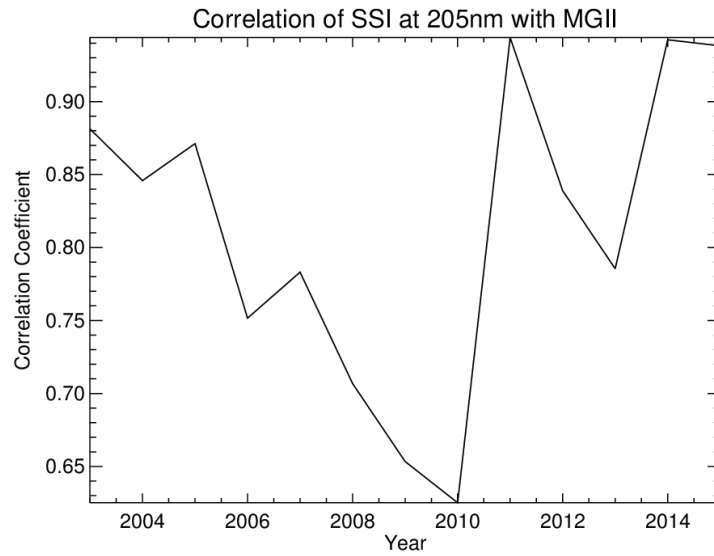
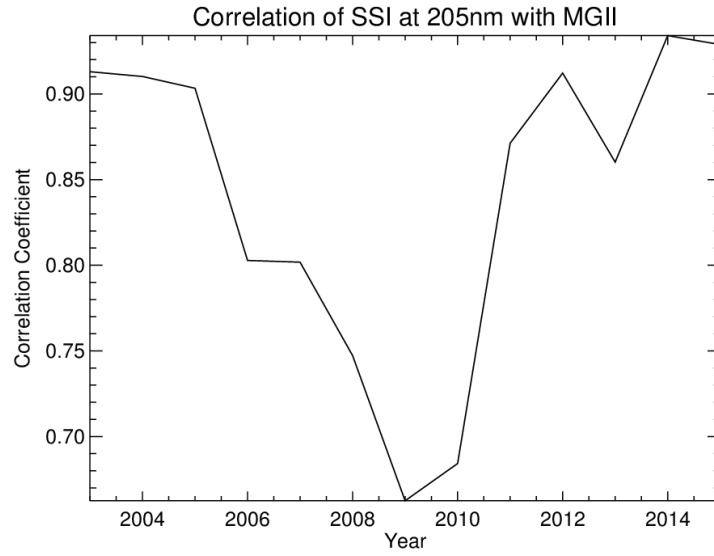


Figure (24): Comparison of correlation coefficients for each year of correlation of detrended SORCE SOLSTICE SSI (top) and undetrended (bottom) at 205 (nm) with Mg II index

# Chapter 5

## Results

This chapter continues the analysis approach, discussed in the previous chapter for all wavelengths in the UV from the dataset SORCE SOLSTICE (2003-2015). Afterwards, the same analysis is done for the other two instruments UARS SOLSTICE (1991-2001) and UARS SUSIM (1991-2005). The sensitivity is discussed for the chosen wavelengths of 130, 205 and 300, and compared between the three instruments. Then summary plots provide information about the whole UV region. In the end the results are compared with the NRLSSI2 model. This comparison will provide information about the difference between the obtained results from the three instruments and the modeled data which has also used the Mg II index as a proxy for its construction. It will be seen how well the results agree, and so give a better view of the suitability of the Mg II index being used in the models.

### 5-1- SORCE SOLSTICE

#### 5-1-1- Analysis at 130 nm and 300 nm

As a representative of the lower wavelengths, 130 nm, and for higher wavelengths, 300nm, has been chosen. The same analysis described in the previous chapter will be performed for both wavelengths in order to compare the changes dependent on wavelength. As discussed before only detrended data are used for analysis.

The scatter plot shows a very firmly spread cloud from the lower left up to the upper right for SORCE SOLSTICE at 130 nm (see Figure (25)). It shows a positive correlation with very good correlation.

The yearly correlation coefficients (Figure (26)) show that the correlation decreases from 2003 until 2009 and is at its minimum in year 2009, during solar minimum. In 2011 and 2012 there is significant increase in the correlation as the activity in the sun increases. In general the years have a high correlation of above 0.5.

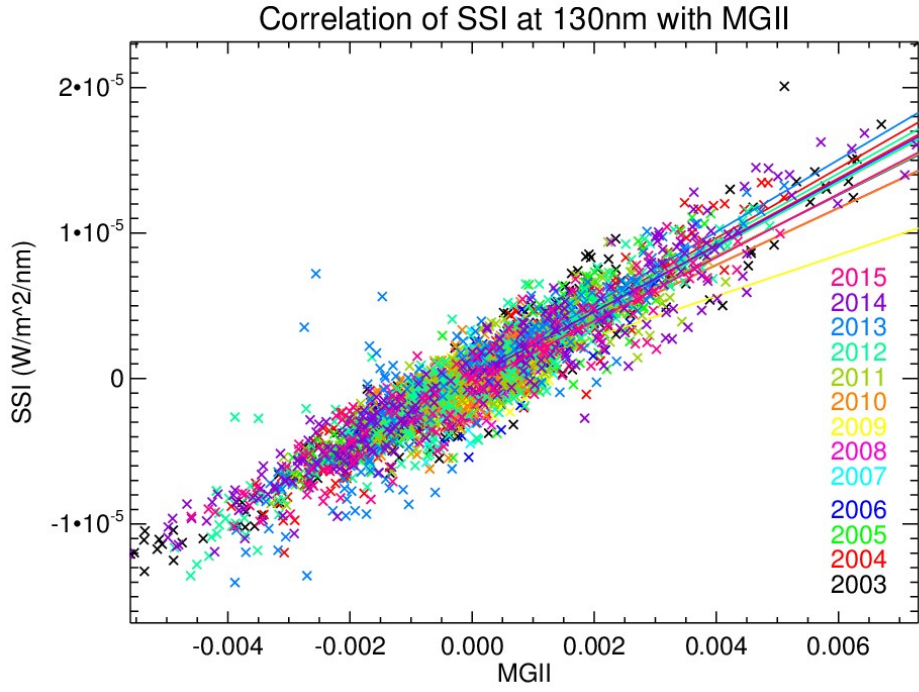


Figure (25): Correlation of SOLSTICE SSI at 130 nm with Mg II index separated in yearly data with their correspondent linear fit results.

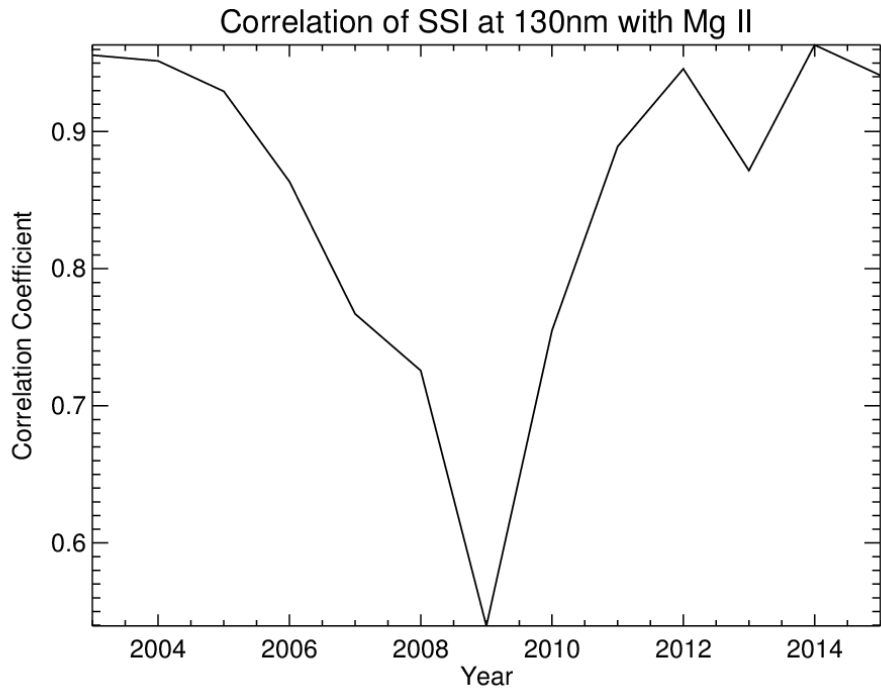


Figure (26): Annual timeseries of correlation coefficients of SOLSTICE SSI at 130 nm with Mg II index

The sensitivity plot in figure (27) shows high stability with time with low error bars. Except for the solar minimum year 2009, with comparably higher errors, the year-to-year can be seen as stable, and are within  $\pm 0.0003$  ( $\text{W}/\text{m}^2/\text{nm}$ ). The variations also remain very good within the error bars region's overlap and also the standard deviation limit except at the minimum peak. If the solar minimum peak year would not be considered then, this plot shows high reliability of the proxy at this low wavelength. The minimum solar cycle change is around 22% and maximum at 36%. There is a quite high spread of about 15 % in general, but excluding the minimum peak in year 2009, the spread reduces to about 5 %. Although the values for sensitivity are very low, there is high percentage of solar cycle change in this low wavelength region. This indicates the higher importance of sensitivity at lower wavelengths, since the relative changes are higher.

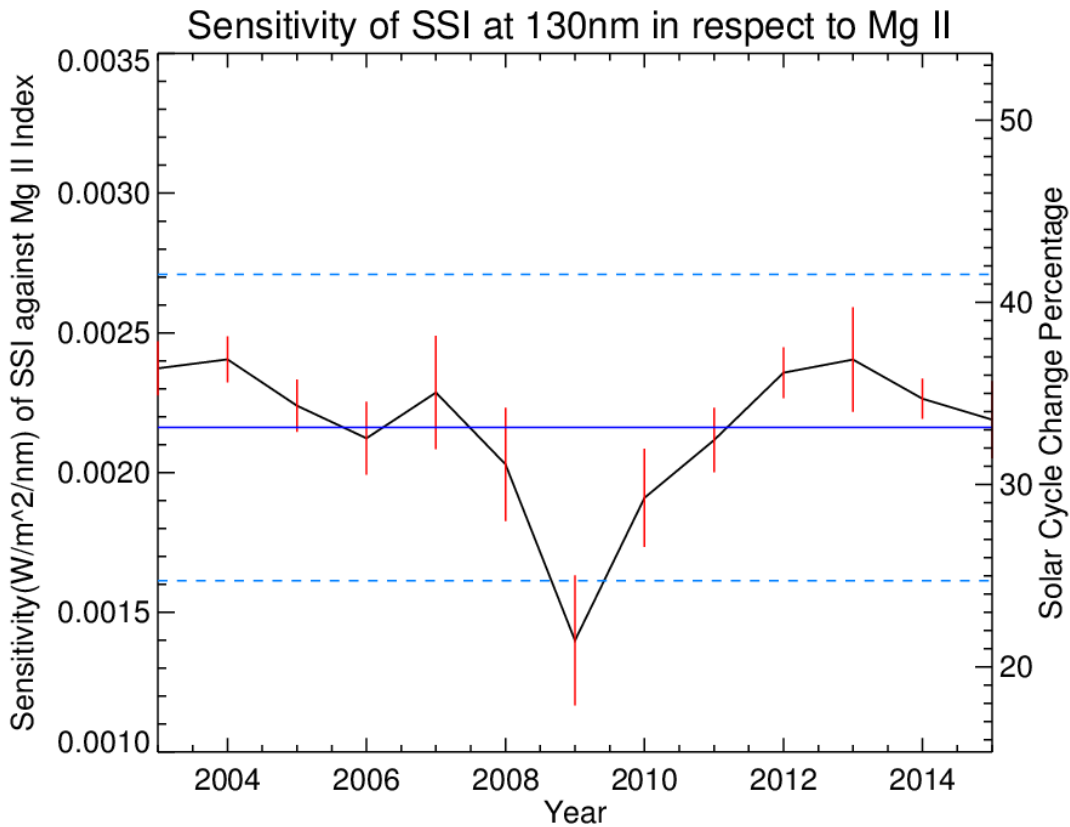


Figure (27): Sensitivity analysis of SOLAR SOLSTICE SSI at 130 nm with respect to the Mg II index with their corresponding 2 sigma uncertainty of the linear fit. Blue line is the mean value over the years along with its 2 times standard deviation.

The same analysis process is repeated at a higher wavelength at 300 nm. Its scatterplot (see figure (29)) shows clearly a widely spread cloud with less uniform distribution. It shows very low correlations.

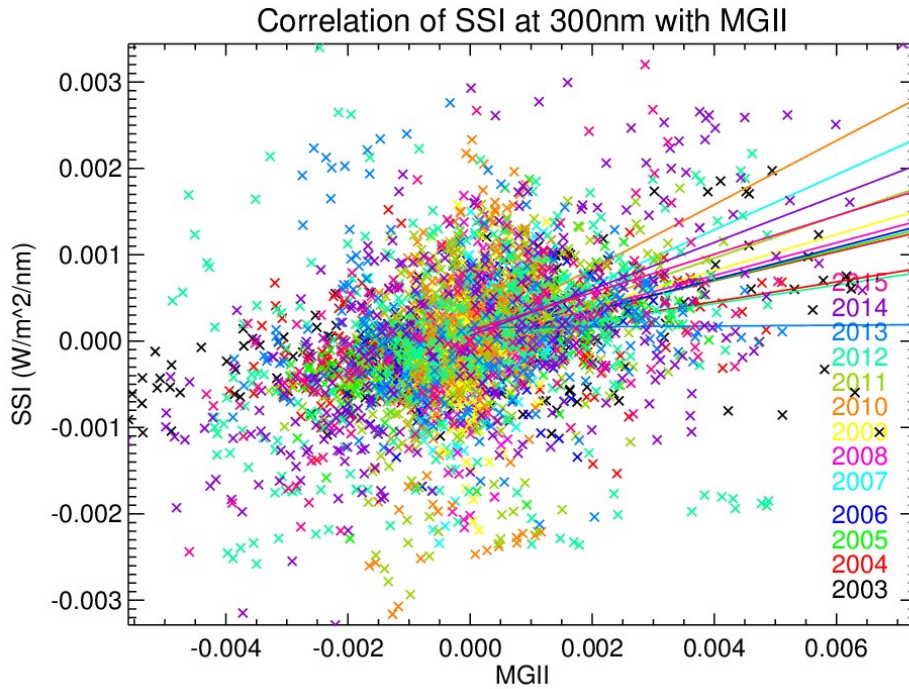


Figure (29): Correlation of SOLAR SOLSTICE SSI at 300 (nm) with Mg II index separated in yearly data with their correspondent linear fit results.

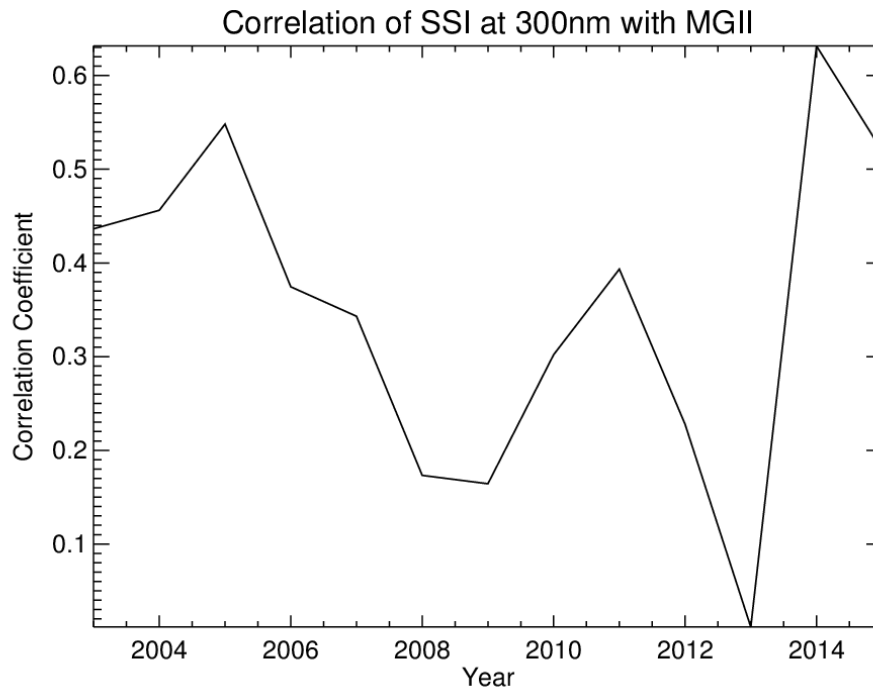


Figure (30): Annual timeseries of correlation coefficients of SOLAR SOLSTICE SSI at 205 nm with Mg II index

The timeseries of rather low correlation coefficients are shown in figure (30). In year 2013 there is very low correlation, which is also effected by the data gap at that specific year.

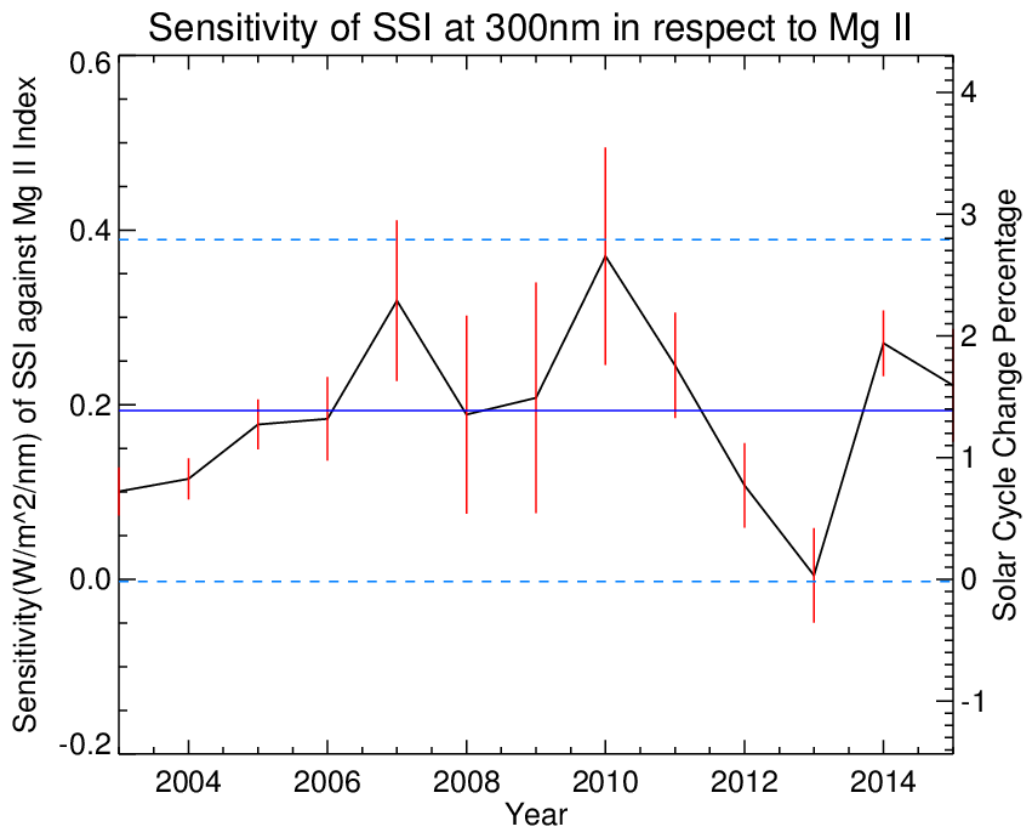


Figure (31): Sensitivity analysis of SORCE SOLSTICE SSI at 300 nm with respect to the Mg II index with their corresponding 2 sigma uncertainty of the linear fit. Blue line is the mean value over the years along with its 2 times standard deviation

The sensitivity diagram shows high fluctuations with large error bars which do not always overlap from their previous points. It shows quite well stability, considering the large error bars, during the solar minimum years. But from 2010 to 2013 there is a drop in sensitivity and the error bars are quite small and so do not overlap with each other. At these points it can no longer be stated that the proxy sensitivity is stable with time.

The solar cycle percentages on the other hand are very low, generally below 2.7%. This is because the sensitivity values were very large, therefore even though there is high change, the percentage remains low. As it was shown previously in figure (5), the TSI varies only 0.1% for wavelengths above near UV

(300 nm), and so where the SSI values peak the changes are small. This low variability change is also seen here. But the lower wavelengths where the SSI absolute values are very low, the variability in the absolute values contribute also very little to TSI changes.

At these higher wavelengths, there are more parameters that play a role and have to be considered in the linear regression in order to achieve better compatibility. Sunspot darkening is one additional parameter that plays an important role at higher wavelengths above approximately 240 nm (Pagaran et al., 2011). Therefore the Mg II index proxy alone is not very suitable for this wavelength region.

### **5-1-2- General Outlook over all Wavelengths**

For a general outlook on the whole UV spectrum, the sensitivities and correlation coefficients for all of wavelengths are plotted in 3D to see its relation to both time and wavelength at the same time.

The sensitivity plot in figure (32) shows very good stability throughout all wavelengths up to 250 nm, then at higher wavelengths there are more fluctuations evident. Throughout the years the sensitivity seems relatively stable in general. At 120 nm there is an expected high peak in proxy sensitivity value, the Lyman-alpha wavelength, which is also often used as a proxy. The same is apparent at 280 nm, which is the peak for Mg II wavelength.

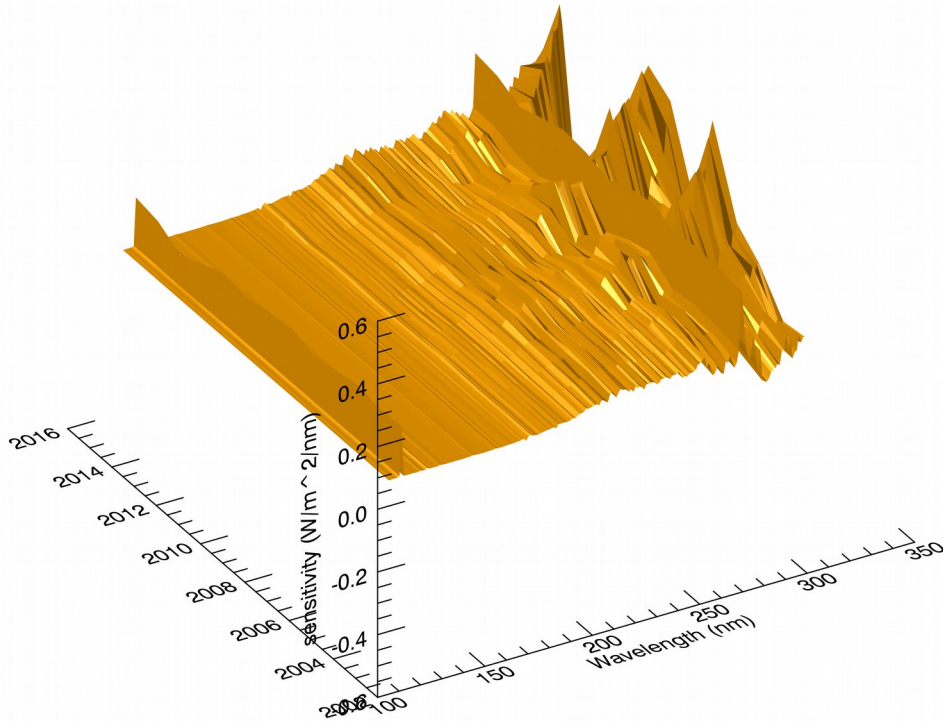


Figure (32): Sensitivity of SORCE SOLSTICE SSI with respect to the Mg II index in the UV

Figure (33) shows very high correlation coefficients for lower wavelengths, and as the wavelength increases the coefficient drops down significantly. For the time dependency, there are lower values around 2008 and 2009 during solar minimum. The lower peak around 2013, is mainly due to lack of SSI data. For wavelength dependency, there are very high correlation coefficients at lower wavelengths, and from around 250 nm the decrease is visible, until very low values are reached at 300 nm. At 280 nm there is a sudden high correlation, which is the wavelength for the Mg II index as expected.

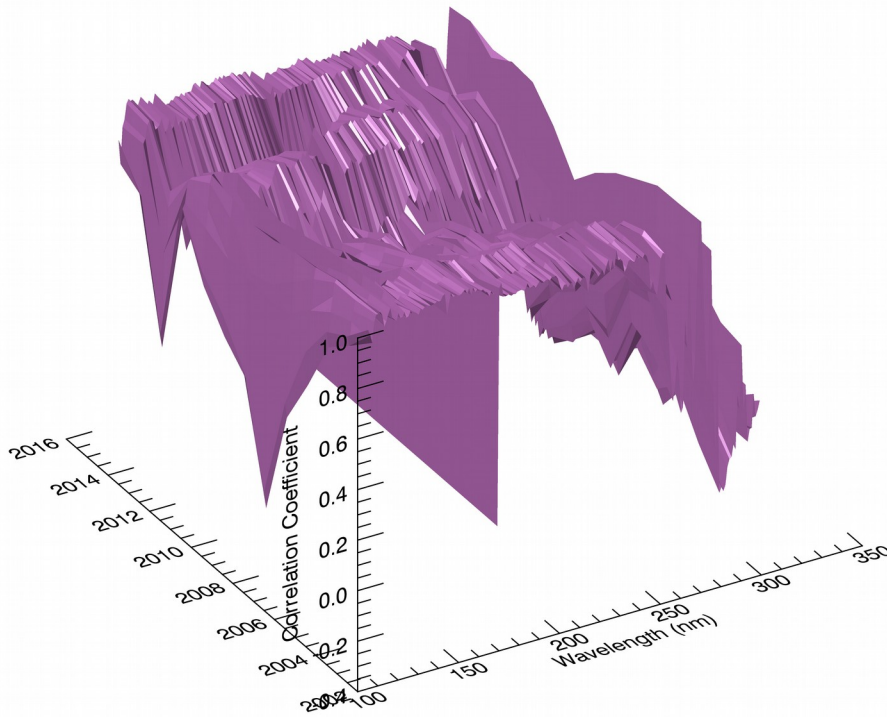


Figure (33): Correlation coefficients of SORCE SOLSTICE SSI with Mg II index in the UV as a function of wavelength and year

In order to examine the wavelength dependency of the sensitivity, its mean value is calculated for each year along with its standard deviation, and then plotted as a function of wavelength is shown in figure (34). It is seen that there are generally low proxy sensitivity in absolute units at lower wavelengths. They increase above around 250 nm, and at the same time the uncertainties strongly increase as well. The two peaks of Lyman-alpha and Mg II are clearly visible here as well. Here the sensitivity can be seen as very stable for the lower wavelengths, but since the values are very low, no firm judgment can be concluded from this plot. Therefore it is better to see the solar cycle percentage plot for these low values in order to be able to come to a better conclusion.

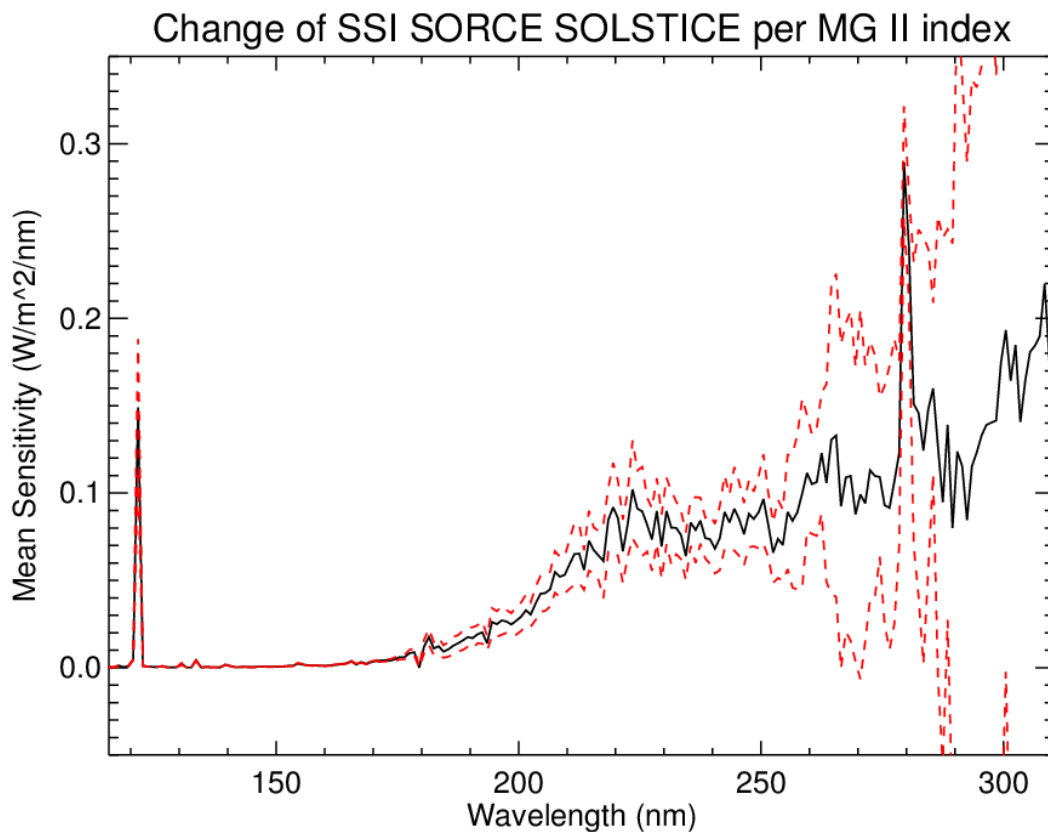


Figure (34): Mean sensitivity for SOLSTICE SSI with respect to Mg II index over the years in the UV spectrum, with 2 sigma standard deviation.

Similar to the previous sensitivity plot, the solar cycle percentage is also averaged over the years to see its wavelength dependency and uncertainty in figure (35). Now the changes in lower wavelengths are visible. There is high percentage change at lower wavelengths below 150 nm, then the changes keep decreasing, and from 200 nm onwards the changes become very low. Therefore at the higher wavelengths the percentage plot does not provide much information for this analysis. The minimum peak at 180 nm is due to the boundary between the two SOLSTICE A and B spectrometer datasets. This plot indicates the importance of the variability at the lower wavelengths of the UV spectrum, and less importance of the variability of the sensitivity in the higher wavelengths of this spectrum. These solar cycle percentage values are more physical quantities, and represent the SSI variability, as described in Section 2-2. There is very low uncertainty for the lower wavelengths, which is favorable. Around 200 nm there is an increase in uncertainty and then decreases for higher wavelengths.

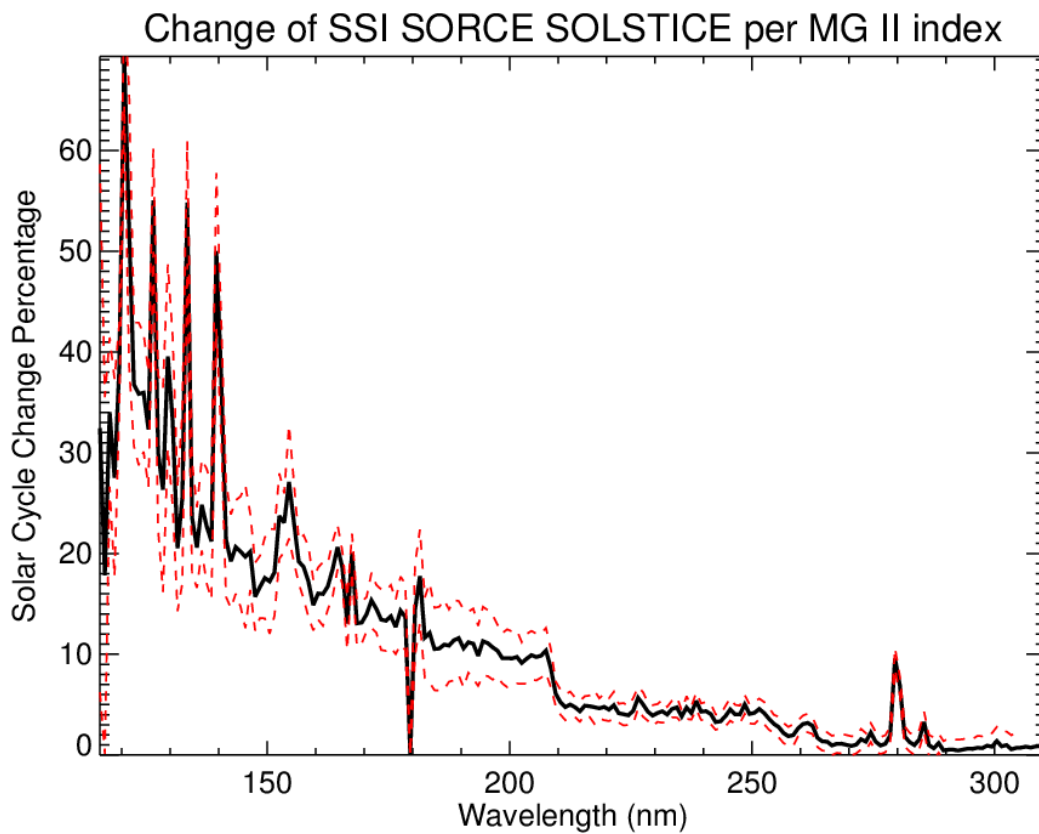


Figure (35): Mean solar cycle change percentage over the years for SOLSTICE SSI with respect to Mg II index for the UV spectrum, with 2 sigma standard deviation.

In figure (36), the solar cycle percentage in this study has been compared to the variability of SSI obtained by (Domingo et al., 2009), for the values of Mg II index at 280 nm and Lyman-alpha at 120 nm. The values of around 10% and 65% respectively, show very good agreement with the latter study. It proves that the obtained values from this study are reliable.

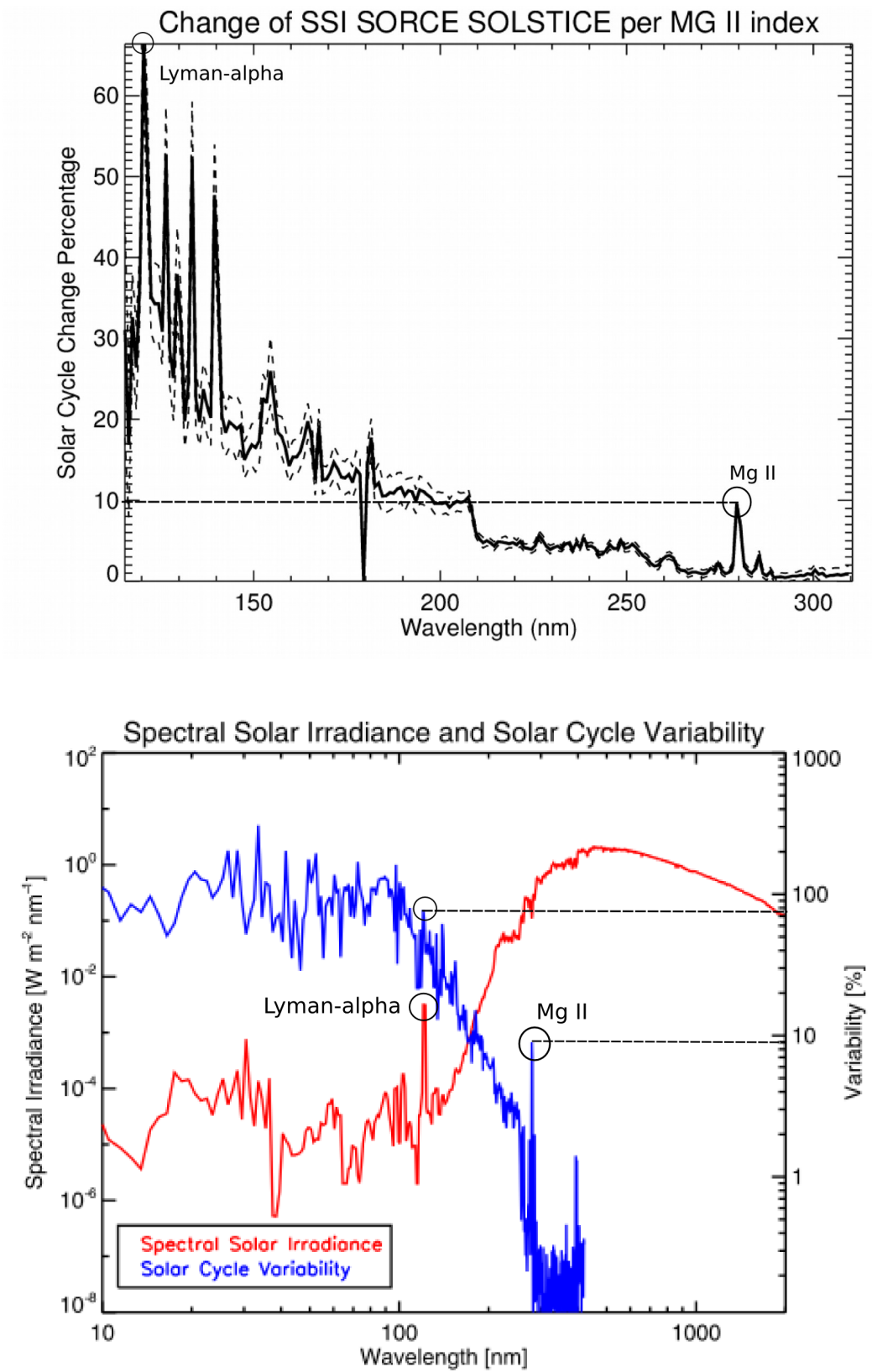


Figure (36): Comparison of derived solar cycle percentage change from this study (top) to the Domingo et.al. (Domingo et al., 2009) (bottom)

## 5-2- UARS SOLSTICE

The UARS SOLSTICE data set of SSI covers almost 10 years from 1991 until 2001. The time series is shown in figure (37). It covers from mid solar cycle 22 to the mid solar cycle 23 covering solar minimum in 1996 and solar maximum in 2000. There is high activity at the beginning of the dataset in 1992 and then goes down to a minimum and then high up to the next maximum in 2000. This data set includes measurements for continuous wavelengths from 120 nm to 410 nm and is gridded for every 1 nm.

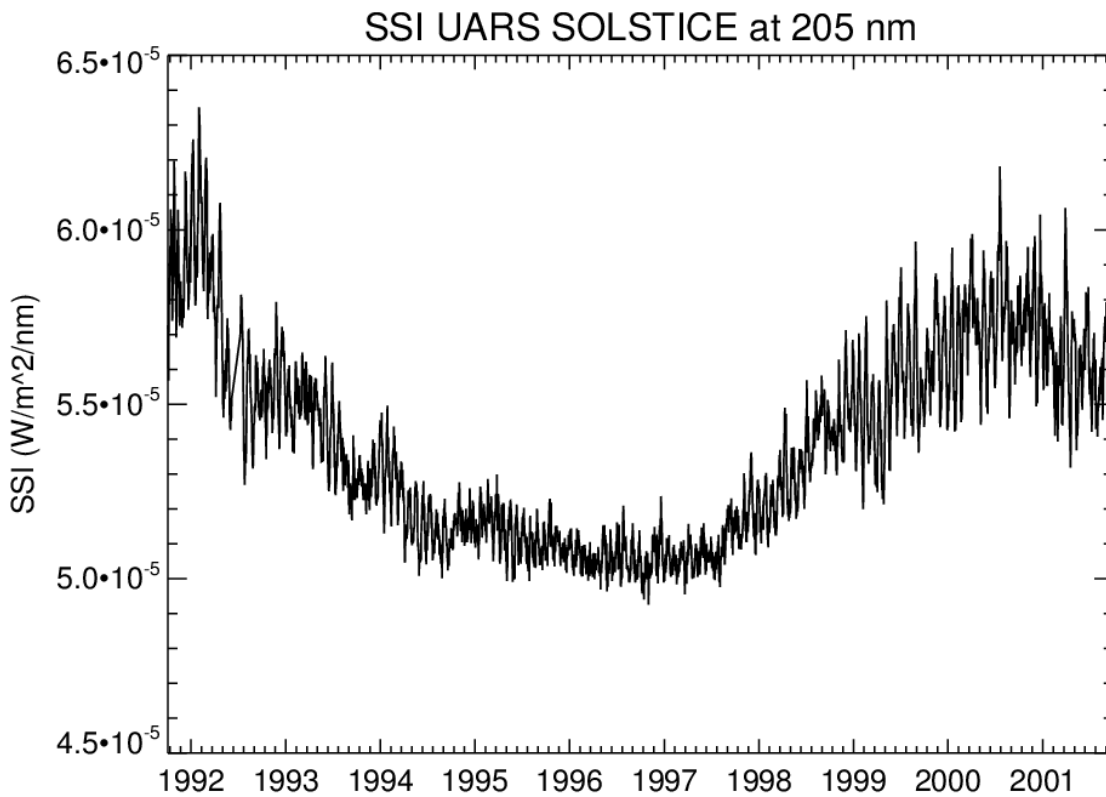


Figure (37): Daily SSI (W/m<sup>2</sup>/nm) from UARS SOLSTICE at 205 nm

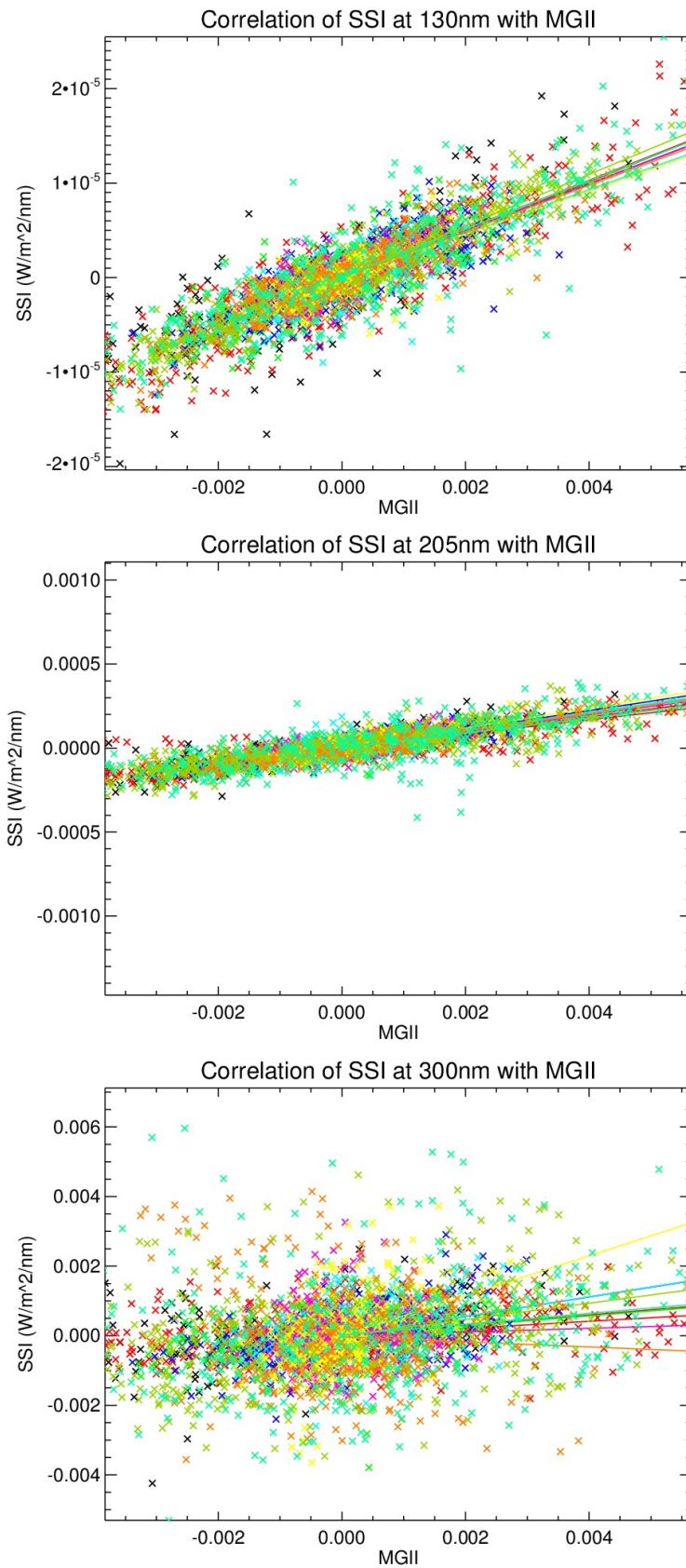


Figure (38): Correlation of UARS SOLSTICE SSI at 130, 205 & 300 nm with Mg II index separated in yearly data with their correspondent linear fit results.

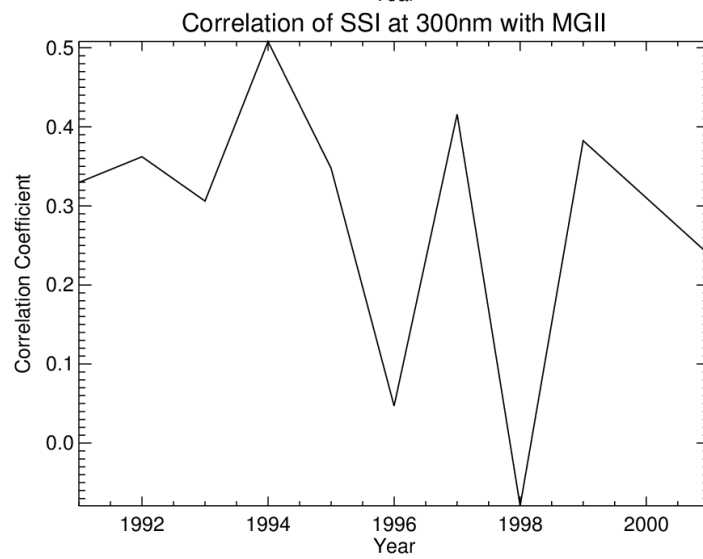
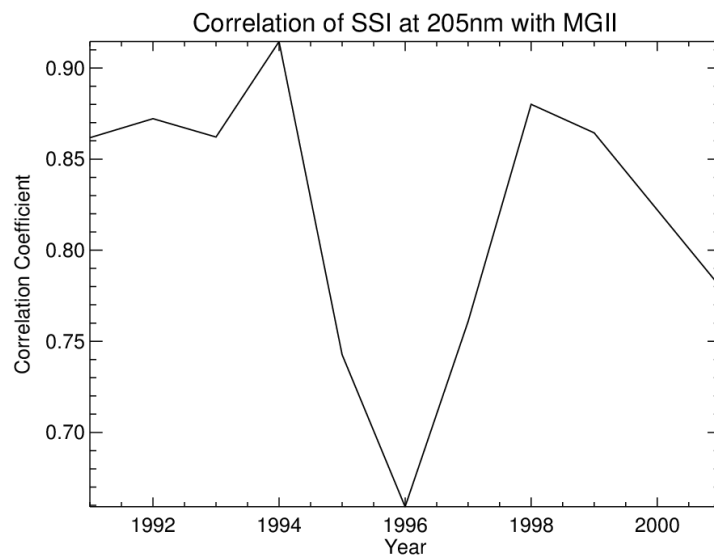
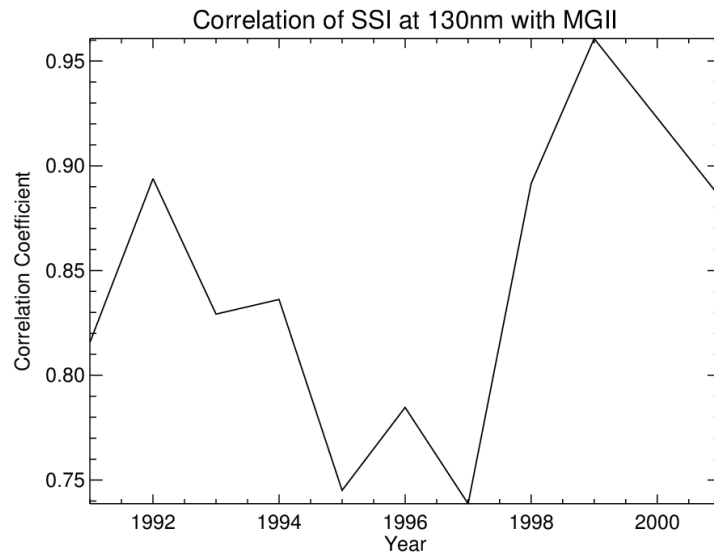


Figure (39): Annual time series of correlation coefficients of UARS SOLSTICE SSI at 130, 205 & 300 nm with respect to the Mg II index

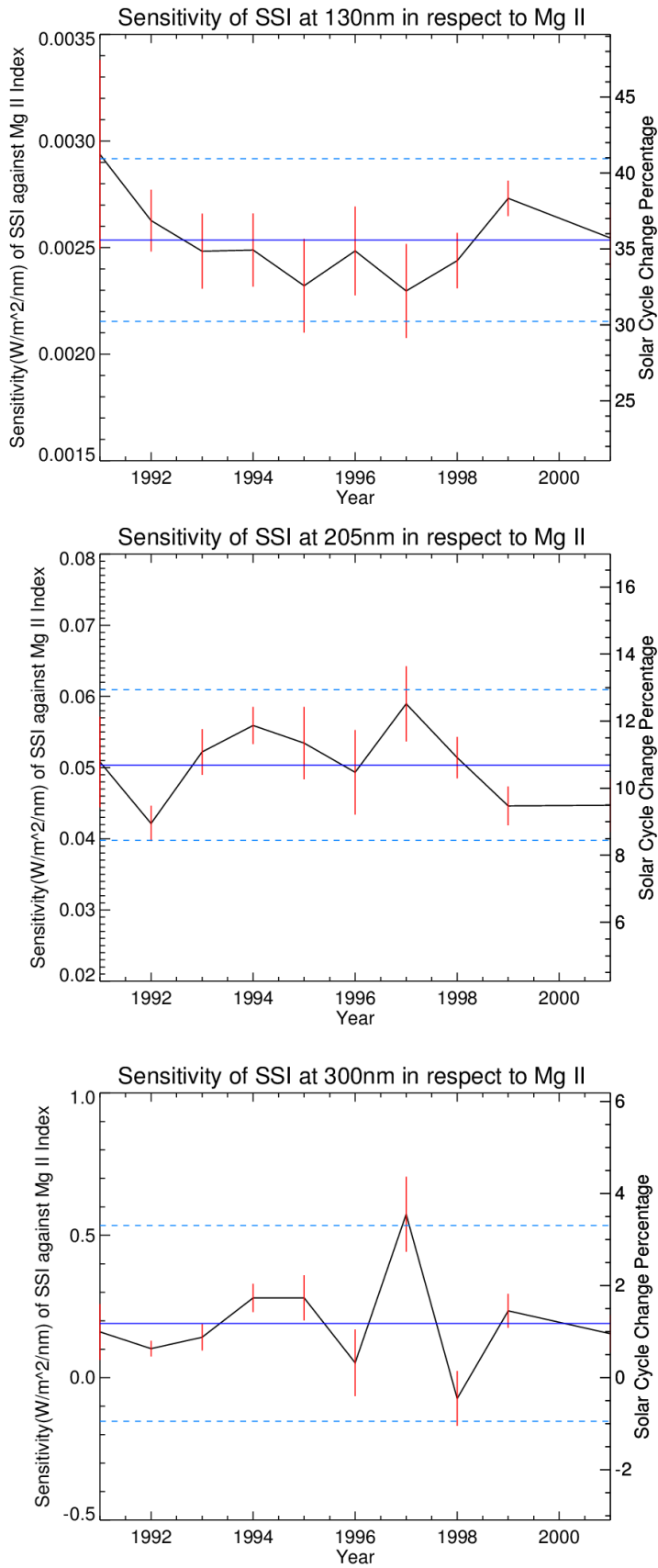


Figure (40): Sensitivity analysis of detrended UARS SOLSTICE SSI at 130, 205, 300 nm with respect to the Mg II index with their corresponding 2 sigma uncertainty of the linear fit.

The scatter plots in figure (38) show similar distributions as for *SORCE SOLSTICE*. There is very good and firmly spread data for the lower wavelengths. For higher wavelengths the distribution gets more spread out.

The correlation coefficients in figure (39) are generally very high, for both 130 and 205 nm, and very low for the higher wavelength. The minimum peak is around 1996 which is also the minimum in solar activity. It rises up when nearing 2000 and was also high at the beginning. For 300 nm the yearly correlations are very low with unpredictable variations and even change sign, as expected from what was visible in its scatter plot.

A similar pattern is also seen with the sensitivity plots in figure (40). For lower wavelengths the sensitivity fluctuations are mainly within the error-bars. The error bars overlap at each point and therefore it can be stated that the proxy sensitivity is stable with time. There are larger error bars indicating higher uncertainties during solar minimum (near 1996). At 205 nm, there is a large change in 1992 with small errors that do not overlap with the previous years. But except for this point, it is mostly stable within the error bars. The values increase with higher wavelengths and there is more fluctuations. At the same time the changes seem more unpredictable. At 300 nm there are large changes seen along with small errors that do not overlap. It can hardly be stated that the sensitivity is stable here. Their corresponding solar cycle percentage, show the same features.

In the two plots of figure (41), a comparison of this instrument with the previous *SORCE SOLSTICE* is shown. It can be seen that both instruments show good agreement at the lower wavelengths, but at higher wavelengths the mean proxy sensitivity starts to differ from each other. *UARS SOLSTICE* has larger standard deviations and its value variations drop down more compared to *SORCE SOLSTICE*. It also shows higher absolute values compared to the previous instrument. The results from *SORCE SOLSTICE* seem to be more reliable as there is less uncertainty.

The solar cycle percentages on the other hand, show very good overlap between the two instruments and only differ slightly near 200 nm. The uncertainties also are very similar between the two instruments for lower wavelengths, but *UARS SOLSTICE* shows higher uncertainties for higher wavelengths.

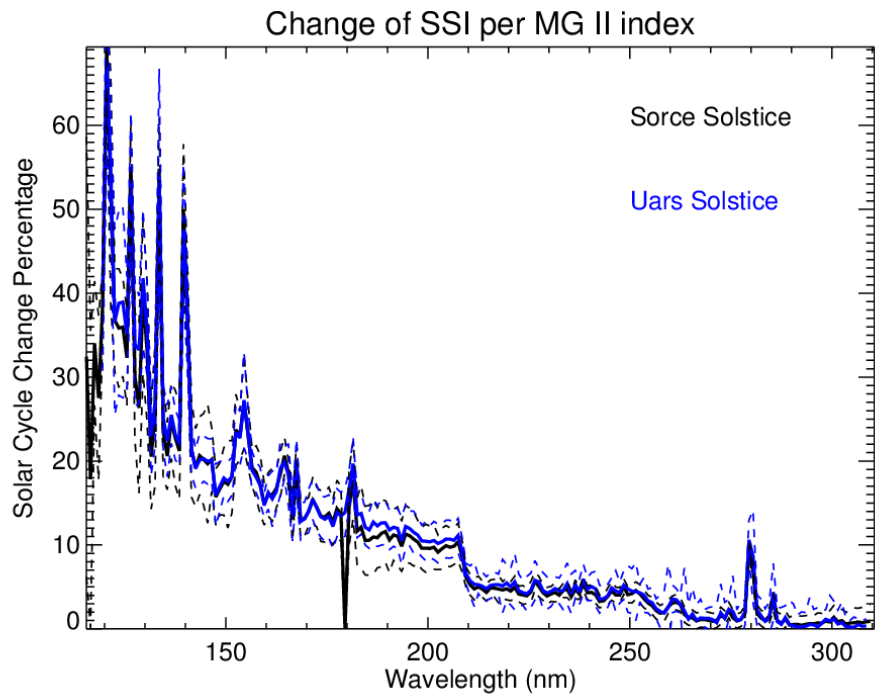
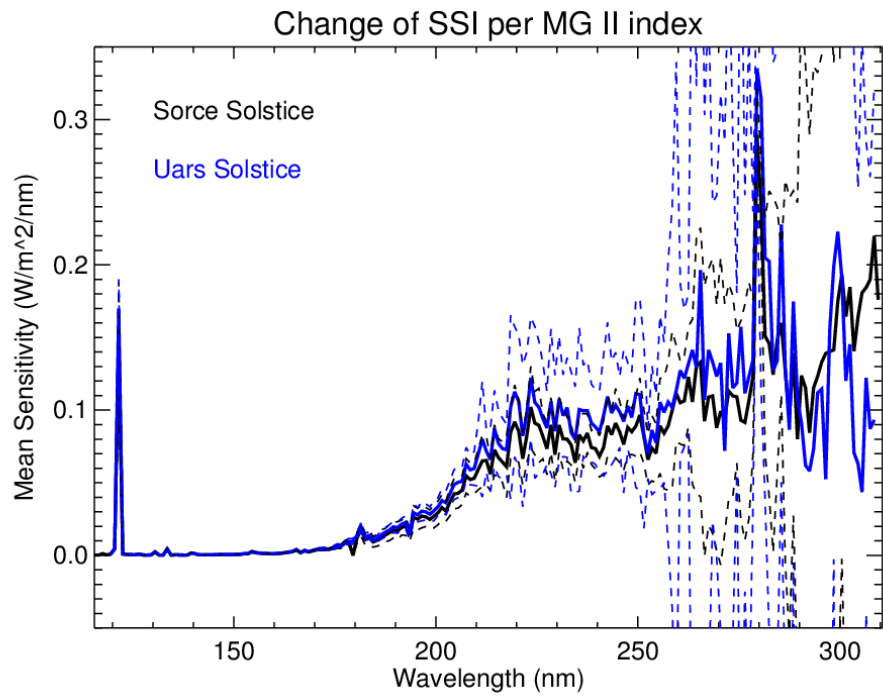


Figure (41): Comparison of the mean sensitivity (above plot) and mean change percentage (below plot) for SORCE SOLSTICE and UARS SOLSTICE, with 2 sigma standard deviation.

### 4-3- UARS SUSIM

The UARS SUSIM data set of SSI covers more years of the solar maximum years, from 1991 until 2005. Its time series is shown in figure (42). It ranges from mid solar cycle 22 to the declining phase of solar cycle 23 with a solar minimum in 1996 and covering solar maximum in 2002. There is high activity at the beginning of the dataset in 1992 and then goes down to a minimum and then high up to the next maximum in 2002. SUSIM covers more of the solar maximum years than UARS SOLSTICE. This data set also includes measurements from 120 nm to 410 nm and is gridded for every 1 nm.

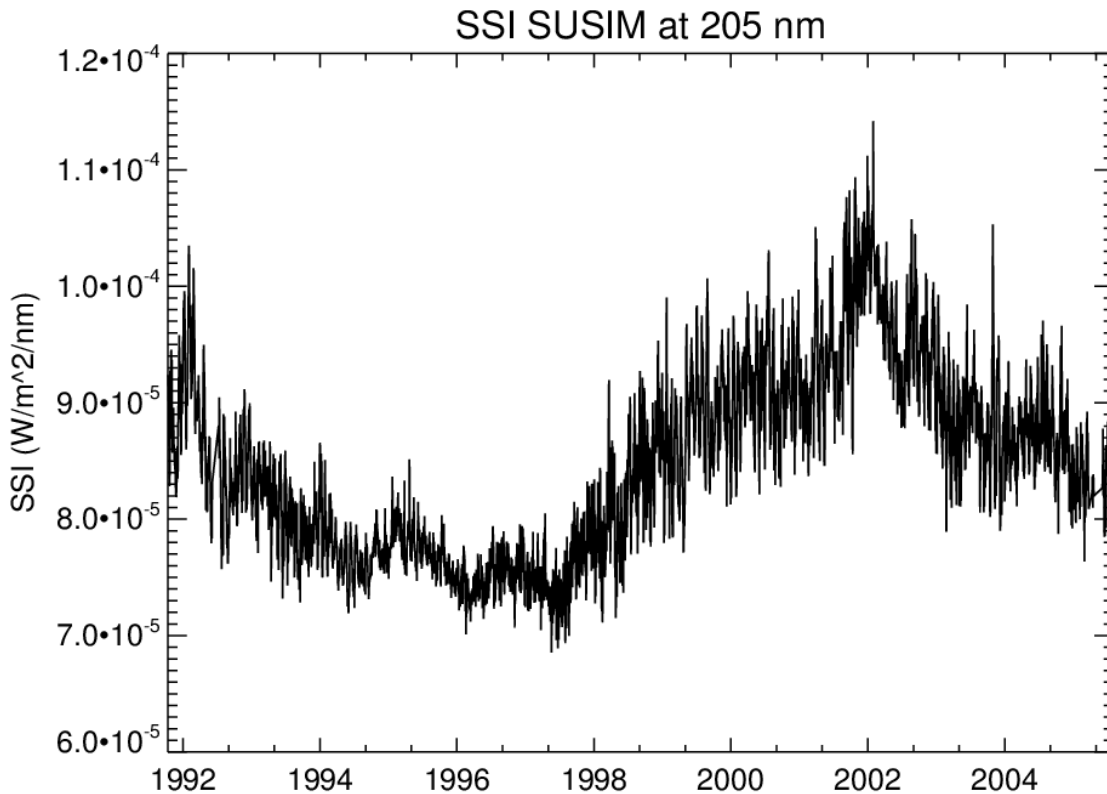


Figure (42): Daily SSI ( $W/m^2/nm$ ) from UARS SUSIM at 205 nm

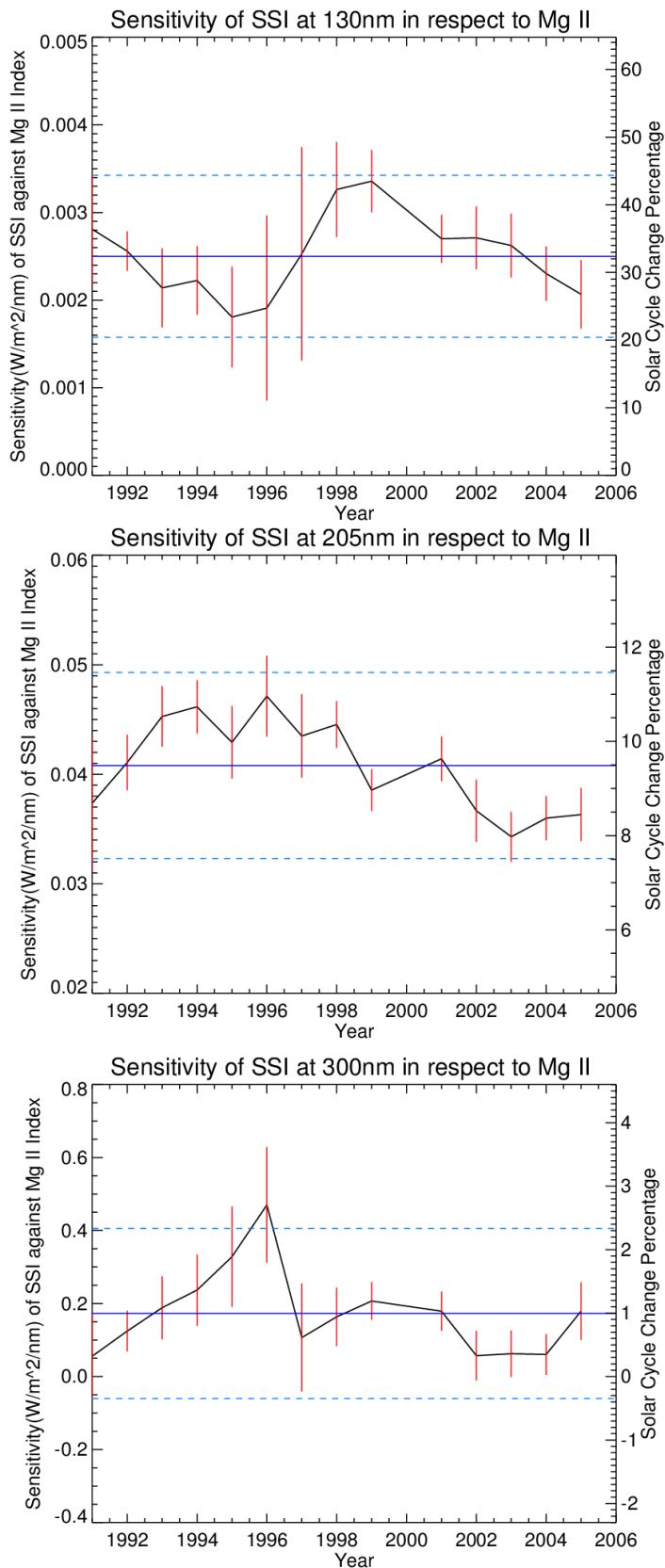


Figure (43): Sensitivity analysis of detrended UARS SUSIM SSI at 130, 205 & 300 nm with respect to the Mg II index with their corresponding 2 sigma uncertainty of the linear fit. Blue line is the mean value over the years along with its 2 times standard deviation.

The sensitivity analysis for this instrument shows generally higher errors than the previous two instruments as shown in figure (43). At 130 nm, the variations with time remain within the error bars and so good stability is seen. The variations of sensitivity from 1995 to 1999 is followed by very large error bars, and the overlap between the error bars is also quite good over the entire time span. From 2000 onwards there is little change along with with a small downward trend, and at the same time smaller error bars. These years are during solar maximum years, where less errors are expected. The decline in sensitivity values may suggest the effects of instrument degradation in this parts. Since at this point the instrument has been operating for a long time, and does not show anymore the expected higher values.

At 205 nm also very good stability is seen. The variations stay mainly within the error bars, however, a small trend is also seen here after 2000. For 300 nm there is a large drop 1997 which is just after the solar minimum year in 1996. Even though at this point the errors are large, still they do not overlap. But at the other years better stability is seen. Specially from 2000 onwards, the solar maximum years, very good stability is seen in the proxy sensitivity. Despite the fact that at higher wavelengths the other instruments were not very stable, SUSIM shows fairly stable results at 300 nm except in 1996.

This data reflects very well the expected accuracy and stability of the correlation between SSI and the Mg II index during solar maximum years. Further correlation and scatter plots can be seen in the appendix.

The mean proxy sensitivity of SUSIM is compared to UARS SOLSTICE as shown in figure (44). It shows lower sensitivity for SUSIM for higher wavelengths and even gets negative at some points. Its standard deviation is lower than SOLSTICE. The solar cycle percentage values are also lower compared to SOLSTICE. It reaches up to only around 45%, compared to 60% by the SOLSTICES instruments at 120 nm, but SUSIM also show higher uncertainty. Compared to both UARS SOLSTICE and SORCE SOLSTICE the standard deviations are higher for this instrument.

The results for UARS SUSIM shows in general very high uncertainties, as compared to the other two instruments. On the other hand it shows good stability of the proxy sensitivity within its uncertainty during solar minimum years as well as solar maximum years. It shows lower absolute values compared

to the previous instruments. During solar maximum years it shows very favorable and stable sensitivity with low uncertainty. However the effect of instrument degradation are also more visible in this dataset.

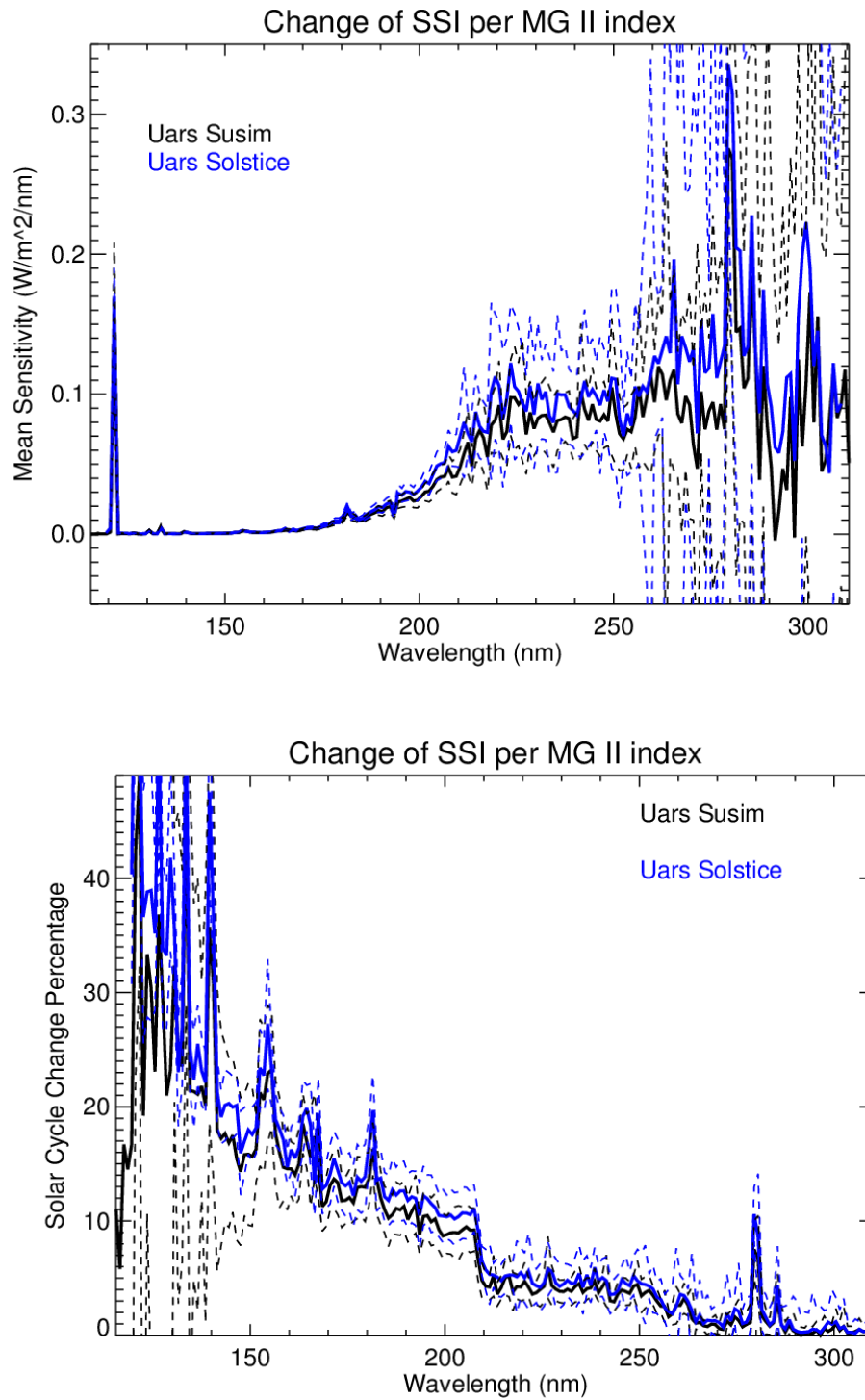


Figure (44): Comparison of the mean sensitivity (top) and mean change percentage (bottom) for SORCE SUSIM and UARS SOLSTICE, with 2 sigma standard deviation.

## 5-4- Sensitivity Comparison for all Instruments

Comparing all three instruments at once at the specific wavelengths can give a better overview on the proxy sensitivity stability. The differences for each instrument is better seen when zoomed in for the specific, chosen wavelengths.

At 130 nm in figure (45), it can be seen that the sensitivity obtained from SUSIM shows very good stability for both solar maximum and minimum years, but at the same time it has the largest errors and standard deviation compared to the other instruments. The sensitivity obtained from UARS SOLSTICE at the same time range has much less errors, but the variations are also not very large compared to SUSIM. Its mean value is almost the same as SUSIM and has less standard deviation compared to the other two instruments. SORCE SOLSTICE shows also very small errors in comparison, and it is mostly stable except for the solar minimum year. It has a lower mean value compared to the other two instruments.

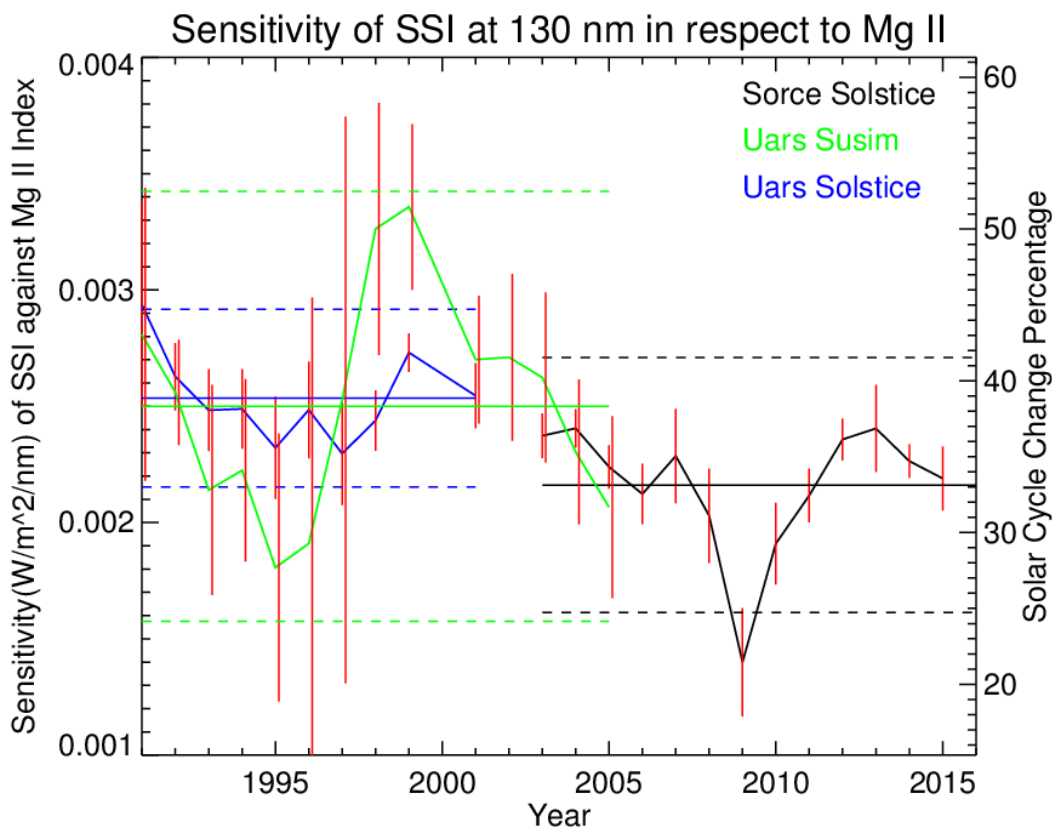


Figure (45): Comparison of the sensitivity at 130 nm for all three instruments

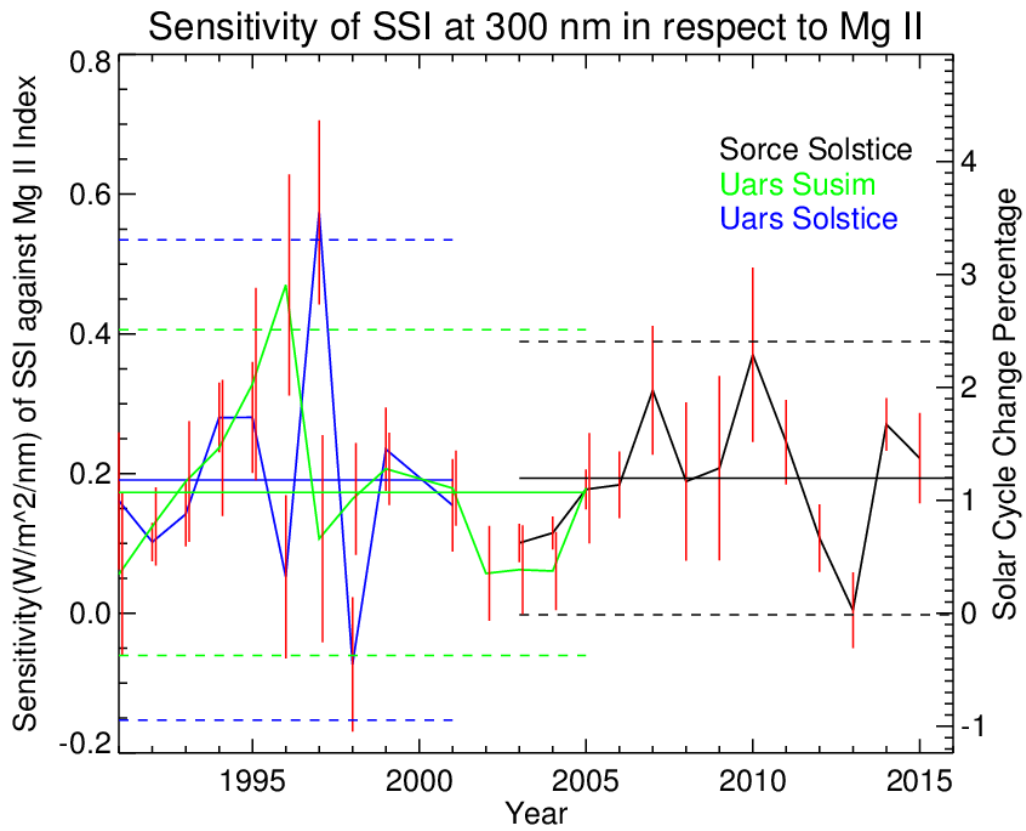
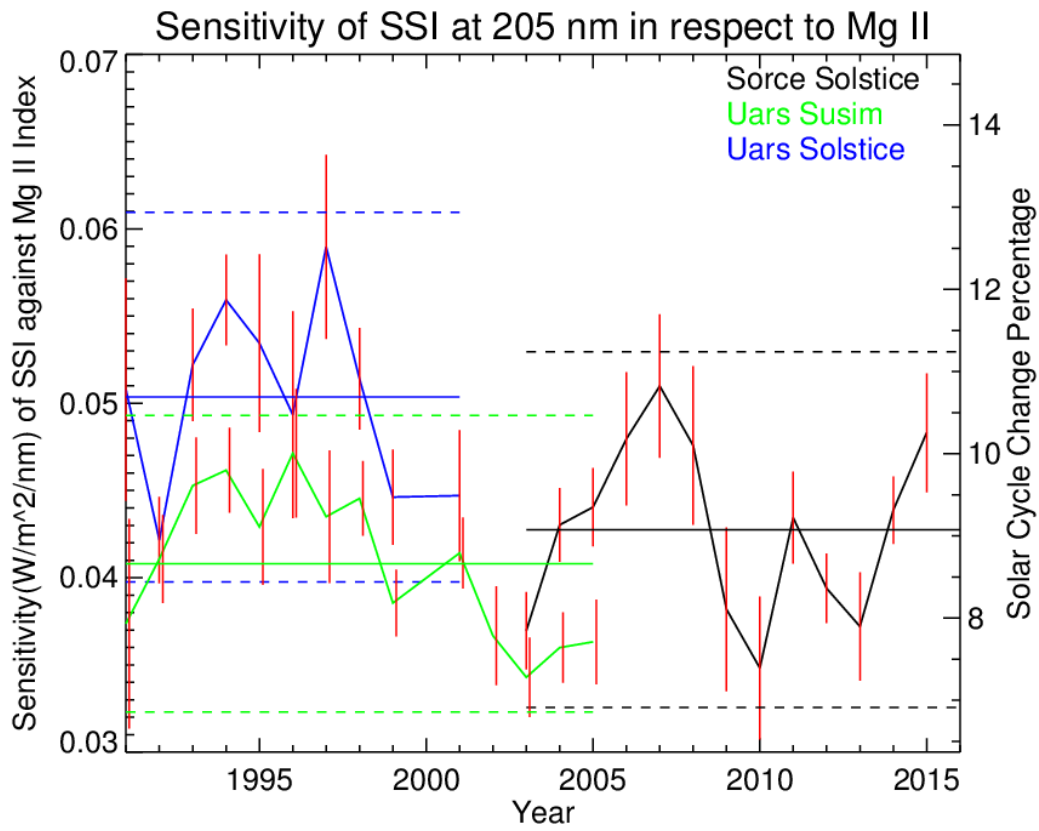


Figure (46): Comparison of the sensitivity at 205 nm (top) and 300 nm (bottom) for all three instruments

The comparison for sensitivity changes at 205 nm is shown in figure (46). All three instruments show quite stable with time. *SORCE SOLSTICE* shows more fluctuations than the other instruments, but it has also larger errors and they mainly overlap, except around 2010. *UARS SUSIM* shows very good stability at the solar minimum years, and has lower values compared to the other two instruments. Also from 2001 its values drop down, but still can be seen as stable within its error bars. *UARS SOLSTICE* shows more fluctuation at the same time span, with higher values and larger errors. But except for the year 1992 it can be seen as stable. At 300 nm, *UARS SOLSTICE* shows very high fluctuations during solar minimum years (1995-1996), with errors that do not overlap. *UARS SUSIM* shows better stability at the same years except for 1995-1996 with a strong drop. There is very good stability during solar maximum years 2000-2005 but with a decrease in values. *SORCE SOLSTICE* also does not show very good stability at several points from 2011-2015, where better stability is expected since there is higher solar activity.

## 5-5- NRLSSI2

For a final comparison, the proxy sensitivities from all the instruments are compared to the solar model *NRLSSI2*. This data has a time span from 1950 until present, but here only the same time span of the *Mg II* index from 1978 until present is considered. The model covers the entire solar spectrum from the UV to the IR, but here only the UV region from 115 to 310 nm is considered. Its time series for the wavelength 205.5 nm is seen in figure (47).

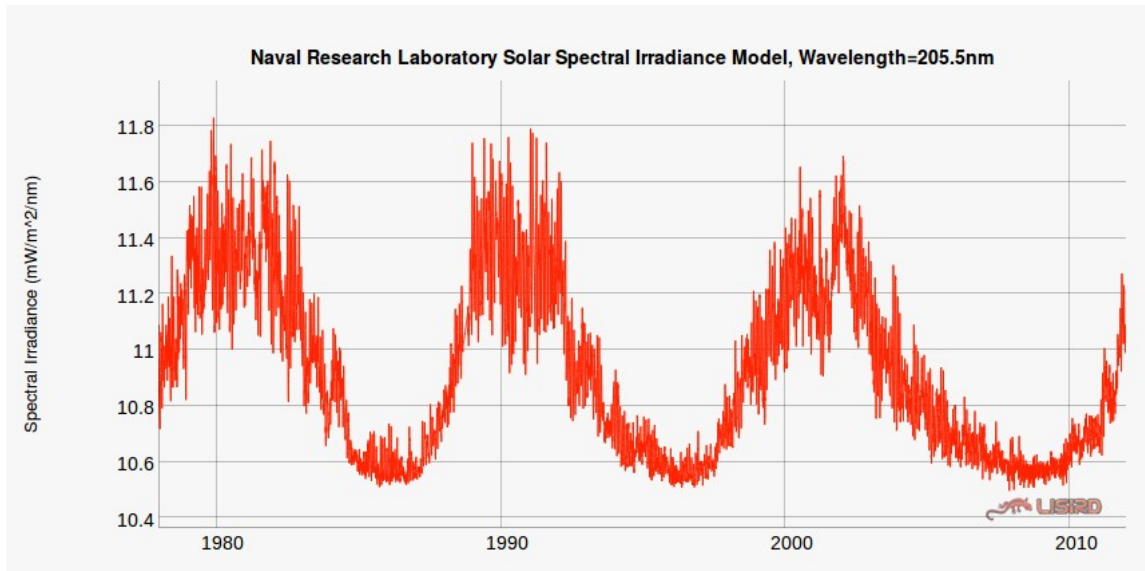


Figure (47): *NRLSSI2* time series at 205.5 nm [<http://lasp.colorado.edu/lisird/nrlssi/>]

The sensitivity obtained from this model is shown in figure (48). It shows firm stability of sensitivity over the years and wavelengths. At higher wavelengths, even though more fluctuations are seen in the values but it is relatively stable. Compared to the proxy sensitivity from the measured data, these results show regular changes and less dramatic variability with time. This high stability is expected since this model uses proxies, including the Mg II index and sunspot darkening, in its linear regression. While the sensitivity analysis of the instruments here only considers one component in the linear regression.

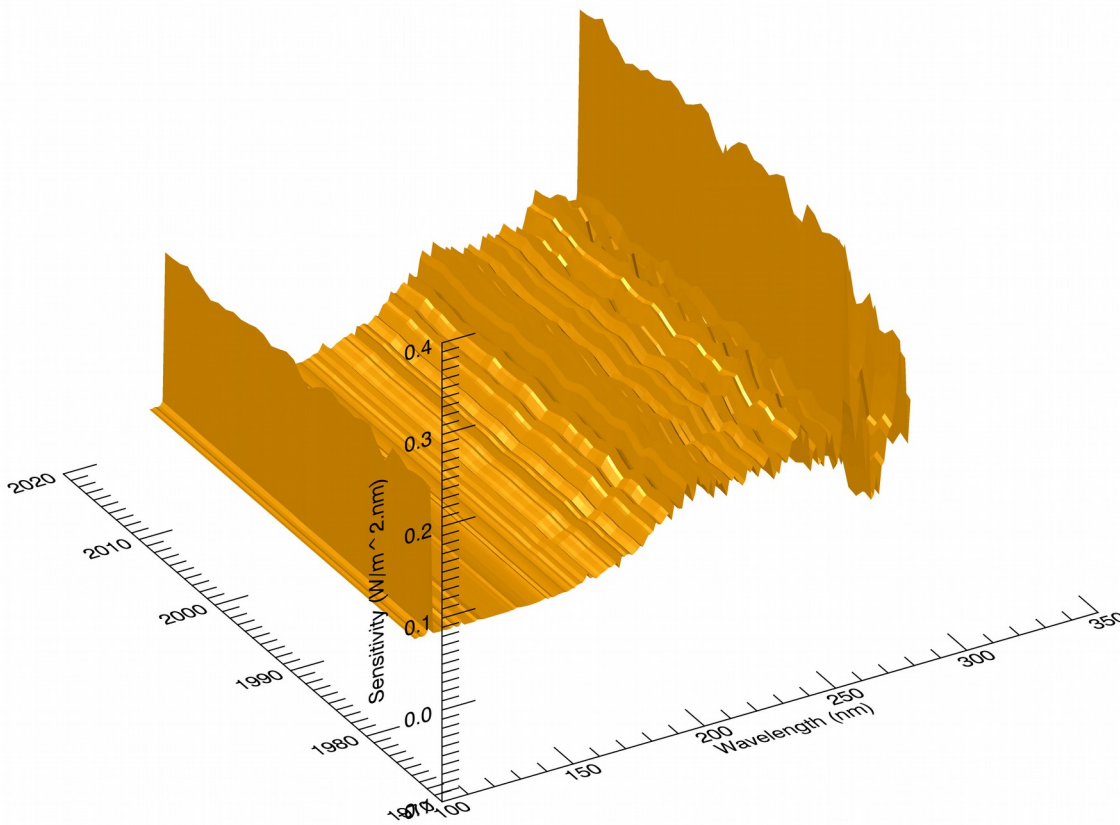


Figure (48) : NRLSSI2 sensitivity over the UV spectrum

## 5-6- Comparisons of all instruments with NRLSSI2

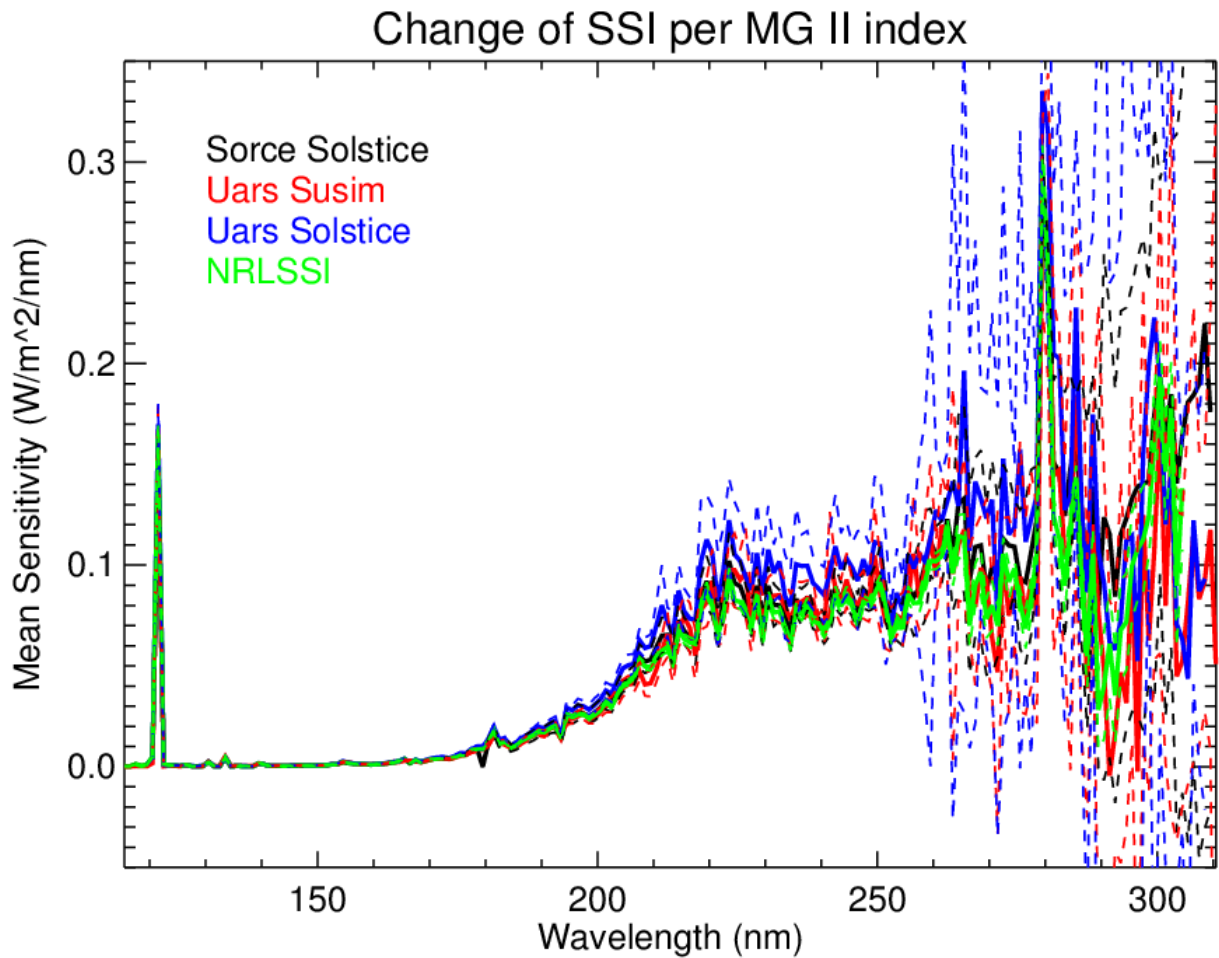


Figure (49): Mean proxy sensitivities for all three instruments and NRLSSI2. Dashed lines show 2 sigma uncertainty.

Figure (49) shows the mean sensitivity data as a function of wavelength from the differently measured data and NRLSSI2 at one place. Here the different data sets are shown with different colors, and their standard deviation with dashed lines of the same color.

From 200-250 nm there is good agreement and variations with wavelength are similar. The values differ slightly and the standard deviation is small in value, but since the values are very low it can not be seen very clearly. Above 250 nm, when the uncertainties are getting larger, the difference between the datasets also increase along with their standard deviation. Above 300 nm the standard deviations get very large. At the peak of Mg II doublet (280 nm) all data agree very well.

Figure (50) shows the difference of the mean sensitivity for each of the instruments and NRLSSI2. It shows that UARS SOLSTICE differs the most from NRLSSI2 than the other two instruments, and SORCE SOLSTICE has the best agreements with this model. But since the NRLSSI2 uses SORCE SOLSTICE as the main data set for its linear regression, this agreement is expected (Lean et al., 1997). All instruments and NRLSSI2 agree well below 200 nm wavelengths. UARS SOLSTICE shows significant difference in the higher wavelengths, along with higher values. It also shows several high peaks not seen with the other instruments. This instrument has three channel boundaries, which can be the cause for these high peaks. The boundaries lie around 119 nm, 180 nm and 280 nm, which might cause the big peaks at 119 nm and 280 nm. UARS SUSIM and SORCE SOLSTICE have differences that become significant only above 280 nm. It also shows that SUSIM has lower absolute values.

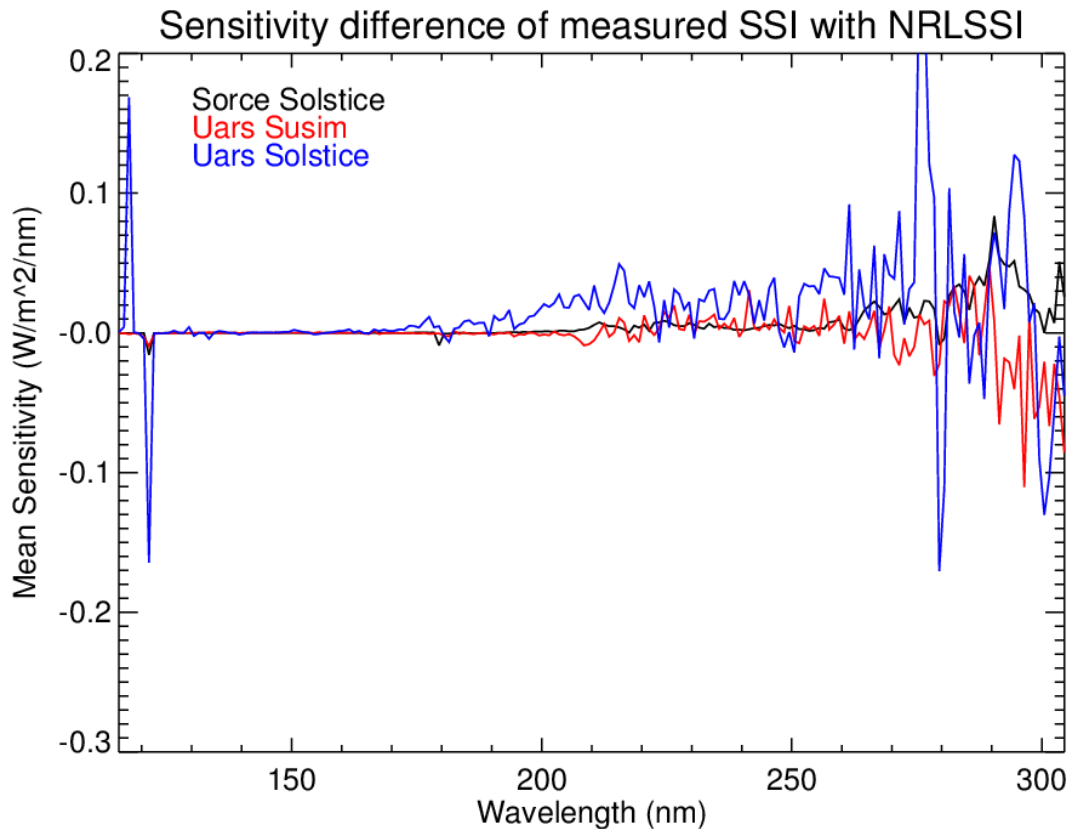


Figure (50): Difference of mean proxy sensitivities for all three instruments and NRLSSI2.

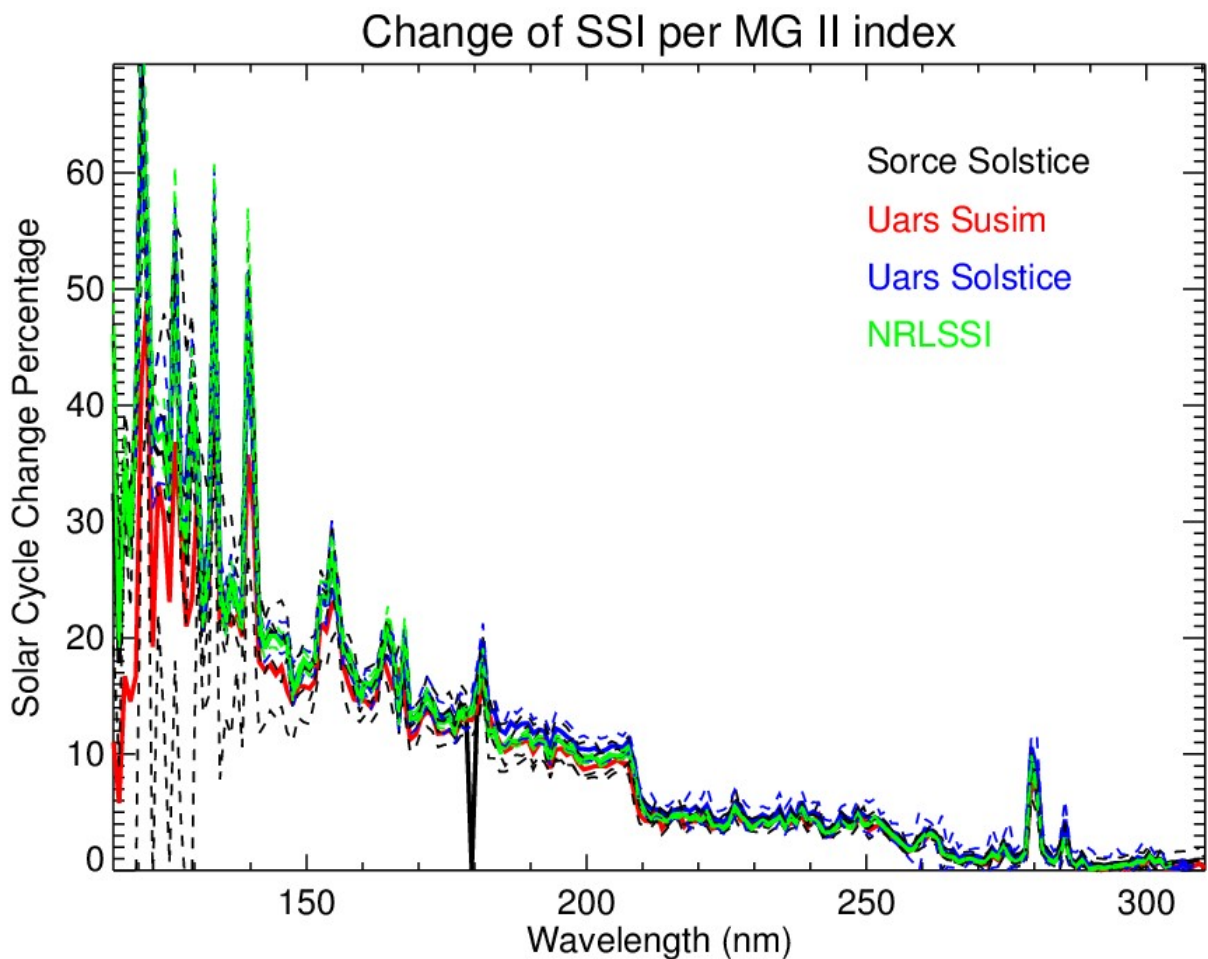


Figure (51): Mean solar cycle change percentages for all three instruments and NRLSSI2

In figure (51), the solar cycle change percentage, for all three instruments and NRLSSI2 are shown.

There is very good agreement of all instruments over the entire spectrum, except for UARS SUSIM at lower wavelengths. For UARS SUSIM the standard deviation is also higher at lower wavelengths, and for UARS SOLSTICE standard deviation is higher at higher wavelengths.

Figure (52) shows the difference for each of the instruments and NRLSSI2, for better visibility. It shows that UARS SOLSTICE differs the most from NRLSSI2 compared to the other two instruments. The differences are seen as specially high in the lower wavelengths for UARS SOLSTICE, where it reaches up to 40% and a change of 5-10% overall. The high peaks seems to be an instrumental issue. The channel boundaries covering the spectrum might be one issue.

UARS SUSIM is lower up to 20% with respect to NRLSSI2 and the other two instruments at lower wavelengths.

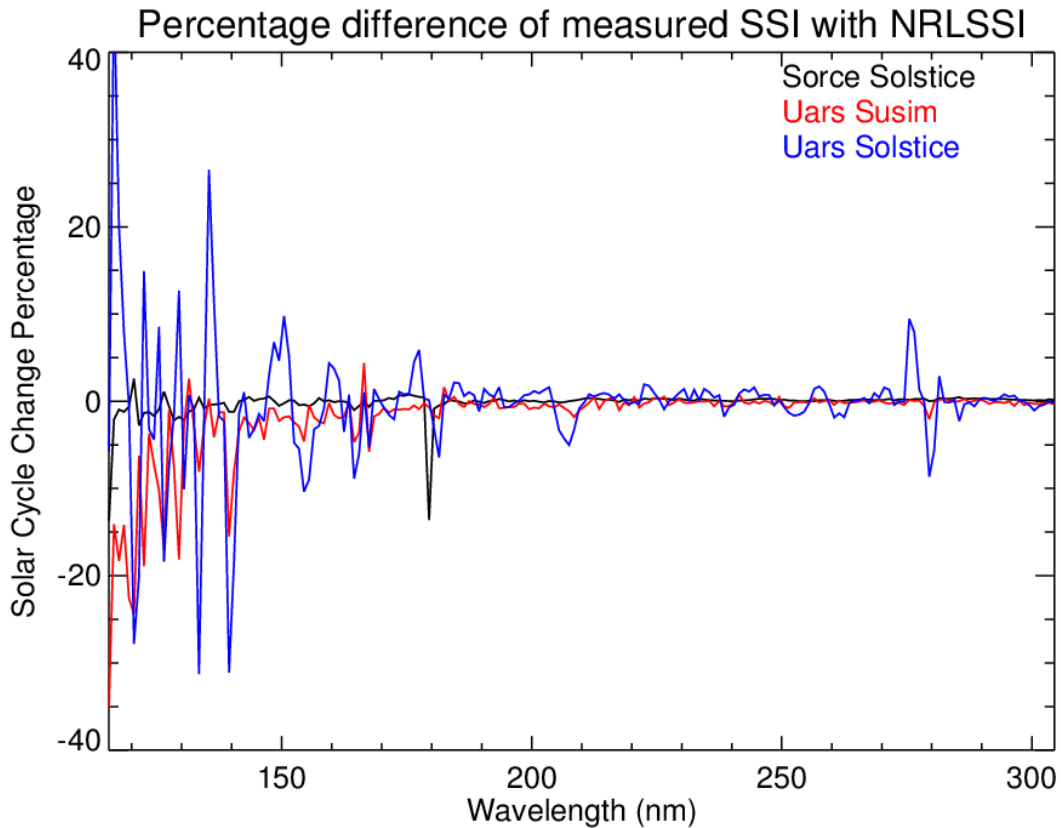


Figure (52): Difference of mean solar cycle change percentages for all three instruments and NRLSSI2

It can be concluded that if the NRLSSI2 model would have used the data from UARS SUSIM it would show lower variability of the SSI, specially at the lower wavelengths, but from the previous analysis we also know that it has higher uncertainties. If UARS SOLSTICE would have been used then it would have higher absolute values and also show more changes of variability, but also include more irregularities caused by the instrument.

# Chapter 6

## Summary

The yearly proxy sensitivity of different SSI datasets in the UVC and UVB spectral region (115-310 nm) with respect to the Mg II index have been analyzed in this thesis. Most of the focus lies during the solar minimum years, when the signals in SSI data is weaker and noisier, causing larger uncertainties in the measured data. During the maximum years of the 11 year solar cycle the SSI signals are strong and result in better reliability of the datasets. Therefore amplifies the need to investigate the stability of the sensitivity during minimum years of the 11 year cycles. The observation of solar minima years has been provided by the satellite instruments SORCE SOLSTICE (2003-2015), UARS SOLSTICE (1991-2001), along with UARS SUSIM (1991-2005) which provides also measurements during the solar maxima years. In addition modeled data from NRLSSI2 is used for a final comparison.

The results from the three instruments show that the yearly sensitivity of SSI with respect to the Mg II index variations is for most parts stable within the error bars over the observation time from the instruments. The uncertainty of this sensitivity parameter is generally higher during solar minimum years along with lower correlation values compared to solar maximum years. At specific years the changes of proxy sensitivity may exceed the error's range and so contradict the stability. The analysis for the UV wavelength region shows, high correlation and good stability of the sensitivity at wavelengths below around 250 nm. For higher wavelengths the correlation drops down and the stability of the sensitivity can not be confirmed at various points. For this wavelength region the effects of instrument degradation and sunspots are more evident. Therefore at higher wavelengths above 250 (nm) Mg II index alone is not a suitable proxy and additional proxies such as sunspot darkening are required to improve solar reconstruction.

Even after detrending the data, there are still signs of instrumental degradation particularly in the SUSIM measurements (decreasing proxy sensitivity during the last five years of the mission). But even though they are not completely removed, it has been shown that within the uncertainty range, the variations are acceptable most of the times, taking into consideration some exceptions.

The data sets of the three instruments show very good agreement in the lower wavelength region below 250 nm. *SORCE SOLSTICE* covers the declining and inclining phase of solar cycles 23 and 24, respectively covering the solar minimum peak very well. Its proxy sensitivities have less uncertainties compared to the other instruments which is favorable, but the stability of the sensitivity can not always be proven. *UARS SOLSTICE* covers part of the solar cycles 22 and 23, covering the solar minimum peak years, and shows good stability of sensitivity within its uncertainties. It shows more variations compared to *SORCE SOLSTICE*, has slightly higher absolute values and uncertainties, and there seem to be some deviation in the channel boundary regions. *UARS SUSIM* shows the highest uncertainties among the three instruments, but also very good stability of sensitivity within its uncertainty region. It also shows lower absolute values, but covers the solar maximum years very well with much less uncertainties.

Comparison of these three instruments with *NRLSSI2*, shows lower values for *UARS SUSIM* in the lower wavelengths, which would indicate less SSI variability if the model used *UARS SUSIM*. *UARS SOLSTICE* shows higher SSI variability than *NRLSSI2* along with higher absolute values, but with more instrument irregularities.

As an outlook for further research in this area, the analysis can be continued by extending to the higher wavelengths. At higher wavelengths there is the need for an additional parameter, the sunspot darkening in the linear regression analysis in order to achieve better regression results. Also increasing the resolution of the study to monthly analysis, instead of yearly analysis of the proxy sensitivity, and establishing it from the 27 days cycle instead of yearly data, would provide additional confirmation. Also further comparison of the datasets with the model *SATIRE-S* (Ermolli et al., 2013), currently an alternative candidate for use in climate models, would provide more information on the optimum use of the Mg II index proxy.

# Appendix

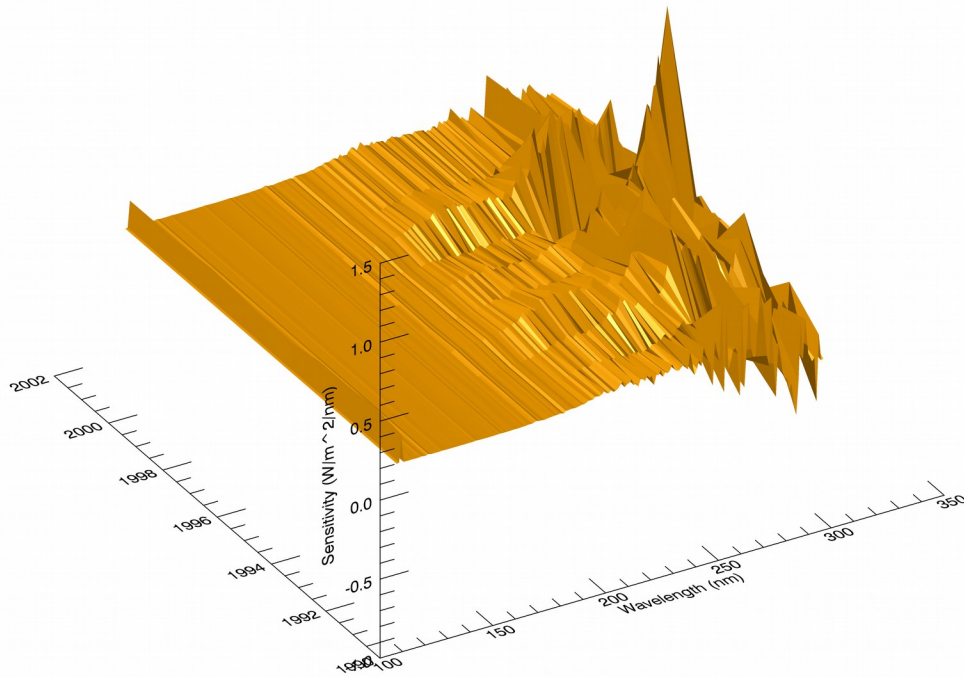


Figure (53): Sensitivity of UARS SOLSTICE SSI with respect to the Mg II index for the UV spectrum

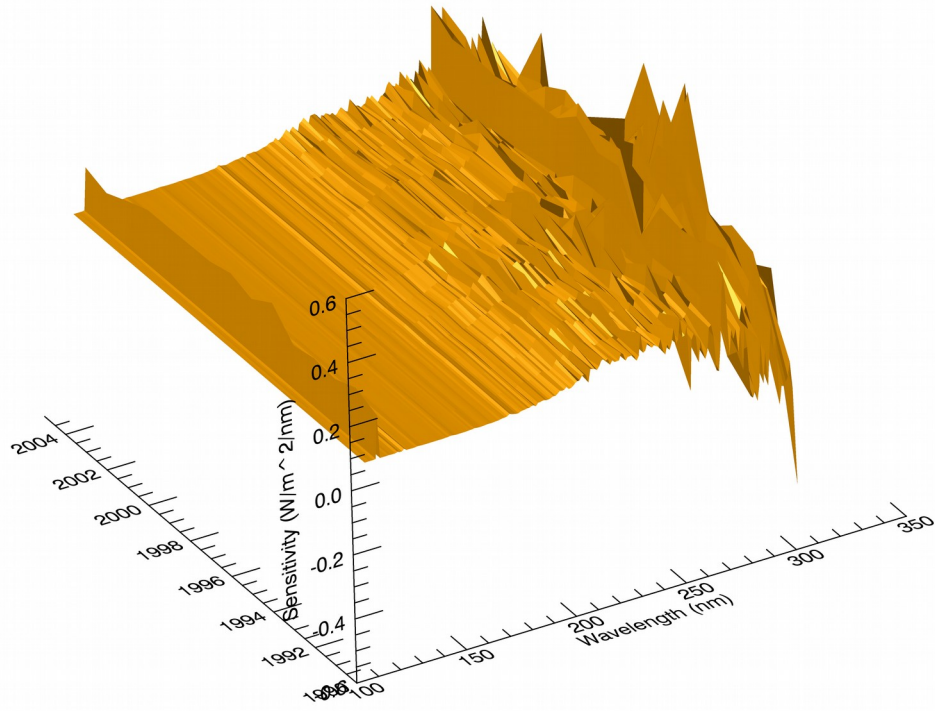


Figure (54): Sensitivity of UARS SUSIM SSI with respect to the Mg II index for the UV spectrum

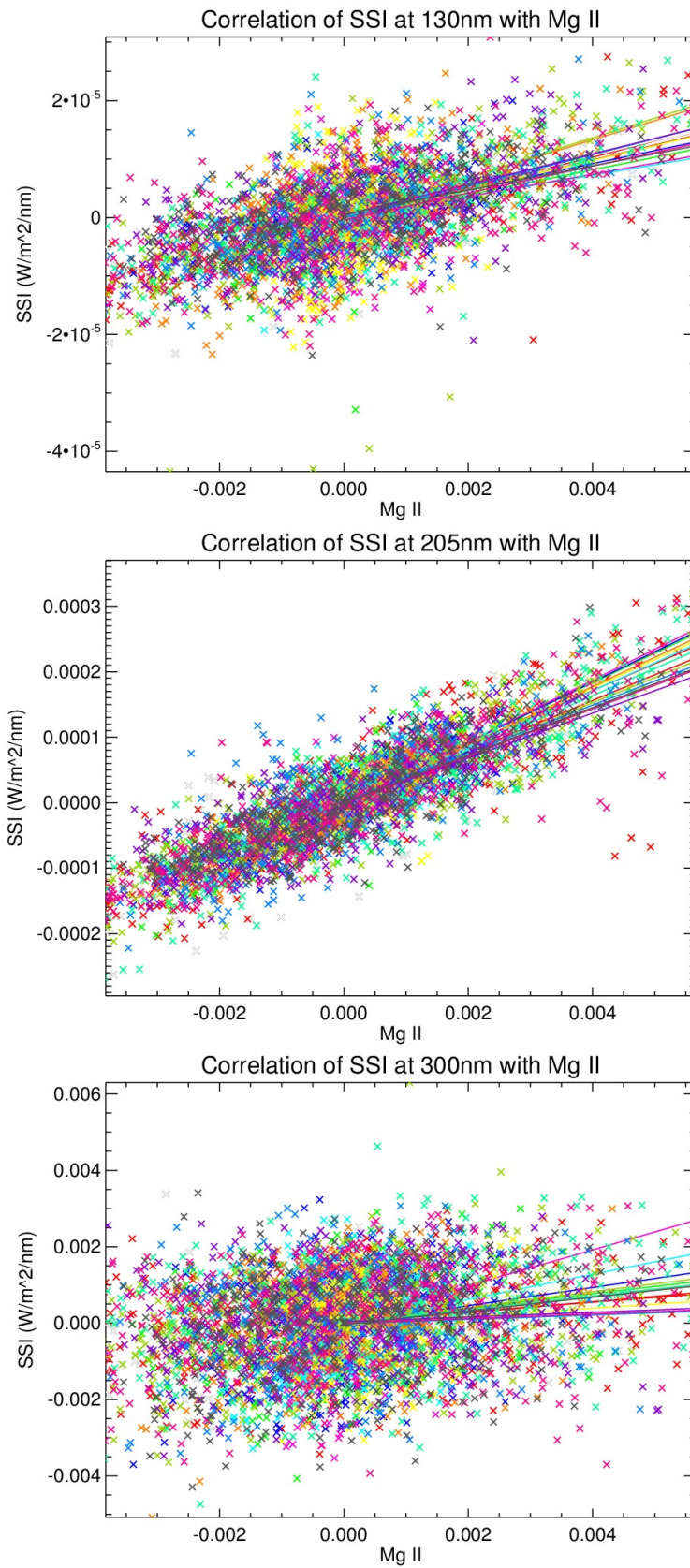


Figure (55): Correlation of UARS SUSIM SSI at 130, 205 & 300 nm with Mg II index separated in yearly data with their correspondent linear fit results.

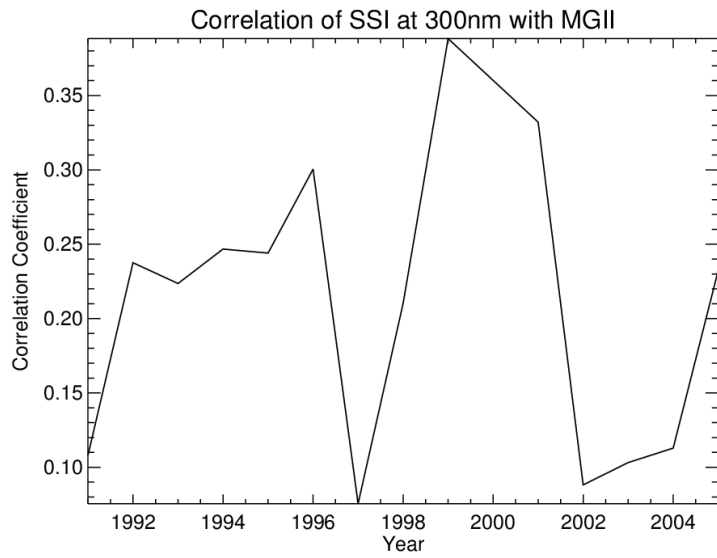
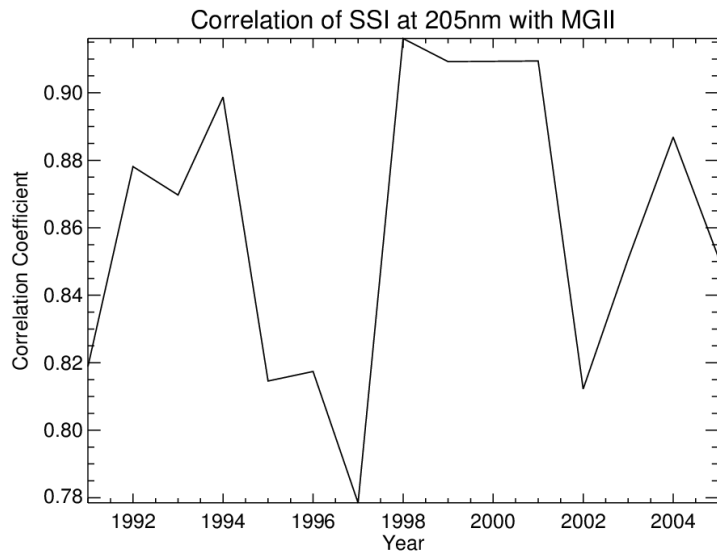
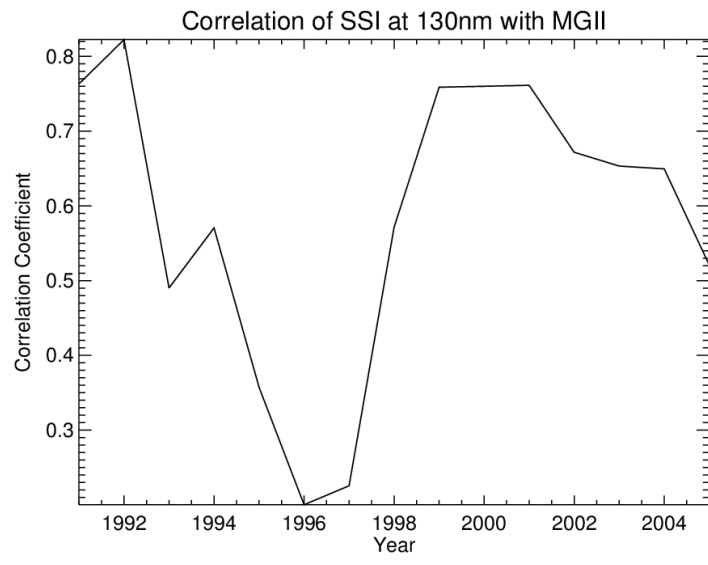


Figure (56): Correlation coefficients for each year of correlation of UARS SUSIM SSI at 130, 205 & 300 (nm) with Mg II index

## Bibliography

V. G. Cholakyan, **Intensities of the resonance lines of neutral and ionized magnesium in stellar spectra**, *Astrophysics*, 25, 2, 1986.

W. Cleveland, M. Hill, N.J. Summit, **Visualizing data**; At & T Bell Laboratories Published by Hobart Press, ISBN 978-0963488404, 1993.

V. Domingo, I. Ermolli, P. Fox, C. Fröhlich, M. Haberreiter, N. Krivova, G. Kopp, W. Schmutz, S.K. Solanki, H.C. Spruit, Y. Unruh, A. VöglerSolar, **Surface Magnetism and Irradiance on Time Scales from Days to the 11-Year Cycle**; *Space Sci Rev* 145: 337–380, DOI 10.1007/s11214-009-9562-1, 2009.

T. Dudok deWit, M. Kretzschmar, J. Liliensten, and T. Woods, **Finding the best proxies for the solar UV irradiance**, *Geophys. Res. Lett.*, 36, L10107, doi:10.1029/2009GL037825, 2009.

I. Ermolli, K. Matthes, T. Dudok de , N. A. Krivova, K. Tourpali, M. Weber, Y. C. Unruh, L. Gray, U. Langematz , P. Pilewskie , E. Rozanov , W. Schmutz , A. Shapiro , S. K. Solanki 4,13 , and T. N. Woods, **Recent variability of the solar spectral irradiance and its impact on climate modelling**; *Atmos. Chem. Phys.*, 13, 3945–3977, DOI 10.5194/acp-13-3945-2013, 2013.

C. Froehlich, J. Lean, **Solar Radiative Output and its Variability: Evidence and Mechanisms**; Solar variability and its effects on climate, American Geophysical Union, 2004.

P. Fox, **Solar Activity and Irradiance Variations**; Solar variability and its effects on climate, American Geophysical Union, 2004.

A. Hanselmeier, **The Solar and Space Weather**; Kluwer Academics Publishers, 2004.

M. T. DeLand, and R. P. Cebula, **Composite Mg II Solar Activity Index for Solar Cycles 21 and 22**; *J. Geophys. Res.*, 98, 12809-12823, 1993.

D. H. Hathaway, **The Solar Cycle**; Living Rev. Solar Phys. 7, 1, 2010.

S. B. Hill, N. S. Faradzhev, L. J. Richter, S. Grantham, C. Tarrío, et al., **Optics contamination studies in support of high-throughput EUV lithography tools**, Proc. SPIE 7969, Extreme Ultraviolet (EUV) Lithography II, 79690M, doi:10.1117/12.879852, 2011.

J. Lean, [http://lasp.colorado.edu/sorce/news/2012ScienceMeeting/docs/presentations/S1-04%20LEAN\\_NRLSSI\\_Sep12.pdf](http://lasp.colorado.edu/sorce/news/2012ScienceMeeting/docs/presentations/S1-04%20LEAN_NRLSSI_Sep12.pdf) , 2012. Accessed on: 23.01.2016

J. Lean, G. Rottman, J. Harder, G. Kopp, **Sorce Contributions To New Understanding Of Global Change And Solar Variability**, Solar Physics 230: 27–53, 2005.

J. Lean, G. Rottman, H. L. Kyle, T. N. Woods, J. R. Hickey, L. C. Puga, **Detection and parameterization of variations in solar mid- and near-ultraviolet radiation (200-400 nm)**; J. Geophys. Res., 102, No. D25, 29939-29956, 1997.

P. Lemaire, & A. Skumanich, **Magnesium II Doublet Profiles of Chromospheric Inhomogeneities at the Center of the Solar Disk**; Astronomy and Astrophysics, 22, 61, 1973.

Lisirid, <http://lasp.colorado.edu/lisird/nrlssi/> Accessed on: 23.01.2016

W. E. McClintock, G. J. Rottman, T. N. Woods, **Solar Stellar Irradiance Comparison Experiment II (SOLSTICE II): Instrument Concept and Design**; Solar Physics, 230, 1, 225-258, 2005.

D. M. Mecko, [http://www.ltrr.arizona.edu/~dmeko/notes\\_7.pdf](http://www.ltrr.arizona.edu/~dmeko/notes_7.pdf),  
<http://www.ltrr.arizona.edu/~dmeko/geos585a.html> , 2015. Accessed on: 05.01.2016

NASA, <http://science.nasa.gov/missions/sorce/> Accessed on: 23.01.2016

J. A. Pagarán, **Solar spectral irradiance variability from SCIAMACHY on daily to several decades timescales**; Ph.D. Thesis, University of Bremen, 2012.

J. Paganan, M. Weber, M.T. DeLand, L.E. Floyd, J.P. Burrows, **Solar Spectral Irradiance Variations in 240 – 1600 nm During the Recent Solar Cycles 21 – 23**; Solar Phys, 272 159–188, DOI 10.1007/s11207-011-9808-4, 2011.

J. Paganan, M. Weber, and J. Burrows, **Solar Variability From 240 to 1750 nm in terms of Faculae Brightening and Sunspot Darkening from SCIAMACHY**; The Astrophysical Journal, 700, 1884–1895, 2009.

A. Riaz, **Error analysis of the long term Mg II index from SCIAMACHY, GOME and GOME-2**; M.Sc. Thesis, University of Bremen, 2012.

I. Rühedi, M. Güdel and W. Schmutz, **The Sun, Solar Analogs and the Climate**; Swiss Society for Astrophysics and Astronomy, 2004.

F. Shakeri, **Investigation of solar variability using satellite measurements of the Mg II index**; M.Sc. Thesis, University of Bremen, 2010.

M. Snow, M. Weber, J. Machol, R. Viereck, E. Richard, **Comparison of Magnesium II core-to-wing ratio observations during solar minimum 23/24**; J. Space Weather Space Clim., 4, 2014.

M. Snow, W. E. McClintock, G. Rottman, T. N. Woods, **Solar Stellar Irradiance Comparison Experiment II (SOLSTICE II): Examination of the Solar Stellar Comparison Technique**; Solar Physics, 230, 1, 295-324, 2005.

SOLSTICE, <http://lasp.colorado.edu/home/SOLSTICE/> Accessed on: 23.01.2016

SUSIM, [http://www.solar.nrl.navy.mil/susim\\_uars.html](http://www.solar.nrl.navy.mil/susim_uars.html) Accessed on: 23.01.2016

C. Tarrío, S. Grantham, S. B. Hill, N. S. Faradzhev, L. J. Richter, C. S. Knurek and T. B. Lucatorto; **A synchrotron beamline for extreme-ultraviolet photoresist testing**, Rev. Sci. Instrum. 82, 073102, doi:10.1063/1.3606484, 2011.

G. Thuillier, M. DeLand, A. Shapiro, W. Schmutz, D. Bolsée, S.M.L. Melo, **The Solar Spectral Irradiance as a Function of the Mg II Index for Atmosphere and Climate Modelling**; DOI 10.1007/s11207-011-9912-5, 2012.

G. Thuillier, and S. Bruinsma, **The Mg II index for upper atmosphere Modeling**; Ann. Geophys., 19, 219 228, 2001.

R. A. Viereck, L. E. Floyd, P. C. Crane, T. N. Woods, B. G. Knapp, G. Rottman, M. Weber, L. C. Puga, M. T. DeLand, **A composite Mg II index spanning from 1978 to 2003**; Space Weather, 2, S10005, DOI 10.1029/2004SW000084, 2004.

R. Viereck, L. Puga, D. McMullin, D. Judge, M. Weber, W. K. Tobiska, **The MG II index: A Proxy for Solar EUV**, **Geophysical Research Letters**; 28, 7, DOI 0094-8276/01/2000GL012551, 2001.

UARS, <http://umpgal.gsfc.nasa.gov/> Accessed on: 23.01.2016